Two Facets of Insect Vision: Polarization Sensitivity and Visual Pigments

Dissertation

zur

Erlangung der naturwissenschaftlichen Doktorwürde

(Dr. sc. nat.)

vorgelegt der

Mathematisch-naturwissenschaftlichen Fakultät

der

Universität Zürich

von

Miriam Judith Henze

aus

Deutschland

Promotionskomitee

Prof. Dr. Stephan Neuhauss (chair)
PD Dr. Thomas Labhart (supervisor)
Prof. Dr. Rüdiger Wehner
Prof. Dr. Uwe Homberg

Zürich 2009

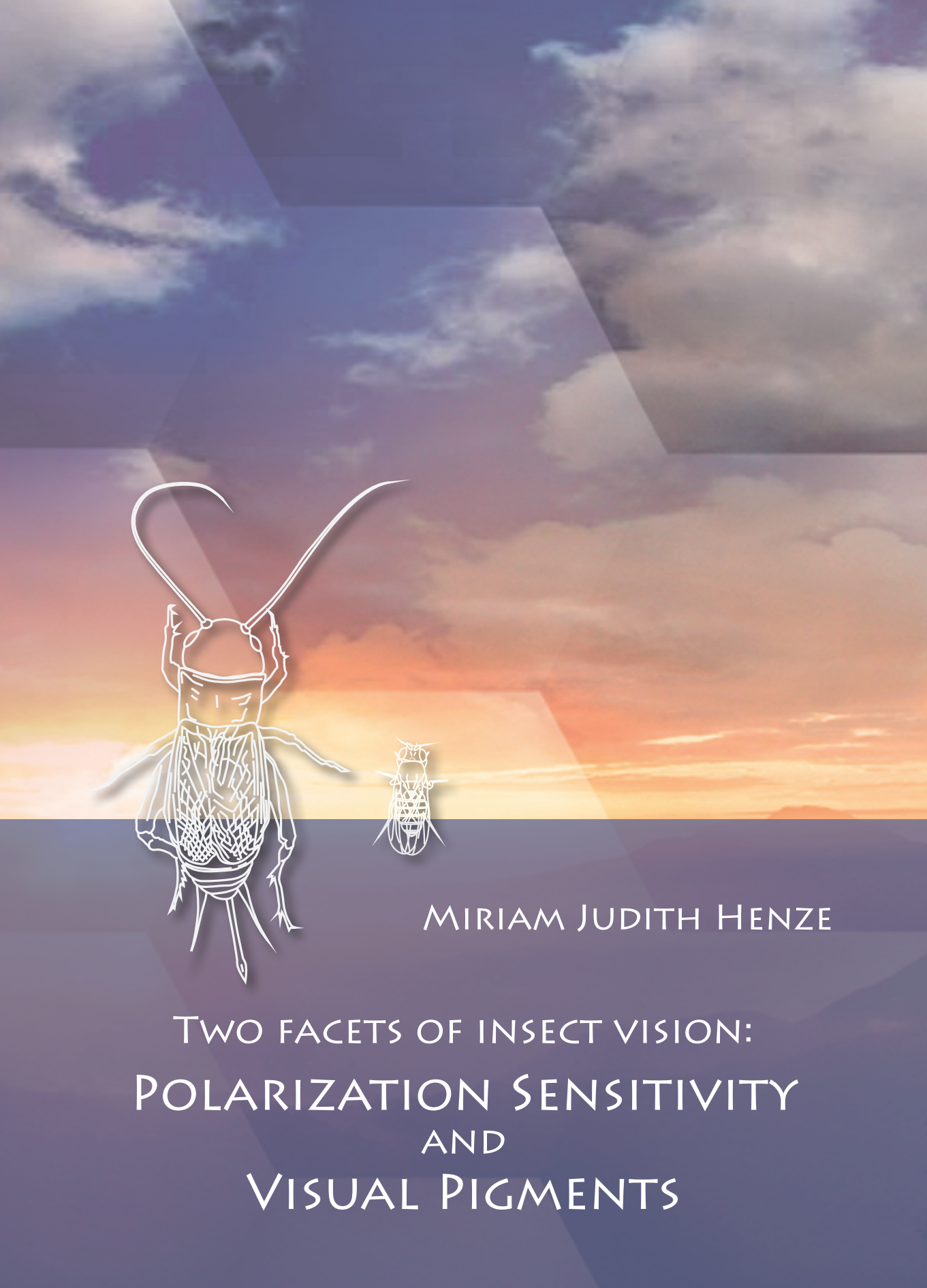

Miriam Judith Henze

Two facets of insect vision: Polarization Sensitivity and Visual Pigments

"If you think you are too small to be effective,
you have never been in bed with a mosquito."

Betty Reese

For Martin
and our little one

Table of contents

Summary

The polarization pattern of the sky serves many insects as a reference for visual compass orientation. Chapter I specifies thresholds for the behavioral response to polarized light in field crickets (*Gryllus campestris*) under conditions mimicking those experienced by the animals in their natural habitat. Our results show that the polarization vision system of crickets is extremely sensitive and robust.

Photoreceptors involved in the detection of polarized skylight are generally confined to a small part of the insect compound eye, the so-called dorsal rim area (DRA). In Chapter II, we construct a model for the sensory input to the polarization vision system of fruit flies (*Drosophila melanogaster*) and compare it with data from crickets, thus demonstrating the consequences of two opposite DRA designs for neuronal coding of orientation.

Group-specific distinctions in the morphology of DRA ommatidia suggest that polarization vision evolved independently in several insect taxa. However, developmental findings indicate that DRA formation in distantly related species is initiated by homologous signaling pathways. We address the question of DRA ancestry in Chapter III where we report pilot experiments that failed to detect the same selector gene for DRA specification in two-spotted crickets (*Gryllus bimaculatus*) as previously identified in fruit flies.

Polarization vision in crickets is mediated by blue receptors. Electrophysiological data imply that the respective visual pigment is exclusively found in the DRA. We have cloned four visual opsins of *G. bimaculatus* and investigated their phylogeny as well as their expression pattern in the compound eyes and the ocelli. Chapter IV reveals that the ocellar opsins diverged from those of the compound eyes and that regionalization in the cricket visual system is more complex than assumed earlier.

Zusammenfassung

Das Polarisationsmuster des Himmels dient vielen Insekten als Kompass zur visuellen Orientierung. Kapitel I beschäftigt sich mit der Reaktionsschwelle, die Feldgrillen (*Gryllus campestris*) auf polarisiertes Licht zeigen, wenn die Versuchsbedingungen die Verhältnisse im natürlichen Lebensraum der Tiere simulieren. Unsere Ergebnisse verdeutlichen, dass das Polarisationssehsystem von Grillen äußerst empfindlich und robust ist.

Die Photorezeptoren, die an der Wahrnehmung von polarisiertem Himmelslicht beteiligt sind, findet man in der Regel nur in der so genannten dorsalen Randregion (DRA) des Komplexauges. In Kapitel II erstellen wir ein Modell für den sensorischen Eingang zum Polarisationssehsystem von Taufliegen (*Drosophila melanogaster*) und vergleichen es mit Daten von der Grille. Dabei demonstrieren wir die Konsequenzen, die zwei konträre DRA-Typen für die Kodierung der Körperorientierung im Gehirn haben.

Taxon-spezifische Unterschiede in der Morphologie der DRA-Ommatidien deuten darauf hin, dass das Polarisationssehen in verschiedenen Insektengruppen unabhängig voneinander entstanden ist. Entwicklungsphysiologische Befunde hingegen lassen vermuten, dass die Ausbildung der DRA selbst in entfernt verwandten Arten durch homologe Signalwege ausgelöst wird. Wir befassen uns mit der Frage der DRA-Herkunft in Kapitel III, wo wir eine Pilotstudie vorstellen, in der das DRA-Selektorgen, das zuvor bei Fruchtfliegen identifiziert wurde, nicht bei Zweifleckgrillen (*Gryllus bimaculatus*) nachzuweisen war.

Polarisationssehen wird bei Grillen durch blauempfindliche Photorezeptoren vermittelt. Elektrophysiologische Daten legen nahe, dass das zugehörige Sehpigment ausschließlich in der DRA vorkommt. Wir haben vier visuelle Opsine von *G. bimaculatus* kloniert und deren Abstammung sowie ihr Expressionsmuster in den Komplexaugen und Ocellen untersucht. Kapitel IV zeigt, dass sich die Opsine der Ocellen von denen der Komplexaugen unterscheiden und dass das visuelle System der Grille regional stärker spezialisiert ist als bisher angenommen.

Introduction

"To understand the success of insects is to appreciate our own shortcomings"
Thomas Eisner

With about a million described species and presumably many more to be discovered, insects constitute by far the most diverse and successful animal group on earth at present (Chapman, 2007; Grimaldi and Engel, 2005). Their leading position is often overlooked since individual insects are rather small due to the size limitation given by their respiratory organ, the tracheal system (Kaiser et al., 2007). A consequence of small body size is a miniature brain. However, the tiny brains of insects are able to deal very efficiently with the everyday challenges of our world. Insects are experts when it comes to the extraction of relevant information from a complex stimulus on a peripheral level. This is especially obvious in vision: Rather than collecting different kinds of information with one type of eye and sorting it out at higher brain levels, insects have evolved eyes for special purposes and dedicated eye regions to specific tasks. The processing of visual cues such as intensity contrasts, wavelength composition (color), plane of vibration (polarization) and motion are based on the absorption of light by visual pigments. In my thesis, I have studied skylight polarization vision in crickets and flies as well as the visual pigments in the eyes of crickets. This introduction shall provide the background knowledge necessary to understand and discuss the results presented in Chapters I to IV. It is not meant as a review of all available literature on insect vision.

1 Rhabdomeric photoreceptors

a) Structure

The sensory elements of insect eyes are elongated neurons termed retinula cells. They consist of a cell body, a photosensitive part and an axon that leaves the eye proximally. On at least one side of each photoreceptor, the membrane is differentiated into tubular protrusions that extend at right angles to the long axis of the cell (Fig. 1A). These so-called microvilli collectively form the photosensitive part, the rhabdomere. The rhabdomeres of several receptors together make up the rhabdom. This structure acts as an optical light- or waveguide since the closely-packed cell membranes composed of phospholipids and proteins have a higher refractive index than the watery surroundings (Stavenga, 2006). The rhabdom contains the visual pigment molecules (Fig. 1C), which are responsible for the detection of light. They are embedded in the microvillar membrane and, due to the tremendous increase in surface area, tens of millions of them can be found in one rhabdom (Eguchi et al., 1989).

b) Polarization sensitivity

Visual pigments are dichroic since their photosensitive part, the chromophore, forms an electrical dipole that maximally absorbs light polarized parallel to it. Tilted about 20° into the surface, the dipole axes of the chromophores are oriented approximately in the plane of the membrane (Goldsmith and Wehner, 1977). In combination with the tubular shape of the microvillus, this results in an intrinsic polarization sensitivity of rhabdomeric photoreceptors. Even if the dipole axes were oriented randomly across the surface of the microvillus, the sensitivity for light polarized parallel to the microvillar axis would be twice as high as for light polarized perpendicular to it (Fig 1D). As the pigment molecules are anchored in the membrane in such a way that the dipole axes of the chromophores are preferentially aligned with the long axis of the microvillus (Fig. 1B), much higher polarization sensitivities are achieved (Goldsmith and Wehner, 1977; Israelachvili and Wilson, 1976; Land, 1991; Moody and Parriss, 1961).

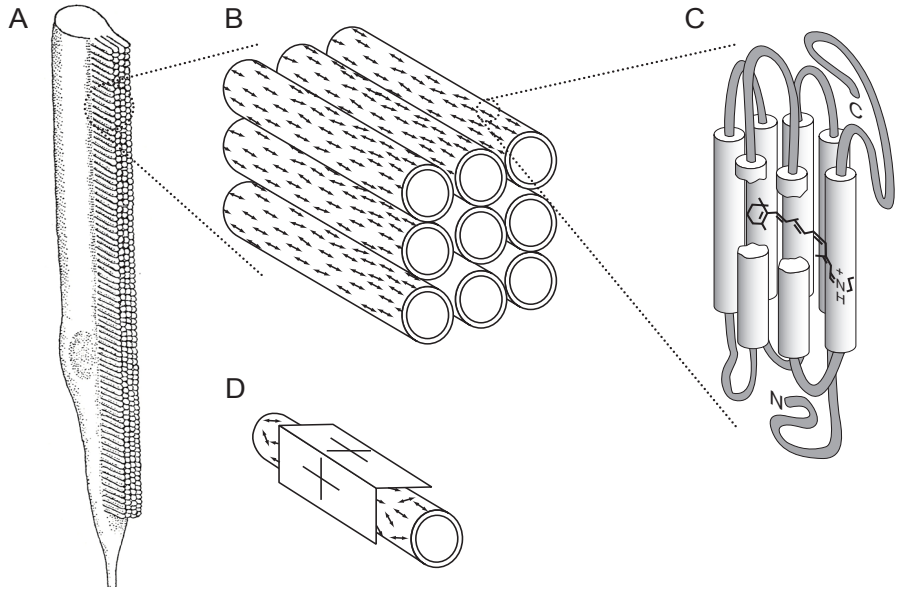

Fig. 1. (A) Schematic drawing of a rhabdomeric photoreceptor. The tubular protrusions of the receptor membrane, the microvilli, conjointly constitute the photosensitive part of the cell, the rhabdomere. (B) Enlarged view on a stack of microvilli. The dipole axes of the pigment molecules embedded in the membrane are indicated by double-headed arrows. They are preferentially aligned with the long axes of the microvilli. (C) A visual pigment molecule is a covalent compound of a protein, opsin, and a chromophore, retinal. The seven transmembrane helices of the opsin surround the chromophore, as shown in this cutaway view. Visual pigments are inherently dichroic, that is the absorption of linearly polarized light is a sinusoidal function of the axes of polarization. (D) A single microvillus is also intrinsically polarization sensitive even if the dipole axis of the photopigments are randomly oriented in the plane of its membrane. Its tubular form results in twice as many molecules being aligned parallel to its long axis as compared with either orthogonal direction. If the dipole axes of the pigment molecules are parallel to the long axis of the microvillus, polarization sensitivity is maximized. Adapted from (Horváth and Varjú, 2004; Land, 1991; Rodieck, 1998; Wehner, 1976).

c) Spectral sensitivity

The spectral sensitivity of a photoreceptor is primarily determined by the absorption spectrum of its visual pigment. Visual pigments are chromoproteins of about 380 amino acids, one of which covalently binds the 11-cis isomer of a light-sensitive prosthetic group, the chromophore (Fig. 1C). Both the amino acid sequence of the apoprotein and the nature of the chromophore affect the wavelength of peak sensitivity. The prevalent chromophore in insect visual pigments is retinal, the aldehyde of vitamin A1. Some species employ 3-hydroxyretinal derived from vitamin A3 (e.g. many flies and butterflies (Seki and Vogt, 1998)) or 3-hydroxyretinal as well as retinal (e.g. dragonflies (Seki et al., 1989) and fireflies (Hariyama et al., 1998)). Whereas both chromophores alone absorb maximally in the ultraviolet, the peak sensitivity of a visual pigment can be located anywhere between ultraviolet and red (Briscoe and Chittka, 2001; Gärtner, 2000). This depends on the composition of the apoprotein part of the visual pigment, the opsin. The seven transmembrane helices of an opsin form a binding pocket harboring the chromophore (Fig. 1C). Specific amino acid side groups interact with the chromophore and influence its absorption properties, thereby tuning it to specific wavelengths (Nathans, 1990; Sakmar et al., 1989; Salcedo et al., 2003; Zhukovsky and Oprian, 1989).

2 The eyes of adult insects

In adult insects rhabdomeric photoreceptors are typically grouped in two kinds of visual organs: lateral compound eyes and dorsal ocelli. Both eye types were probably present in the first euarthropods already (Bitsch and Bitsch, 2005; Paulus, 1979; Paulus, 2000), which indicates that their evolutionary divergence dates back at least to the early Cambrian, more than 500 million years ago (Waloszek, 2003).

2.1 Ocelli

Ocelli are cup-shaped, isolated camera-type eyes. In general, there are three in number which are positioned in an inverted triangle dorsally on the front (Fig. 2A) or on the vertex of the head. The two lateral ocelli are directed to the right and left respectively, while the median ocellus is oriented frontally. In several insect species - particularly in wingless forms, but also in most Coleoptera (beetles) and Lepidoptera (butterflies, moths) - the median or all of the ocelli are secondarily reduced or absent (Chapman, 1998; Mizunami, 1994).

a) Phylogeny

Ocelli were inherited from the arthropod ancestor (Bitsch and Bitsch, 2005; Mayer, 2006; Paulus, 2000). They are found in the fossils of predecessors as well as in representatives of all extant arthropod subphyla except for the myriapods. It is assumed that the three dorsal ocelli of insects are homologous to the nauplius eyes of crustaceans, the ocelli (median eyes)

of horseshoe crabs, the principal (anterior median) eyes of spiders and the eyes of sea spiders (Bitsch and Bitsch, 2005; Paulus, 1979; Paulus, 2000). The arthropod predecessor presumably had only one pair of ocellus-like visual organs which was then duplicated and modified in several arthropod lineages (Mayer, 2006). According to this theory the median ocellus of insects resulted from a fusion event. Indeed, there is developmental and morphological evidence of a paired origin (e.g. (Caesar, 1913; Chapman, 1998; Mobbs, 1979)).

b) Structure

An ocellus has a single curved lens (Fig. 2B) or a flat window consisting of transparent cuticle. Sometimes a clear zone is located between it and the underlying photoreceptor layer, which comprises a large number of closely packed retinula cells in an irregular arrangement. Each retinula cell has a rhabdomere on at least one of its sides and the rhabdomeres of two or more cells join to form rhabdoms. A reflecting tapetum and pigment cells, enclosing the ocellus and providing a moveable iris, are present in several species but are lacking in others. Proximally each retinula cell extends as an axon through the basal lamina and terminates in a synaptic plexus immediately behind the ocellus (Chapman, 1998).

c) Function

Dorsal ocelli possess high-aperture dioptrics exhibiting wide visual fields. In most cases the refractive power is not sufficient to form a focused image on the retinal layer (reviewed by (Goodman, 1981)), and a large number of photoreceptors converge on to a small number of interneurons. Thus the ocelli are not suited for fine-scale form perception, but are extremely light sensitive and can detect subtle changes of intensity integrated over their wide visual field. Given the giant diameter of some ocellar interneurons and the small number of synapses between detector and effector, the system is also considered to be very fast.

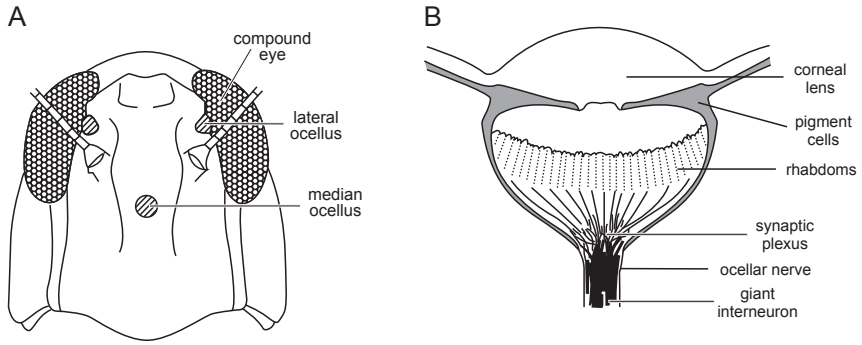

Fig. 2. (A) Frontal view of the head of a grasshopper showing its three ocelli. (B) Schematic longitudinal section through an ocellus of a grasshopper. The light-adapted condition in which the pigment restricts the entry of light is illustrated. Adapted from (Chapman, 1998; Wilson, 1978).

Because of these features, ocelli are well adapted to monitor the position of the horizon as an insect rolls or pitches around its body axis during flight (Guy et al., 1979; Taylor, 1981; Wilson, 1978). A role in the maintenance of flight stability has been demonstrated in locusts and dragonflies (Stange, 1981; Stange and Howard, 1979; Taylor, 1981). Ocelli have also been considered to act as general light meters that influence the sensitivity of the compound eyes and entrain circadian rhythms (reviewed by (Mizunami, 1994)). In desert ants, ocellar photoreceptors are strongly polarization sensitive and are used to read compass information from the sky (Fent and Wehner, 1985; Mote and Wehner, 1980). Recent studies have shown that the ocelli of some insects are capable to resolve spatial details of the world (Berry et al., 2007; Warrant et al., 2006). Furthermore, the ocelli of dragonflies show a directional response to motion if ultraviolet light is used as a stimulus (van Kleef et al., 2008).

2.2 Compound eyes

Compound eyes have a repetitive architecture (Fig. 3A). They consist of individual photoreception units called ommatidia which are located on a convex surface, thus pointing in slightly different directions. A pair of compound eyes, one on each side of the head, is present in most adult insects (Fig. 2A) and in the larvae of hemimetabolous species. The number of ommatidia per eye can be as high as 30 000 in aerial hunters such as dragonflies (Wehner and Gehring, 1995). On the other hand, in parasitic groups, cave-dwelling species and habitually subterranean stages compound eyes may be reduced to very few ommatidia or be completely absent (Chapman, 1998).

a) Phylogeny

Compound eyes arose together with the first euarthropods in the early Cambrian and are considered an autapomorphy (novel acquisition) of this group (Bitsch and Bitsch, 2005; Nilsson and Kelber, 2007; Paulus, 1979; Paulus, 2000; Waloszek, 2003). They are missing in pycnogonids (sea spiders), but are found in representatives of all other subphyla. The only extant chelicerates possessing compound eyes are horseshoe crabs (Xiphosura), which have remained almost unchanged for millions of years. More recent chelicerates, such as scorpions and spiders, have converted the ancestral compound organs into several camera-type eyes by fusing groups of ommatidia (Bitsch and Bitsch, 2005; Harzsch et al., 2005; Land and Nilsson, 2002; Nilsson and Kelber, 2007; Paulus, 1979; Paulus, 2000). Even though the evolution of compound eyes might have proceeded along at least two independent lineages, a crustacean/insect and a myriapod/chelicerate one, from a very primitive ancestor (Nilsson and Kelber, 2007), comparative studies of the nervous system leave little doubt that the lateral eyes of euarthropods, i.e. the compound eyes of insects, crustaceans, myriapods and horseshoe crabs, the secondary eyes of spiders and the lateral eyes of modern scorpions, are homologous (Harzsch, 2002; Sinakevitch et al., 2003; Strausfeld, 2005).

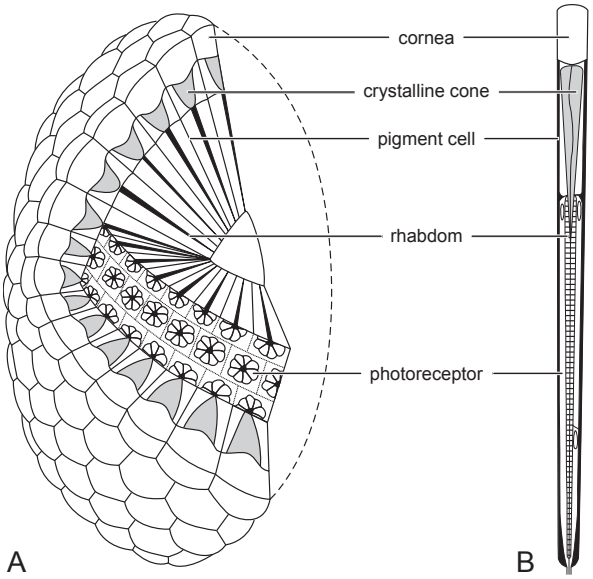

Fig. 3. Compound eye of the apposition type. (A) Diagrammatic three-dimensional drawing showing cross-sections and longitudinal sections through a compound eye. (B) Schematic longitudinal section of an ommatidium. Adapted from (Burghause, 1979; Wehner and Gehring, 1995).

b) Structure

The cuticle covering a compound eye is transparent and usually forms a biconvex corneal lens at the distal end of each ommatidium. In surface view, these structures make up an array of hexagonal facets. Apart from the corneal lens, each ommatidium is generally composed of two primary and several secondary pigment cells, four semper cells which produce the crystalline cone, a clear intracellular structure, and eight retinula (receptor) cells (e.g. (Bitsch and Bitsch, 2005; Paulus, 1979; Paulus, 2000)). In most insects, the rhabdomeres of all retinula cells abut on each other along the optical axis of the ommatidium forming a fused rhabdom. In Diptera (flies), Dermaptera (earwigs), some Heteroptera (bugs) and Coleoptera (beetles), however, the rhabdomeres are separated and constitute an open rhabdom (Chapman, 1998). In an ommatidium with a fused rhabdom, all receptors have the same field of view. If the rhabdom is open, the receptors in an ommatidium have different visual fields, but share it with individual cells in each of the adjacent ommatidia. The axons from all receptors imaging the same point in space congregate in the lamina. This type of eye is called neural superposition eye (Kirschfeld, 1967). It is a special case of the apposition compound eye (Fig. 3) typically found in diurnal insects. In apposition eyes the rhabdoms directly adjoin the crystalline cones. Nocturnal and crepuscular insects, in contrast, often have optical superposition eyes, in which the lens system and the rhabdoms are separated by a clear zone such that each rhabdom receives light from many facets (e.g. (Chapman, 1998; Land and Nilsson, 2002)).

c) Function

Compound eyes are the main visual organs of most adult insects and of the larvae of hemimetabolous species. They fulfill a number of different functions including intensity, color, polarization and motion vision, distance and form perception. Insects with well-developed compound eyes generally have an extensive field of view which may cover almost 360° (Chapman, 1998). The spatial resolution of a compound eye is lower than the one of a well-focused camera-type eye of the same diameter, but still reaches values of 0.25° in the most acute zone of dragonfly eyes (Land and Nilsson, 2002). Many insects can see very well in dim light, experience a great variety of colors, and can clearly distinguish extremely rapid movements with their compound eyes (Warrant and Nilsson, 2006).

3 Detection of polarized skylight

Several insect species have been shown to detect skylight polarization which they exploit as a reference for visual orientation (for reviews see (Horváth and Varjú, 2004; Labhart and Meyer, 1999; Wehner and Labhart, 2006)).

3.1 The celestial polarization pattern

On its way through the atmosphere, light is scattered by air molecules (Fig. 4A) and is thereby linearly polarized, i.e. the electric vector (*e*-vector) of light waves preferentially vibrates in one orientation. The proportion oscillating in the prevailing orientation is called the degree of (linear) polarization. Both the orientation of the *e*-vector (axis of polarization) and the

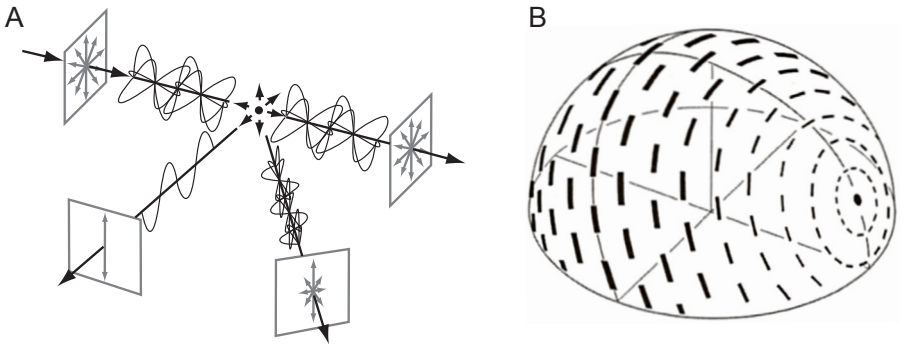

Fig. 4. (A) Skylight polarization originates from scattering processes in the atmosphere. The wave traces in the diagram depict the oscillations of the electric vector (*e*-vector) of light propagating in the direction of the black arrows. Grey, double-headed arrows inside the panels mark *e*-vector orientation as seen by an earthbound observer. Whereas direct sunlight is unpolarized (upper left and right panel), light scattered by an air molecule is linearly polarized, maximally at a scattering angle of 90° (lower left panel). (B) Celestial *e*-vector pattern shown in a three-dimensional representation for an elevation of the sun (black disc) of 25°. Tilt and size of the bars indicate the prevailing *e*-vector orientation and the degree of polarization, respectively. The line connecting the bars at an angular distance of 90° from the sun marks the region of the sky that exhibits maximal polarization. Adapted from (Wehner, 1982; Wehner, 2001).

degree of polarization depend on the scattering angle. As a result, a pattern of polarized skylight is generated (Fig. 4B) that is linked to the dominant light source illuminating the celestial hemisphere, i.e. the sun during the day and the moon at night (Coulson, 1988; Cronin et al., 2006; Gál et al., 2001; Horváth and Wehner, 1999; Strutt, 1871).

Celestial cues are effectively at infinity. Thus, their retinal position in a terrestrial observer does not shift with translational motions but only with rotations, which makes them useful references for visual compass orientation. In contrast to the sun and the moon as orientation cues, the polarization pattern has the advantage that it extends over the whole sky, and therefore it is not shielded completely by scattered clouds or terrestrial objects. Other stray light parameters in the sky, such as the gradients of spectral composition and intensity, are highly susceptible to atmospheric disturbances. This is also true for the degree of polarization whereas the distribution of *e*-vector orientations is rather stable. Depending on illumination conditions, it can even continue underneath clouds, haze or under a canopy (Barta and Horváth, 2004; Brines and Gould, 1982; Können, 1985; Pomozi et al., 2001). The *e*-vector pattern thus provides a very reliable reference for visual compass orientation.

3.2 The polarization-sensitive dorsal rim area (DRA)

In all insect species studied so far, the photoreceptors mediating celestial *e*-vector detection are confined to a small part of the compound eye, the so-called dorsal rim area (DRA) (e.g. (Labhart and Meyer, 1999)).

a) Common functional adaptations

DRA ommatidia show a number of characteristic features (Labhart and Meyer, 1999): (1) They are directed towards the sky and (2) their optics is often degraded. (3) The microvilli forming the rhabdomere of each photoreceptor are well aligned. (4) Each ommatidium contains two sets of photoreceptors with mutually orthogonal microvilli orientations but (5) with the same spectral sensitivity. (6) The rhabdoms are comparatively short and have large cross-sectional areas. Together, these functional adaptations provide the basis for a color-blind and intensity-independent visual system that is highly sensitive to the *e*-vector orientation of linearly polarized light from above.

In Chapter I, we demonstrate by a behavioral study on field crickets (*Gryllus campestris*) that the properties described above ensure an extremely robust sensory system that can deal with very low light intensities (Herzmann and Labhart, 1989; Labhart et al., 2001), low degrees of polarization and small stimulus sizes.

b) Different DRA designs

Despite common properties, there are also considerable differences between the DRAs of insect species. The disparities concern for instance the arrangement and the optical specializations of DRA ommatidia. In some insects, the polarization-sensitive area is

restricted to the dorsalmost part of the eye and is many ommatidia wide (field cricket (Blum and Labhart, 2000), locust (Homberg and Paech, 2002), cockchafer (Labhart et al., 1992), dung beetles (Dacke et al., 2003, Dacke et al., 2002)). In others, it extends all the way from the caudal to the frontal eye rim, but comprises only one or two ommatidial rows (dragonfly (Meyer and Labhart, 1993), fruit fly (Tomlinson, 2003; Wernet et al., 2003)). Several insects take an intermediate position, with a DRA that is relatively short and rather narrow (honey bee, desert ant (Wehner, 1982), halactid bee (Greiner et al., 2007), monarch butterfly (Labhart et al., 2009; Stalleicken et al., 2006)). In many cases, the optics of DRA ommatidia is degraded in ways that significantly increase the visual field (for a review see (Labhart and Meyer, 1999)). In other species such adaptations are missing (ants (Aepli et al., 1985; Herrling, 1976; Labhart and Meyer, 1999; Wehner, 1982), monarch butterflies (Labhart et al., 2009; Stalleicken et al., 2006), some flies (review (Labhart and Meyer, 1999))). These differences have not received much attention so far, even though they strongly affect the sensory input to the polarization vision system and possibly have a functional basis. The arrangement and optics of the DRA ommatidia define direction and size of the visual fields and thus ultimately determine which parts of the celestial polarization pattern are exploited.

In Chapter II, we construct a model for the sensory input to the polarization vision system of fruit flies (*Drosophila melanogaster*) and compare it with data from crickets, thus demonstrating the consequences of two opposite DRA designs for neuronal coding of orientation.

c) Phylogeny of the DRA

Whereas similar constellations concerning the arrangement and optical specializations of DRA ommatidia are found in distantly related insect species, fine-structural disparities in the design of DRA ommatidia are group-specific. They include for instance the configuration and the spectral sensitivity of the receptors used for polarization vision. Based on these differences, it has been suggested that celestial *e*-vector detection arose independently in several insect taxa (Labhart and Meyer, 1999). In addition to morphological and physiological comparisons, developmental studies can provide evidence for evolutionary relationships. Data from fruit flies and grasshoppers suggest that DRA formation during metamorphosis of the derived Diptera and during embryogenesis of the phylogenetically more primitive Orthoptera is initiated by homologous signaling pathways (Dong and Friedrich, 2005; Tomlinson, 2003; Wernet et al., 2003). A promising route to further address the question of DRA ancestry is to study downstream mediators of DRA specification in different taxa. The general employment of one selector gene would support a monophyletic origin while group-specific selector genes would favor polyphyly. So far homothorax (hth), the DRA selector gene in the fruit fly (Wernet et al., 2003), could not be detected in the eye field of the embryonic grasshopper (Dong and Friedrich, 2005).

In Chapter III we report pilot experiments that failed to detect the expression of hth in the DRA of another orthopteran species, the cricket (*Gryllus bimaculatus*). Thus, skylight polarization vision in insects might be a case of convergent evolution of morphological traits via the recruitment of homologous upstream signaling pathways.

4 Visual pigments

The concomitance of different kinds of visual organs in one organism makes insects an interesting model to study visual pigment evolution. Visual pigments are crucial in the sensory process of vision and one would expect that their fate is related to the function as well as to the history of the eyes.

4.1 Spectral sensitivities of insect eyes

A possibility to characterize visual pigments is their absorption spectrum. Spectral sensitivities of photoreceptors have already been investigated in many insect taxa and are to a major extent determined by the visual pigments they contain.

a) Ocelli

The ocelli of most species show absorption maxima in both the ultraviolet (UV) and the blue-green spectral range (dragonflies (Chappell and DeVoe, 1975; Ruck, 1965), mantis (Sontag, 1971), locust (Wilson, 1978), bumblebee (Meyer-Rochow, 1980), honeybee (Goldsmith and Ruck, 1958), moths (Eaton, 1976; Pappas and Eaton, 1977)). Exceptions are the dragonfly *Anax junius* with potentially three visual pigments (UV, blue and blue-green (Chappell and DeVoe, 1975)) and a few cases in which only one of the two typical peak sensitivities was found (UV in the desert ant *Cataglyphis bicolor* (Mote and Wehner, 1980); blue-green in the cockroach *Periplaneta americana* (Goldsmith and Ruck, 1958) and the cricket *Gryllus firmus* (Lall and Trouth, 1989)). Flies possess a single receptor type in their ocelli which is unusual in two respects: it has a longwavelength sensitivity maximum shifted towards blue-violet and it achieves UV-sensitivity by a sensitizing pigment (*Musca* (Kirschfeld et al., 1988); *Calliphora* (Kirschfeld et al., 1988; Kirschfeld and Lutz, 1977); *Drosophila* (Feiler et al., 1988; Hu et al., 1978)).

In Chapter IV, we demonstrate by electroretinogram recordings that the ocelli of the two-spotted cricket *Gryllus bimaculatus* show the two typical sensitivity peaks generally found in insects.

b) Compound eyes

Insect compound eyes typically contain three spectral classes of receptors: UV, blue and green (Briscoe and Chittka, 2001). In some species blue receptors are missing (e.g. in the cockroach *Periplaneta americana* (Mote and Goldsmith, 1971), the red flour beetle

Tribolium castaneum (Jackowska et al., 2007; Richards et al., 2008) and the desert ant *Cataglyphis bicolor* (Labhart, 1986)), in others additional red receptors are present (e.g. in the dragonfly *Hemicordulia tau* (Yang and Osorio, 1991), some butterflies (Bernard, 1979) and hymenopterans (Peitsch et al., 1992)). These features seem to have evolved independently in several groups, though. From the spectral sensitivity data superimposed on the phylogeny of Insecta, it was concluded that the Devonian ancestor of all winged (pterygote) insects likely possessed UV, blue and green receptors (Briscoe and Chittka, 2001).

4.2 Phylogeny of insect visual opsins

Spectral sensitivity data do not necessarily mirror phylogenetic relationships and it is therefore more informative to compare the amino acid sequences of the opsins, the apoproteins that together with a chromophore constitute visual pigments.

Insect visual opsins fall into three major clades (Briscoe and Chittka, 2001): UV-sensitive SW opsins, blue-sensitive MW opsins and LW opsins whose sensitivities vary from blue-violet (Rh2 in *Drosophila* (Feiler et al., 1988)) through green to red (e.g. in some Lepidoptera (Briscoe, 2000)). Most insect species investigated so far possess at least one opsin of each type. Exceptions such as the red flour beetle *Tribolium castaneum* which only encodes an SW and an LW opsin are thought to have lost their MW paralog secondarily (Jackowska et al., 2007). Few studies have analyzed the relationship between the two types of visual organs of adult insects. Honey bees express the same ultraviolet opsin (AmUVop) in both the ocelli and the compound eyes (Velarde et al., 2005). This has also been shown for bumblebees (Spaethe and Briscoe, 2005). Long-wavelength opsins, in contrast, differ between the ocelli and the compound eyes in all insect species investigated so far. AmLop2 of the honey bee (Velarde et al., 2005) and Rh2 of the fruit fly (Pollock and Benzer, 1988) are ocellus-specific. However, up to now molecular studies concentrated on Hymenoptera, Diptera, Lepidoptera and Coleoptera, all of which are highly derived, holometabolous insect orders. Based on such a restricted data set, general conclusions on the evolution of insect opsins are questionable.

In Chapter IV, we report the results of a study in which we cloned retinal opsins of the cricket *Gryllus bimaculatus*, a comparatively primitive, hemimetabolous insect. We investigated the phylogenetic origin as well as the spatial expression pattern of the identified opsin paralogs in the compound eyes and the ocelli.

4.3 Regionalization and opsin distribution in the insect retina

Regionalization is a common property of insect eyes (e.g. (Kelber, 2006)). Two basic types can be distinguished. In the first case, confined parts of the eye are principally different from the remainder, often expressing another set of opsins, and used for a specific purpose. Examples are the polarization-sensitive DRAs in many insect species (Labhart and Meyer, 1999), the part of the dragonfly eye specialized for prey detection (Labhart and Nilsson, 1995) or the

mating zone of the honey bee drone (Menzel et al., 1991). The second case of regionalization involves more subtle differences. In many insects the number and frequency of receptor types changes gradually across the eye. In the hawkmoth *Manduca sexta* and in the butterfly *Vanessa cardui*, for instance, ommatidia with blue receptors are more frequent ventrally than dorsally (Briscoe et al., 2003; White et al., 2003). These regional characteristics are thought to be adaptations to the light distribution in the habitat optimizing spectral discrimination (Stavenga et al., 2001).

In Chapter IV, we reanalyze retinal regionalization in the cricket *Gryllus bimaculatus* by *in situ* hybridization. Our results object some of the previous assumptions on visual pigment distribution in the compound eyes of this species and include the description of a yet unknown ventral blue-green region.

5 The frame encompassing the different projects of this thesis

The four projects that were carried out during this thesis are related in the following way: While the experiments described in Chapter I test polarization vision in crickets under naturalistic stimulus conditions, optical and histological measurements as well as computer models reported in Chapter II compare the polarization vision systems of flies and crickets on a functional level. The pilot project presented in Chapter III extends the comparison between both insect species in a developmental context. Chapter IV is the only section that does not focus on polarization vision. However, dealing with the visual opsins of the cricket and their distribution in the eyes, it touches on this topic as well. The study was prompted by the need for a reliable marker of the DRA in the *in situ* hybridizations performed in Chapter III. As previous electrophysiological studies had shown a region-specific distribution of spectral types of photoreceptors (Labhart et al., 1984; Zufall et al., 1989), visual opsins seemed well suited to discriminate between the functionally different parts of the cricket compound eye.

6 References

Aepli, F., Labhart, T. and Meyer, E. P. (1985). Structural specializations of the cornea and retina at the dorsal rim of the compound eye in Hymenopteran insects. *Cell Tissue Res.* **239**, 19-24.

Barta, A. and Horváth, G. (2004). Why is it advantageous for animals to detect celestial polarization in the ultraviolet? Skylight polarization under clouds and canopies is strongest in the UV. *J. Theor. Biol.* **226**, 429-437.

Bernard, G. D. (1979). Red-absorbing visual pigment of butterflies. *Science* **203**, 1125-1127.

Berry, R. P., Stange, G. and Warrant, E. J. (2007). Form vision in the insect dorsal ocelli: an anatomical and optical analysis of the dragonfly median ocellus. *Vision Res.* **47**, 1394-1409.

Bitsch, C. and Bitsch, J. (2005). Evolution of eye structure and arthropod phylogeny. In *Crustacea and Arthropod Relationships* (ed. S. Koenemann, R. A. Jenner and F. R. Schram), pp. 185-214. New York: CRC Press, Taylor and Francis Book Inc.

Blum, M. and Labhart, T. (2000). Photoreceptor visual fields, ommatidial array, and receptor axon projections in the polarisation-sensitive dorsal rim area of the cricket compound eye. *J. Comp.*

Physiol. A **186**, 119-128.
Brines, M. L. and Gould, J. L. (1982). Skylight polarization patterns and animal orientation. *J. Exp. Biol.* **96**, 69-91.
Briscoe, A. and Chittka, L. (2001). The evolution of color vision in insects. *Annu. Rev. Entomol.* **46**, 471-510.
Briscoe, A. D. (2000). Six opsins from the butterfly *Papilio glaucus*: Molecular phylogenetic evidence for paralogous origins of red-sensitive visual pigments in insects. *J. Mol. Evol.* **51**, 110-121.
Briscoe, A. D., Bernard, G. D., Szeto, A. S., Nagy, L. M. and White, R. H. (2003). Not all butterfly eyes are created equal: Rhodopsin absorption spectra, molecular identification, and localization of ultraviolet-, blue-, and green-sensitive rhodopsin-encoding mRNAs in the retina of *Vanessa cardui*. *J. Comp. Neurol.* **458**, 334-349.
Burghause, F. M. H. R. (1979). Die strukturelle Spezialisierung des dorsalen Augenteils der Grillen (Orthoptera, Grylloidea). *Zool. Jb. Physiol.* **83**, 502-525.
Caesar, C. J. (1913). Die Stirnaugen der Ameisen. *Zool. Jahrb. Abt. Anat.* **35**, 161-242.
Chapman, A. D. (2007). *Numbers of Living Species in Australia and the World*. Toowoomba, Australia: Australian Biodiversity Information Services.
Chapman, R. F. (1998). *The Insects: Structure and Function*. Cambridge, New York, Melbourne, Madrid, Cape Town, Singapore, São Paulo: Cambridge University Press.
Chappell, R. L. and DeVoe, R. D. (1975). Action spectra and chromatic mechanisms of cells in the median ocelli of dragonflies. *J. Gen. Physiol.* **65**, 399-419.
Coulson, K. L. (1988). *Polarization and Intensity of Light in the Atmosphere*. Hampton, Virginia USA: A. Deepak Publishing.
Cronin, T. W., Warrant, E. J. and Greiner, B. (2006). Celestial polarization patterns during twilight. *Appl . Optics* **45**, 5582-5589.
Dacke, M., Nordström, P. and Scholtz, C. (2003). Twilight orientation to polarised light in the crepuscular dung beetle *Scarabaeus zambesianus*. *J. Exp. Biol.* **206**, 1535-1543.
Dacke, M., Nordström, P., Scholtz, C. H. and Warrant, E. J. (2002). A specialized dorsal rim area for polarized light detection in the compound eye of the scarab beetle *Pachysoma striatum*. *J. Comp. Physiol. A* **188**, 211-216.
Dong, Y. and Friedrich, M. (2005). Comparative analysis of Wingless patterning in the embryonic grasshopper eye. *Dev. Genes Evol.* **215**, 177-197.
Eaton, J. L. (1976). Spectral sensitivity of ocelli of adult cabbage looper moth, *Trichoplusia ni*. *J. Comp. Physiol.* **109**, 17-24.
Eguchi, E., Seki, T. and Suzuki, T. (1989). Comparative studies of chromophore contents inside and outside the rhabdoms of arthropod compound eyes. *J. Comp. Physiol. A* **165**, 589-604.
Feiler, R., Harris, W. A., Kirschfeld, K., Wehrhahn, C. and Zuker, C. S. (1988). Targeted misexpression of a *Drosophila* opsin gene leads to altered visual function. *Nature* **333**, 737-741.
Fent, K. and Wehner, R. (1985). Ocelli - a celestial compass in the desert ant *Cataglyphis*. *Science* **228**, 192-194.
Gál, J., Horváth, G., Barta, A. S. and Wehner, R. D. (2001). Polarization of the moonlit clear night sky measured by full-sky imaging polarimetry at full moon: Comparison of the polarization of moonlit and sunlit skies. *J. Geophys. Res.* **106**, 22647-22653.
Gärtner, W. (2000). Invertebrate visual pigements. In *Handbook of Biological Physics* (ed. D. G. Stavenga, W. J. De Grip and E. N. Pugh), pp. 297-388. New York: Elsevier.
Goldsmith, T. H. and Ruck, P. R. (1958). The spectral sensitivities of the dorsal ocelli of cockroaches and honeybees; an electrophysiological study. *J. Gen. Physiol.* **41**, 1171-1185.
Goldsmith, T. H. and Wehner, R. (1977). Restrictions on rotational and translational diffusion of pigment in the membranes of a rhabdomeric photoreceptor. *J. Gen. Physiol.* **70**, 453-490.
Goodman, L. J. (1981). Organisation and physiology of the insect dorsal ocellar system. In *Handbook of Sensory Physiology*, vol. VII 6C (ed. H. Autrum), pp. 201-286. Berlin: Springer-Verlag.
Greiner, B., Cronin, T. W., Ribi, W. A., Wcislo, W. T. and Warrant, E. J. (2007). Anatomical and physiological evidence for polarisation vision in the nocturnal bee *Megalopta genalis*. *J. Comp. Physiol. A* **193**, 591-600.
Grimaldi, D. and Engel, M. S. (2005). *Evolution of the Insects*. Cambridge: Cambridge University Press.

Guy, R. G., Goodman, L. J. and Mobbs, P. G. (1979). Visual interneurons in the bee brain: Synaptic organisation and transmission by graded potentials. *J. Comp. Physiol.* **134**, 253-264.

Hariyama, T., Terakita, A., Sakayori, M., Katsukura, Y., Ozaki, K. and Tsukahara, Y. (1998). Chromophore distribution and ultraviolet visual pigment in the compound eyes of the Japanese fireflies *Luciola cruciata* and *L. lateralis* (Coleoptera, Lamphyridae). *J. Comp. Physiol. A* **183**, 165-170.

Harzsch, S. (2002). The phylogenetic significance of crustacean optic neuropils and chiasmata: a re-examination. *J. Comp. Neurol.* **453**, 10-21.

Harzsch, S., Müller, C. H. and Wolf, H. (2005). From variable to constant cell numbers: cellular characteristics of the arthropod nervous system argue against a sister-group relationship of Chelicerata and "Myriapoda" but favour the Mandibulata concept. *Dev. Genes Evol.* **215**, 53-68.

Herrling, P. (1976). Regional distribution of three ultrastructural retinula types in retina of *Cataglyphis bicolor* Fabr. (Formicidae, Hymenoptera). *Cell Tissue Res.* **169**, 247-266.

Herzmann, D. and Labhart, T. (1989). Spectral sensitivity and absolute threshold of polarization vision in crickets - a behavioral study. *J. Comp. Physiol. A* **165**, 315-319.

Homberg, U. and Paech, A. (2002). Ultrastructure and orientation of ommatidia in the dorsal rim area of the locust compound eye. *Arthropod Struct. Dev.* **30**, 271-280.

Horváth, G. and Varjú, D. (2004). *Polarized Light in Animal Vision - Polarization Patterns in Nature*. Berlin, Heidelberg, New York: Springer-Verlag.

Horváth, G. and Wehner, R. (1999). Skylight polarization as perceived by desert ants and measured by video polarimetry. *J. Comp. Physiol. A* **184**, 1-7, 347-349.

Hu, K. G., Reichert, H. and Stark, W. S. (1978). Electrophysiological characterization of *Drosophila* ocelli. *J. Comp. Physiol.* **126**, 15-24.

Israelachvili, J. N. and Wilson, M. (1976). Absorption characteristics of oriented photopigments in microvilli. *Biol. Cybern.* **21**, 9-15.

Jackowska, M., Bao, R., Liu, Z., McDonald, E. C., Cook, T. A. and Friedrich, M. (2007). Genomic and gene regulatory signatures of cryptozoic adaptation: Loss of blue sensitive photoreceptors through expansion of long wavelength-opsin expression in the red flour beetle *Tribolium castaneum*. *Front. Zool.* **4**, 24.

Kaiser, A., Klok, C. J., Socha, J. J., Lee, W. K., Quinlan, M. C. and Harrison, J. F. (2007). Increase in tracheal investment with beetle size supports hypothesis of oxygen limitation on insect gigantism. *Proc. Natl. Acad. Sci. USA* **104**, 13198-13203.

Kelber, A. (2006). Invertebrate colour vision. In *Invertebrate Vision* (ed. E. Warrant and D.-E. Nilsson), pp. 250-290. Cambridge, New York, Melbourne, Madrid, Cape Town, Singapore, São Paulo: Cambridge University Press.

Kirschfeld, K. (1967). Die Projektion der optischen Umwelt auf das Raster der Rhabdomere im Komplexauge von Musca. *Exp. Brain Res.* **3**, 248-270.

Kirschfeld, K., Feiler, R. and Vogt, K. (1988). Evidence for a sensitizing pigment in the ocellar photoreceptors of the fly (*Musca*, *Calliphora*). *J. Comp. Physiol. A* **163**, 421-423.

Kirschfeld, K. and Lutz, B. (1977). Spectral sensitivity of ocelli of *Calliphora* (Diptera). *Z. Naturforsch. C* **32**, 439-441.

Können, G. P. (1985). *Polarized Light in Nature*. Cambridge, New York, Melbourne, Madrid, Cape Town, Singapore, São Paulo: Cambridge University Press.

Labhart, T. (1986). The electrophysiology of photoreceptors in different eye regions of the desert ant, *Cataglyphis bicolor*. *J. Comp. Physiol. A* **158**, 1-7.

Labhart, T., Baumann, F. and Bernard, G. D. (2009). Specialized ommatidia of the polarization-sensitive dorsal rim area in the eye of Monarch butterflies have non-functional reflecting tapeta. *Cell Tissue Res.*, in press.

Labhart, T., Hodel, B. and Valenzuela, I. (1984). The physiology of the cricket's compound eye with particular reference to the anatomically specialized dorsal rim area. *J. Comp. Physiol.* **155**, 289-296.

Labhart, T. and Meyer, E. (1999). Detectors for polarized skylight in insects: A survey of ommatidial specializations in the dorsal rim area of the compound eye. *Microsc. Res. Tech.* **47**, 368-379.

Labhart, T., Meyer, E. P. and Schenker, L. (1992). Specialized ommatidia for polarization vision in the compound eye of cockchafers, *Melolontha melolontha* (Coleoptera, Scarabaeidae). *Cell Tissue Res.* **268**, 419-429.

Labhart, T. and Nilsson, D.-E. (1995). The dorsal eye of the dragonfly *Sympetrum* - Specializations for prey detection against the blue sky. *J. Comp. Physiol. A* **176**, 437-453.
Labhart, T., Petzold, J. and Helbling, H. (2001). Spatial integration in polarization-sensitive interneurones of crickets: A survey of evidence, mechanisms and benefits. *J. Exp. Biol.* **204**, 2423-2430.
Lall, A. B. and Trouth, C. O. (1989). The spectral sensitivity of the ocellar system in the cricket *Gryllus firmus* (Orthoptera, Gryllidae). *J. Insect Physiol.* **35**, 805-808.
Land, M. F. (1991). Polarizing the world of fish. *Nature* **353**, 118-119.
Land, M. F. and Nilsson, D.-E. (2002). *Animal eyes*. Oxford: Oxford University Press.
Mayer, G. (2006). Structure and development of onychophoran eyes: What is the ancestral visual organ in arthropods? *Arth. Struct. Dev.* **35**, 231-245.
Menzel, J. G., Wunderer, H. and Stavenga, D. G. (1991). Functional morphology of the divided compound eye of the honeybee drone (*Apis mellifera*). *Tissue Cell* **23**, 525-535.
Meyer-Rochow, V. B. (1980). Electrophysiologically determined spectral efficiencies of the compound eye and median ocellus in the bumblebee *Bombus hortorum tarhakimalainen* (Hymenoptera, Insecta). *J. Comp. Physiol.* **139**, 261-266.
Meyer, E. P. and Labhart, T. (1993). Morphological specializations of dorsal rim ommatidia in the compound eye of dragonflies and damselflies (Odonata). *Cell Tissue Res.* **272**, 17-22.
Mizunami, M. (1994). Information processing in the insect ocellar system: Comparative approaches to the evolution of visual processing and neural circuits. *Adv. Insect Physiol.* **25**, 151-265.
Mobbs, P. G. (1979). Development of the dorsal ocelli of the desert locust, *Schistocerca gregaria* Forsk (Orthoptera: Acrididae). *Int. J. Insect Morphol. Embryol.* **8**, 237-255.
Moody, M. F. and Parriss, J. R. (1961). The discrimination of polarized light by Octopus: a behavioural and morphological study. *Z. Vergl. Physiol.* **44**, 268-291.
Mote, M. I. and Goldsmith, T. H. (1971). Compound eyes: localization of two color receptors in the same ommatidium. *Science* **171**, 1254-1255.
Mote, M. I. and Wehner, R. (1980). Functional-characteristics of photoreceptors in the compound eye and ocellus of the desert ant, *Cataglyphis bicolor*. *J. Comp. Physiol.* **137**, 63-71.
Nathans, J. (1990). Determinants of visual pigment absorbance: identification of the retinylidene Schiff's base counterion in bovine rhodopsin. *Biochemistry* **29**, 9746-9752.
Nilsson, D. E. and Kelber, A. (2007). A functional analysis of compound eye evolution. *Arthropod. Struct. Dev.* **36**, 373-385.
Pappas, L. G. and Eaton, J. L. (1977). Internal ocellus of *Manduca sexta* - Electroretinogram and spectral sensitivity. *J. Insect. Physiol.* **23**, 1355-1358.
Paulus, H. F. (1979). Eye structure and the monophyly of the Arthropoda. In *Arthropod Phylogeny* (ed. A. P. Gupta), pp. 299-383. New York: Van Nostrand Reinhold.
Paulus, H. F. (2000). Phylogeny of the Myriapoda-Crustacea-Insecta: a new attempt using photoreceptor structure. *J. Zool. Sys. Evol. Res.* **38**, 189-208.
Peitsch, D., Fietz, A., Hertel, H., de Souza, J., Ventura, D. F. and Menzel, R. (1992). The spectral input systems of hymenopteran insects and their receptor-based colour vision. *J. Comp. Physiol. A* **170**, 23-40.
Pollock, J. A. and Benzer, S. (1988). Transcript localization of four opsin genes in the three visual organs of *Drosophila*; RH2 is ocellus specific. *Nature* **333**, 779-782.
Pomozi, I., Horváth, G. and Wehner, R. (2001). How the clear-sky angle of polarization pattern continues underneath clouds: full-sky measurements and implications for animal orientation. *J. Exp. Biol.* **204**, 2933-2942.
Richards, S. Gibbs, R. A. Weinstock, G. M. Brown, S. J. Denell, R. Beeman, R. W. Gibbs, R. Beeman, R. W. Brown, S. J. Bucher, G. et al. (2008). The genome of the model beetle and pest *Tribolium castaneum*. *Nature* **452**, 949-955.
Rodieck, R. W. (1998). *The First Steps in Seeing*. Sunderland, Massachusetts: Sinauer Associates, Inc.
Ruck, P. (1965). The components of the visual system of a dragonfly. *J. Gen. Physiol.* **49**, 289-307.
Sakmar, T. P., Franke, R. R. and Khorana, H. G. (1989). Glutamic acid-113 serves as the retinylidene Schiff base counterion in bovine rhodopsin. *Proc. Natl. Acad. Sci USA* **86**, 8309-8313.
Salcedo, E., Zheng, L., Phistry, M., Bagg, E. E. and Britt, S. G. (2003). Molecular basis for ultraviolet vision in invertebrates. *J. Neurosci.* **23**, 10873-10878.

Seki, T., Fujishita, S. and Obana, S. (1989). Composition and distribution of retinal and 3-hydroxyretinal in the compound eye of the dragonfly. *Exp. Biol.* **48**, 65-75.
Seki, T. and Vogt, K. (1998). Evolutionary aspects of the diversity of visual pigment chromophores in the class Insecta. *Comp. Biochem. Phys. B* **119**, 53-64.
Sinakevitch, I., Douglass, J. K., Scholtz, G., Loesel, R. and Strausfeld, N. J. (2003). Conserved and convergent organization in the optic lobes of insects and isopods, with reference to other crustacean taxa. *J. Comp. Neurol.* **467**, 150-172.
Sontag, C. (1971). Spectral sensitivity studies on the visual system of the praying mantis, *Tenodera sinensis*. *J. Gen. Physiol.* **57**, 93-112.
Spaethe, J. and Briscoe, A. D. (2005). Molecular characterization and expression of the UV opsin in bumblebees: three ommatidial subtypes in the retina and a new photoreceptor organ in the lamina. *J. Exp. Biol.* **208**, 2347-2361.
Stalleicken, J., Labhart, T. and Mouritsen, H. (2006). Physiological characterization of the compound eye in Monarch butterflies with focus on the dorsal rim area. *J. Comp. Physiol. A* **192**, 321-331.
Stange, G. (1981). The ocellar component of flight equilibrium control in dragonflies. *J. Comp. Physiol.* **141**, 335-347.
Stange, G. and Howard, J. (1979). An ocellar dorsal light response in a dragonfly. *J. Exp. Biol.*, 351-355.
Stavenga, D. G. (2006). Invertebrate photoreceptor optics. In *Invertebrate Vision* (ed. E. Warrant and D.-E. Nilsson), pp. 1-42. Cambridge, New York, Melbourne, Madrid, Cape Town, Singapore, São Paulo: Cambridge University Press.
Stavenga, D. G., Kinoshita, M., Yang, E. C. and Arikawa, K. (2001). Retinal regionalization and heterogeneity of butterfly eyes. *Naturwissenschaften* **88**, 477-481.
Strausfeld, N. J. (2005). The evolution of crustacean and insect optic lobes and the origins of chiasmata. *Arth. Struct. Dev.* **34**, 235-256.
Strutt, J. L. R. (1871). On the light from the sky, its polarization and colour. *Phil. Mag.* **41**, 107-120.
Taylor, C. P. (1981). Contribution of compound eyes and ocelli to steering of locusts in flight: I. Behavioural analysis. *J. Exp. Biol.* **93**, 1-18.
Tomlinson, A. (2003). Patterning the peripheral retina of the fly: decoding a gradient. *Dev. Cell* **5**, 799-809.
van Kleef, J., Berry, R. and Stange, G. (2008). Directional selectivity in the simple eye of an insect. *J. Neurosci.* **28**, 2845-2855.
Velarde, R. A., Sauer, C. D., Walden, K. K. O., Fahrbach, S. E. and Robertson, H. M. (2005). Pteropsin: A vertebrate-like non-visual opsin expressed in the honey bee brain. *Insect Biochem. Mol. Biol.* **35**, 1367-1377.
Waloszek, D. (2003). The "Orsten" window - Three-dimensionally preserved Upper Cambrian meiofauna and its contribution to our understanding of the evolution of Arthropoda. *Paleontol. Res.* **7**, 71-88.
Warrant, E. and Nilsson, D.-E. (2006). *Invertebrate Vision*. Cambridge, New York, Melbourne, Madrid, Cape Town, Singapore, São Paulo: Cambridge University Press.
Warrant, E. J., Kelber, A., Wallen, R. and Wcislo, W. T. (2006). Ocellar optics in nocturnal and diurnal bees and wasps. *Arth. Struct. Dev.* **35**, 293-305.
Wehner, R. (1976). Polarized-light navigation by insects. *Sci. Am.* **235**, 106-115.
Wehner, R. (1982). Himmelsnavigation bei Insekten. Neurophysiologie und Verhalten. *Neujahrsbl. Naturforsch. Ges. Zürich* **184**, 1-132.
Wehner, R. (2001). Polarization vision - A uniform sensory capacity? *J. Exp. Biol.* **204**, 2589-2596.
Wehner, R. and Gehring, W. (1995). *Zoologie*. Stuttgart, New York: Georg Thieme Verlag.
Wehner, R. and Labhart, T. (2006). Polarisation vision. In *Invertebrate Vision* (ed. E. Warrant and D.-E. Nilsson), pp. 291-348. Cambridge, New York, Melbourne, Madrid, Cape Town, Singapore, São Paulo: Cambridge University Press.
Wernet, M. F., Labhart, T., Baumann, F., Mazzoni, E. O., Pichaud, F. and Desplan, C. (2003). Homothorax switches function of *Drosophila* photoreceptors from color to polarized light sensors. *Cell* **115**, 267-279.
White, R. H., Xu, H., Munch, T. A., Bennett, R. R. and Grable, E. A. (2003). The retina of *Manduca sexta*: rhodopsin expression, the mosaic of green-, blue- and UV-sensitive photoreceptors, and regional specialization. *J. Exp. Biol.* **206**, 3337-3348.

Wilson, M. (1978). Functional organization of locust ocelli. *J. Comp. Physiol.* **124**, 297-316.
Yang, E. C. and Osorio, D. (1991). Spectral sensitivities of photoreceptors and lamina monopolar cells in the dragonfly, *Hemicordulia tau*. *J. Comp. Physiol. A* **169**, 663-669.
Zhukovsky, E. A. and Oprian, D. D. (1989). Effect of carboxylic acid side chains on the absorption maximum of visual pigments. *Science* **246**, 928-930.
Zufall, F., Schmitt, M. and Menzel, R. (1989). Spectral and polarized-light sensitivity of photoreceptors in the compound eye of the cricket (*Gryllus bimaculatus*). *J. Comp. Physiol. A* **164**, 597-608.

Haze, clouds and limited sky visibility: polarotactic orientation of crickets under difficult stimulus conditions

Miriam J. Henze* and Thomas Labhart

Department for Neurobiology, Zoological Institute, University of Zürich, Winterthurerstrasse 190, CH-8057 Zürich, Switzerland

*Author for correspondence (e-mail: miriam.henze@zool.uzh.ch)

I

II

III

IV

Published by The Company of Biologists 2007
The Journal of Experimental Biology 210, 3266-3276
doi:10.1242/jeb.007831

Author contributions statement

MJH conducted the experiments, analyzed the data, prepared the figures and wrote the manuscript.

TL supervised the experiments and edited the manuscript.

The Journal of
Experimental Biology

VOLUME 210 (18) SEPTEMBER 2007

Cover picture. Imagine yourself in a dense forest: nothing from which to get your bearings except for trees that all look alike and patches of sky visible through the leaf canopy. Field crickets cope with a similar situation when foraging in a meadow. In contrast to humans, however, crickets can detect skylight polarization and use it for compass orientation (see article by Henze and Labhart, pp. 3266−3276). Their polarization sense is robust enough to rely on even if sky visibility is restricted to pinhole size. Photograph taken in a meadow with a 180° fisheye lens, by Martin Kohler and Miriam Henze.

The Journal of Experimental Biology 210, 3266-3276
Published by The Company of Biologists 2007
doi:10.1242/jeb.007831

Haze, clouds and limited sky visibility: polarotactic orientation of crickets under difficult stimulus conditions

Miriam J. Henze* and Thomas Labhart

Department for Neurobiology, Zoological Institute, University of Zürich, Winterthurerstrasse 190, CH-8057 Zürich, Switzerland

*Author for correspondence (e-mail: miriam.henze@zool.uzh.ch)

Accepted 23 July 2007

Summary

Field crickets (*Gryllus campestris* L.) are able to detect the orientation of the electric vector (e-vector) of linearly polarized light. They presumably use this sense to exploit the celestial polarization pattern for course control or navigation. Polarization vision in crickets can be tested by eliciting a spontaneous polarotactic response. Previously, wide and 100% polarized stimuli were employed to induce this behavior. However, field crickets live on meadows where the observation of the sky is strongly limited by surrounding vegetation. Moreover, degrees of polarization (*d*) in the natural sky are much lower than 100%. We have therefore investigated thresholds for the behavioral response to polarized light under conditions mimicking those experienced by the insects in the field. We show that crickets are able to rely on polarized stimuli of just 1° diameter. We also provide evidence that they exploit polarization down to an (average) polarization level of less than 7%, irrespective of whether the stimulus is homogeneous, such as under haze, or patched, such as a sky spotted by clouds. Our data demonstrate that crickets can rely on skylight polarization even under unfavorable celestial conditions, emphasizing the significance of polarized skylight orientation for insects.

Key words: skylight navigation, polarization vision, behavior, *Gryllus campestris*.

Introduction

The sky offers a variety of useful references for visual compass orientation. Celestial cues are effectively at infinity and thus their retinal position in a terrestrial observer does not shift with translational motions but only with rotations. Apart from the sun, the moon, the stars and intensity and spectral gradients, there is a prominent directional signal in the sky that is invisible to the human eye: the celestial polarization pattern. On its way through the atmosphere, sunlight is scattered by air molecules (Rayleigh scattering) and is thereby linearly polarized; i.e. the electric vector (e-vector) of light waves preferentially vibrates in one orientation. The proportion oscillating in the prevailing orientation is called the degree of (linear) polarization (*d*). Both the orientation of the e-vector (angle of polarization) and the degree of polarization depend on the scattering angle (the angle between incoming and outgoing rays). As a result, a pattern of polarized skylight is generated that is linked to the dominant light source illuminating the celestial hemisphere; i.e. the sun during the day and the moon at night (Coulson, 1988; Cronin et al., 2006; Gál et al., 2001; Horváth and Wehner, 1999; Strutt, 1871). In contrast to the sun and the moon, the polarization pattern has the advantage that it extends over the whole sky and therefore it is not shielded completely by scattered clouds or terrestrial objects. Other stray light parameters in the sky, such as the gradients of spectral composition and intensity, are highly susceptible to atmospheric disturbances. This is also true for the degree of polarization whereas the distribution of e-vector orientations is rather stable. Depending on illumination conditions, it can even continue underneath clouds, haze or under a canopy (Barta and Horváth, 2004; Brines and Gould, 1982; Können, 1985; Pomozi et al., 2001). The e-vector pattern thus provides a reliable reference for visual compass orientation or course control.

In crickets, as in many other insect species, a specialized, upward-directed region at the dorsal margin of the compound eye, the so-called dorsal rim area (DRA), is dedicated to polarization vision (Brunner and Labhart, 1987; Burghause, 1979; Labhart and Meyer, 1999). The photoreceptors of the cricket DRA are homochromatic, containing exclusively blue-absorbing visual pigment (λ_{max} ~440 nm), and are strongly sensitive to the e-vector of linearly polarized light. In each ommatidium, two sets of photoreceptors are tuned to mutually orthogonal e-vector orientations. Due to the absence of corneal faceting, missing screening pigment and wide rhabdoms, the visual fields of these ommatidia are substantially increased (half-width of average angular sensitivity ~20°) (Blum and Labhart, 2000; Burghause, 1979; Labhart et al., 1984; Nilsson et al., 1987; Ukhanov et al., 1996; Zufall et al., 1989).

Polarization-sensitive neurons (POL neurons) in the optic lobe are thought to represent the first processing layer in the polarization vision system of crickets. Their spiking activity is a sinusoidal function of e-vector orientation with a 180° period. POL neurons receive antagonistic input through two channels with orthogonal orientations of maximal e-vector sensitivity,

which are most likely represented by the two sets of photoreceptors in each ommatidium. The receptive fields of POL neurons are directed to the upper part of the sky and are extremely wide (>60°). This is the result of both optical integration by the photoreceptors and neural integration by the POL neurons, which collect input from about 200 DRA ommatidia (one-third of all dorsal rim ommatidia). POL neurons condition the e-vector information for further processing: as a consequence of the antagonistic input, the contrast of the polarization signal is enhanced and fluctuations in ambient light intensity are ineffective. Spatial integration increases the absolute sensitivity and causes the neurons to respond to the mean e-vector within their visual field rather than to structural details of the polarization pattern (Labhart, 1988; Labhart and Meyer, 2002; Labhart et al., 2001; Petzold, 2001).

Behaviorally, a spontaneous polarotactic response could be elicited by exposing crickets to a large, 100%-polarized stimulus from above (Brunner and Labhart, 1987; Burghause, 1979; Herzmann and Labhart, 1989). However, field crickets live on meadows where sky visibility is often restricted by surrounding vegetation to little more than the zenith. Furthermore, in the blue range of the spectrum, d does not exceed 75% in the upper part of the sky even under optimal conditions when the sun is low and the air is dry and clear (Coulson, 1988). In fact, field crickets are normally confronted with considerably lower zenithal d-values, since they are active around the clock (Rost and Honegger, 1987) and live in temperate regions (Zahradník, 2002), where haze and clouds are frequent. Yet, there is some evidence that they do indeed rely on skylight polarization when homing to their burrows in the ground (Beugnon and Campan, 1989).

In the present study, we have investigated cricket polarization vision in the laboratory under stimulus conditions mimicking those experienced by the animals in the field. We measured the strength of a spontaneous polarotactic response (Brunner and Labhart, 1987) and assessed the behavioral thresholds of polarization vision by varying stimulus size and degree of polarization. The data are discussed in the light of structural and physiological properties of insect polarization vision systems.

Materials and methods

Animals

Wild field crickets (*Gryllus campestris* L.) were collected near Zurich, Switzerland, as late-instar larvae or adults and kept indoors under long-day conditions (14 h:10 h light:dark cycle; L20W/10S daylight lamps; Osram, Munich, Germany) at 23°C and 60% relative humidity. For our experiments, we used both sexes after the imaginal molt.

Experimental setup

Our testing procedure was based upon the approach used by Brunner and Labhart (Brunner and Labhart, 1987). A small metal pin was attached to the pronotum of the crickets with wax. Therewith, they could be mounted to a balanced arm that kept them in a fixed position and orientation on a white, air-suspended Styrofoam™ ball (diameter 8 cm) with a regular pattern of 32 black dots (diameter 6.5 mm) on its surface (Fig. 1A). Translational and rotational walking movements of the cricket were conveyed to the ball and detected by two pairs of photodiodes that registered the dots on the ball passing by.

The ball protruded from a platform surrounded by a cylinder (inner diameter 19 cm), both painted in matt white. A slowly rotating turntable (1.8 ° s^{-1}) holding the visual stimuli was located 46 mm above the head of the cricket. The position of the turntable was registered by a counter that was reset every 360° by a reed switch to avoid error accumulation. A cone of light produced by a blue LED (Luxeon™ Star Royal Blue; Roithner Lasertechnik, Vienna, Austria; λ_{max}=455 nm, spectral half-width 20 nm) equipped with a collimator lens (Roithner Lasertechnik; beam width 30°) evenly illuminated a circular window (diameter 9.5 cm) in the center of the turntable.

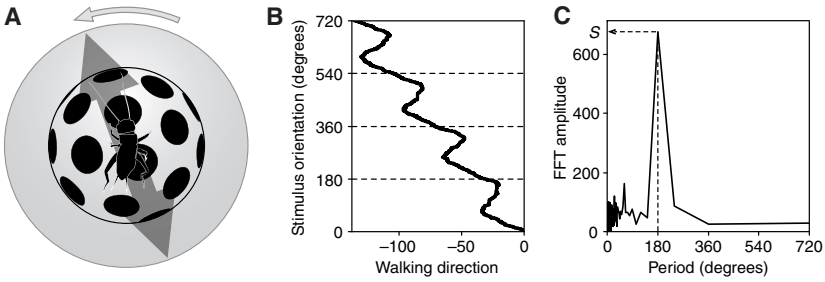

Fig. 1. Data recording and evaluation. (A) Top view of a cricket walking on a Styrofoam™ ball under a slowly rotating, polarized stimulus. The animal is kept on the spot by a balanced arm (not shown). Its walking movements are transferred to the ball and registered by detecting the moving dots on the surface of the ball. (B) Rotational movements of the cricket recorded during two full revolutions of the stimulus (4×180°). Abscissa: walking direction (rotational component of the run) given by the number of dots that passed the detector; positive and negative values indicate right and left turns, respectively. Ordinate: stimulus orientation. Provided that the translation (forward movement) of the cricket was constant, the resulting curve also reflects the virtual walking path. Note the bias in walking direction caused by the inherent turning tendency of the animal. (C) Fourier spectrum of turning speed per degree. Data shown in B were differentiated to remove the bias and then analyzed by a fast Fourier transform (FFT). Abscissa: period of modulation of walking direction. Ordinate: amplitude of FFT signal. Because of the 180° periodicity of the polarized signal, the amplitude at 180° (S) was taken as a measure of the strength of the polarotactic response.

Depending on the experiment, different insets were fitted into the window.

The signals encoding the position of the turntable and the walking movements of the cricket were sent to a computer and recorded by a custom-made program based on LabView software (National Instruments, Austin, TX, USA). To eliminate stray light of short wavelengths, the computer monitor was fitted with a yellow Plexiglas window.

Visual stimuli

In all experiments, the basic optical element ('polarization screen') consisted of a linear polarizer (HNP'B; Polaroid Corporation, Waltham, MA, USA) overlaid with a diffuser (two sheets of translucent drawing paper) (Fig. 2). It provided a strongly polarized stimulus (d=100%) of a diameter of 92°. For zero controls, this polarization screen was inverted, such that the animal faced the diffuser instead of the polarizer and was thus presented with an unpolarized stimulus (d=0%) of the same intensity.

Depending on the experiment, we combined the polarization screen with additional optical elements (see below).

Stimulus size: To examine the influence of stimulus size on the polarotactic performance of the crickets, the radius (r) of the stimulus was narrowed down stepwise from $2r$=92° to 1° by placing black cardboard annuli below the polarization screen (irradiance 4.0×10^{14} to 1.6×10^{11} quanta cm^{-2} s^{-1}).

Haze: To simulate a hazy sky we combined the polarization screen with an optical retarder (a quarter-wave plate made of overhead projector transparency film). This produced a uniform stimulus of an effective degree of linear polarization between 100% and 0% depending on the ellipticity of light. The ellipticity could be changed by adjusting the principal axis of the retarder relative to the transmission axis of the polarizer. For theoretical reasons, and as demonstrated experimentally, partially plane-polarized light and elliptically polarized light with the same d-value are equivalent for an insect photoreceptor (Labhart, 1996). To make sure that light rays reaching the cricket passed approximately perpendicular through the retarder, the size of the stimulus was limited to 25° (irradiance 6.5×10^{13} quanta cm^{-2} s^{-1}).

Clouds: We also tested the response of the animals to a large (92°) compound stimulus composed of a polarized centre (d=100%) and an unpolarized periphery (d=0%). This simulated an overcast sky with a window in the zenith. We reduced the mean degree of polarization ($\bar{d}$) progressively from 100% to 0% by placing diffuser annuli of different sizes (two sheets of translucent drawing paper with a central aperture) below the polarization screen. In order to avoid strong differences in light intensity, a circular diffuser equal in size to the central aperture was positioned on top of the polarization screen for apertures larger than 8.2°. For the same reason, an additional diffuser was placed below the inverted polarization screen in zero controls and above the polarization screen in motivation controls (irradiance range 2.2×10^{14} to 1.9×10^{14} quanta cm^{-2} s^{-1}).

Light intensities and degrees of polarization were determined by a radiometer (photodiode 222AUV with model 161 optometer; United Detector Technology, Santa Monica, CA,

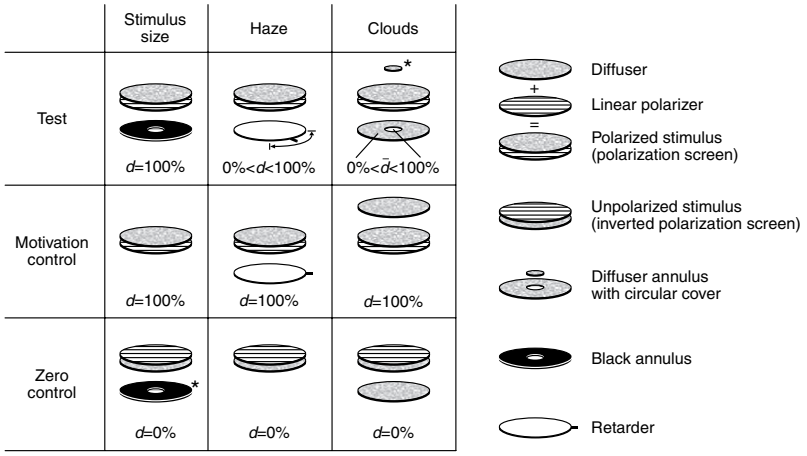

Fig. 2. Optical elements and their combinations for generating the visual stimuli. To produce polarized stimuli for tests and motivation controls, we used a linear polarizer overlaid with a diffuser, a combination termed 'polarization screen'. For the zero controls, the polarization screen was inverted, thus resulting in an unpolarized stimulus. Depending on the experiment, the polarization screen was combined with an additional diffuser, with an optical retarder or annuli consisting of opaque or diffusing material (for details see text). Note that the maximal diameter of the stimulus (not shown) was 92° for Stimulus size and Clouds experiments but 25° for the Haze experiment due to technical reasons. Elements marked with an asterisk were used under specific experimental conditions only. The resulting degree of polarization (d or $\bar{d}$) is indicated at the bottom of each table cell.

USA) at the position of the cricket head. For polarization measurements, the detector was fitted with a wideband blue filter (BG 28; Schott AG, Mainz, Germany) and a high-quality linear polarizer (HNP'B; Polaroid Corporation). The degree of polarization d for homogeneous stimuli (Haze) and $\tilde{d}$ for composed stimuli (Clouds) was calculated from the photometer signals (intensity I) as follows: d or $\tilde{d}=(I_{max}-I_{min})/(I_{max}+I_{min})$, with I_{max} and I_{min} being the mean values of the two maximal and the two minimal intensities recorded during a full rotation (360°) of the turntable.

Testing procedure

All three experiments (Stimulus size, Haze, Clouds) were carried out in a darkroom at 24–28°C and 45–60% relative humidity. A single run (recording of walking movements) lasted for 400 s. During this time, the turntable completed two full revolutions, i.e. each e-vector orientation (if present) occurred four times because of the 180° periodicity of the linear polarizer. A series of runs (recordings from one individual for all different conditions of an experiment) included tests, zero controls (runs under an unpolarized stimulus) and motivation controls (runs under a large or medium-sized, 100%-polarized stimulus). Depending on the experiment, either every single test run (Clouds) or each complete series recorded in one session (Stimulus size, Haze) was preceded and followed by a motivation control. Stimulus transitions were smooth, in order not to startle the walking cricket, and took just a few seconds.

Data evaluation

Recordings were analyzed by custom-made programs in MATLAB® (The MathWorks, Natick, MA, USA). For each run, we calculated a value S, which quantifies the strength of the behavioral response to polarized light by taking the amplitude and the regularity of periodic changes in walking direction into account. Several measures have previously been used for this purpose (Brunner and Labhart, 1987; Herzmann and Labhart, 1989; Mappes and Homberg, 2004; von Philipsborn and Labhart, 1990). They were derived empirically and were defined in a slightly different way depending on the aim of the study. Our approach is based on the theoretical consideration that the behavioral data must show a periodicity of 180°. Developed in our laboratory, this idea was also taken up for recent experiments on locust orientation (Mappes and Homberg, 2007). We calculated the measure S in two steps: (1) a differentiation and (2) a Fourier transformation. (1) From the raw data (stimulus orientation and walking direction) (Fig. 1B), we computed the change in walking direction as a function of stimulus orientation, i.e. turning speed per degree. This differentiation step removes a generally observed linear offset (bias) in the raw data caused by a directional preference of the animal (see Fig. 1B). (2) After differentiation, the data were analyzed by a fast Fourier transformation (FFT). Given the 180° periodicity of the polarization signal, any responses to it should occur with a periodicity of 180°. Hence, we took the amplitude of the 180° component in the Fourier spectrum as a measure of the polarotactic response of the cricket. This value was called S (strength of response) (Fig. 1C).

If S was >200 and at least 2.5 times the mean of the amplitudes at 120° and 240°, a motivation control was regarded as positive (clear polarotactic response present). No signals are expected at 120° nor at 240°, and therefore the corresponding FFT amplitudes were chosen as references reflecting the strength of random noise in the Fourier spectrum.

Previous behavioral studies have shown that the readiness of the crickets to walk and to respond to polarized light varies considerably in the behavioral assay employed (Brunner and Labhart, 1987; Herzmann and Labhart, 1989). Data were therefore analyzed only if they met the following criteria: (1) The animal walked without interruption for at least three of the four 180° periods of a run and (2) a clear response to polarized light was present in both the preceding and the following motivation control. For statistical evaluations, we also corrected for daily or individual differences in responsiveness of the crickets by determining the strength of the polarotactic response relative to the mean response strength in the two motivation controls (S/S_{mot}). Unless mentioned otherwise, the statistics rely on Wilcoxon signed rank tests for Stimulus size and Haze experiments, and on Mann–Whitney tests for the Clouds experiment. Significance levels were corrected for multiple comparisons by Bonferroni-Holm.

Results

Motivation

In Stimulus size and Haze experiments, an entire test series with a positive motivation control at the beginning and at the end had to be recorded from an individual in one session. This implied that the cricket had to walk for at least 1–2 hours without interruption. Animals that accomplished this task showed no reduction in the strength of their polarotactic response in spite of the long walking time: responses in the first and last positive motivation control did not differ significantly from each other (P=0.93 and 0.44; compare gray triangles and diamonds in Fig. 3B and Fig. 4B, respectively). Two good performers actually kept on responding to the polarized light stimulus for over 8 h and were finally stopped by the experimenter. However, most of the individuals did not walk and respond continuously over an extended period of time (see also Brunner and Labhart, 1987; Herzmann and Labhart, 1989); in our study, 87% of the crickets never completed a series within one session and all of their data had to be discarded. For the Clouds experiment, we therefore adopted another testing protocol. We subjected the crickets to a motivation control before and after every single test run. Thus, all data recorded up to the last positive motivation control could be evaluated.

Stimulus size

In sun-exposed meadows, which is the preferred habitat of field crickets, sky visibility can be restricted by terrestrial objects, e.g. by grass and flowers (Fig. 3A), bushes or trees. To examine the influence of stimulus size on the polarotactic orientation behavior, we stepwise reduced the radius r of a strongly polarized stimulus (d=100%) presented at the zenith. For each individual, a complete series of runs was recorded in one session. If two or more series could be measured from the same individual (four cases), they were averaged to avoid a bias caused by multiple contribution of one individual to the data. The results from 11 individuals (16 series) are plotted in Fig. 3B–D. Test data ($2r$=48° to 1°; d=100%) are indicated by

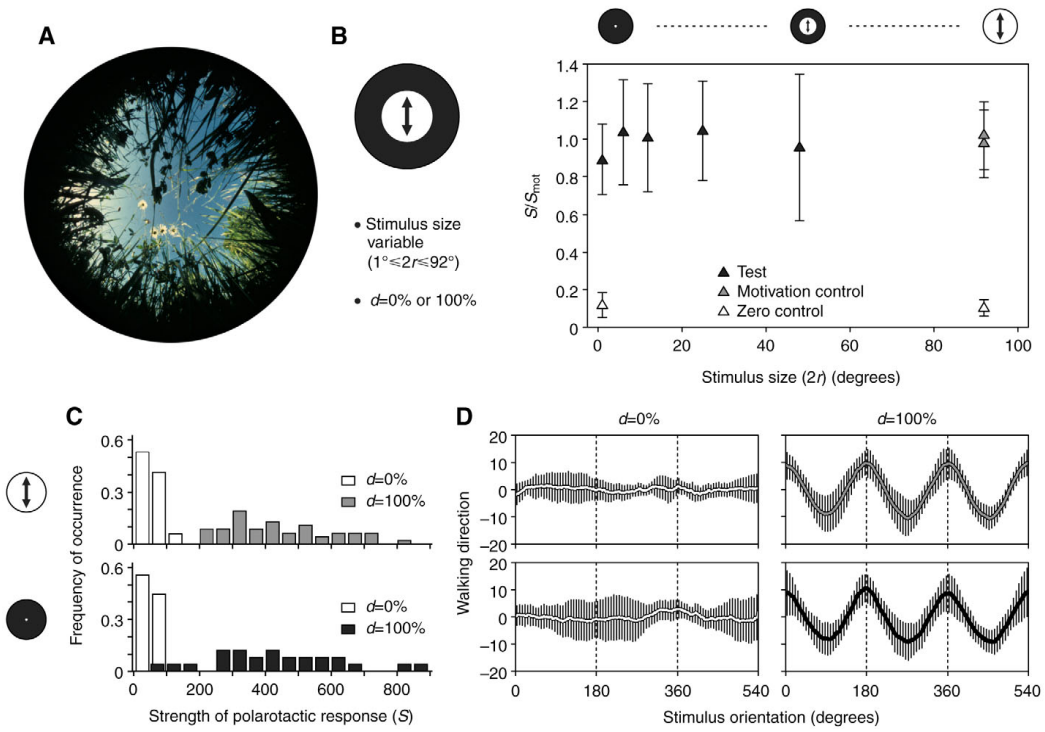

Fig. 3. Stimulus size experiment. (A) 180° fisheye view of the celestial hemisphere taken by a camera positioned in a meadow. A considerable part of the sky is obstructed by vegetation. (B–D) Polarotactic response as a function of stimulus size. The radius (r) of a zenithal stimulus was reduced from $2r$=92° to 1° with a degree of polarization (d) of either 100% or 0%. Tests ($2r$=1° to 48°, d=100%) are indicated by black, motivation controls ($2r$=92°, d=100%) by gray, and zero controls ($2r$=1° or 92°, d=0%) by white (16 series of 11 individuals). (B) Survey of results. The relative strength of the polarotactic response (S/S_{mot}, mean ± s.d.) is plotted against stimulus size. (C,D) Comparison between the largest (92°, top row) and the smallest (1°, bottom row) stimulus. (C) Distribution of S-values. (D) Walking direction of the crickets given by the number of dots that passed the detector (mean ± s.d.; positive and negative values indicate right and left turns, respectively) plotted *versus* stimulus orientation. Prior to averaging, data were standardized, i.e. the runs were phase-adjusted and corrected for an overall deviation from a straight walking path by subtraction of the inherent turning tendency. Note: a reduction in stimulus size to a diameter as low as 1° did not impair the polarotactic response.

black, motivation controls ($2r$=92°; d=100%) by gray, and zero controls ($2r$=92° or 1°; d=0%) by white (triangles in Fig. 3B, columns in Fig. 3C, lines in Fig. 3D).

Fig. 3B summarizes the relative strength of the polarotactic response (S/S_{mot}; mean ± s.d.) under all experimental conditions. A reduction of stimulus size down to $2r$=1° did not significantly influence the strength of the polarotactic response (P=0.41; Friedman test; see black triangles in Fig. 3B). However, for identical stimulus sizes, the response values dropped significantly if the degree of polarization was lowered to 0% (P<0.01 for $2r$=92° or 1°; see white triangles in Fig. 3B).

This overall behavior is further elucidated by the following details: Fig. 3C depicts the distribution of S-values (absolute strength of polarotactic response given by the amplitude of the 180° component in the Fourier spectrum) measured for the largest ($2r$=92°, upper diagram) and the smallest ($2r$=1°, lower diagram) stimulus. In spite of the discrepancy in stimulus size, the results are very similar. In both situations, the S-values for unpolarized (d=0%, white columns) and polarized light (d=100%, gray or black columns) differ clearly. For unpolarized light, S-values do not exceed 150, whereas for polarized light they are broadly distributed between 50 and 900, with two-thirds of all data between 300 and 650. S-values for the test situation (black columns) scatter slightly more than for the motivation controls (gray columns) as a consequence of our evaluation criteria: motivation controls had to be positive (clear polarotactic response present), otherwise the whole series was discarded, but for the tests no such screening took place. In Fig. 3D, the walking direction of the crickets (mean ± s.d.) is plotted *versus* stimulus orientation for the largest ($2r$=92°, top row) and the smallest ($2r$=1°, bottom row) stimulus. Before averaging, data had to be standardized. The runs were therefore

corrected for an overall deviation from a straight walking path by subtraction of the inherent turning tendency and phase-adjusted if the *S*-value was higher than the 99% quantile of the zero control, i.e. if the presence of a polarotactic response was likely. For constant forward translation of the cricket, the curves in Fig. 3D can also be considered as normalized walking paths.

It is evident that the polarotactic response is not impaired if stimulus size is reduced from 92° to 1°: independent of stimulus size, the crickets' walking direction changes periodically with stimulus orientation for high *d*-values following a sinusoidal function (right column). Only under unpolarized light does this modulation of walking direction disappear (left column).

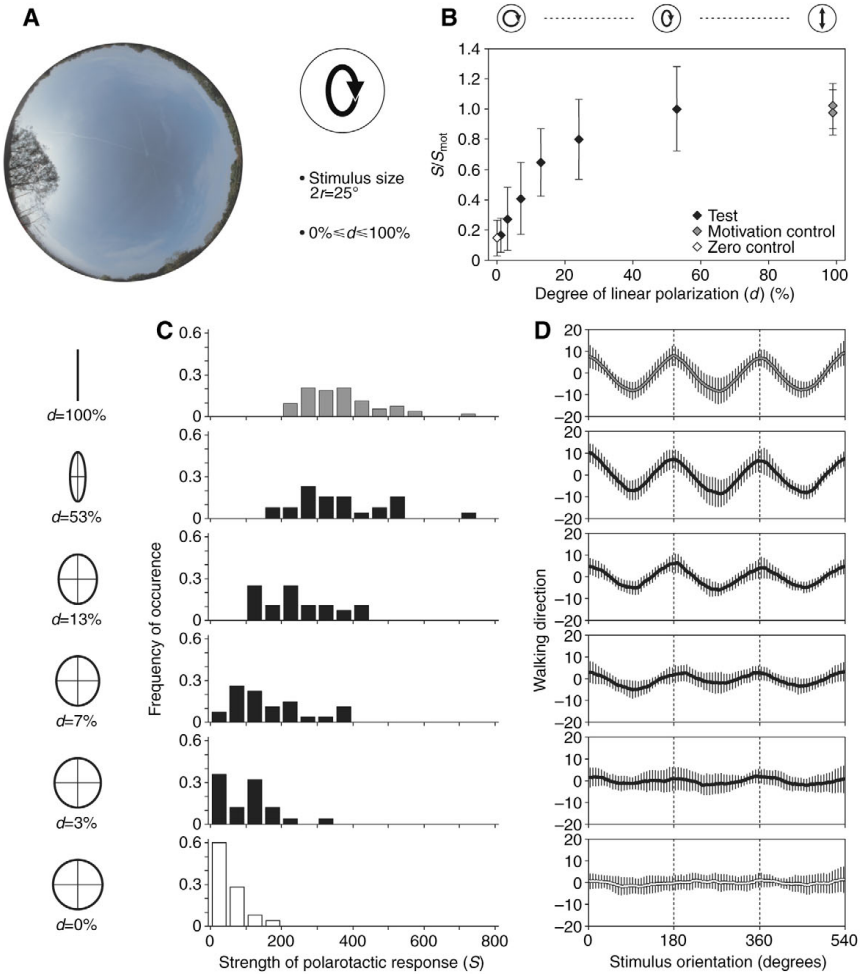

Fig. 4. Haze experiment. (A) 180° fisheye view of the celestial hemisphere on a hazy morning. Compared with clear atmospheric conditions, the degree of polarization across the whole sky is reduced. (B,C) Polarotactic response as a function of the degree of polarization for a uniform stimulus. The effective degree of linear polarization (*d*) of a medium-sized (25°) zenithal stimulus was reduced from *d*=100% to 0% by changing the ellipticity of light (see Materials and methods). Test data (*d*=1% to 53%) are indicated by black, motivation controls (*d*=100%) by gray, and zero controls (*d*=0%) by white (24 series of 17 individuals). (B) Survey of results. Relative strength of the polarotactic response (S/S_{mot}; mean ± s.d.) plotted against the effective degree of linear polarization. (C) Distribution of *S*-values and (D) modulation of walking direction with stimulus orientation for some of the polarization levels tested (see polarization ellipses to the left). Data in D are normalized and plotted as described in Fig. 3D. Note: a reduction in polarization to *d*=53% did not impair the polarotactic response. With lower *d*-levels, the response strength decreased. However, there was a statistically significant orientation to polarized light at least down to a *d*-level of 7% ($P<0.01$).

Haze

From the perspective of a field cricket in a meadow, the zenith is the part of the sky that is most often free of terrestrial objects (Fig. 3A) and that is therefore available for orientation. However, according to the law of Rayleigh scattering, the higher the solar elevation the lower the degree of polarization becomes in the zenith. Even at low solar elevations, which would allow high degrees of polarization in the zenith, d can be substantially reduced by the presence of haze (Fig. 4A). With this natural situation in mind, we investigated the polarotactic performance of crickets under a medium-sized ($2r$=25°) zenithal stimulus for which the degree of polarization was gradually lowered from 100% to 0% by changing the ellipticity of light. Data acquisition and evaluation were as described for Stimulus size. The results from 17 individuals (24 series) are plotted in Fig. 4B–D. Again, test data (d=1% to 53%) are indicated in black, motivation controls (d=100%) in gray, and zero controls (d=0%) in white (diamonds in Fig. 4B, columns in Fig. 4C, lines in Fig. 4D).

Fig. 4B resumes the relative strength of the polarotactic response (S/S_{mot}; mean ± s.d.) for all conditions investigated in this experiment. A reduction in polarization level to 53% had no significant effect on the strength of the polarotactic response (P=0.83). With lower degrees of polarization, response values declined (P<0.01 for d≤24%), but a significant difference to the zero control (white diamond) was present at least down to d=7% (P<0.01). For d=3% the response values were also still higher than those of the zero control (P=0.044); however, this distinction was not significant after a Bonferroni-Holm correction for multiple comparisons.

More details are given in Fig. 4C,D. Fig. 4C shows the distribution of S-values, and Fig. 4D illustrates the modulation of walking direction with stimulus orientation for some of the polarization levels tested. The respective d-values are depicted by polarization ellipses to the left. With lower degrees of polarization, the distribution of S-values (Fig. 4C) gradually shifts towards the distribution of the zero control (bottom row). S-values decline since the modulation of walking direction (Fig. 4D) decreases in both amplitude and precision: maxima, for instance, become less prominent and do not occur every 180° at exactly the same stimulus orientation any more. Note again that a reduction in d to ~50% does not reduce the response (compare the first and second rows). Furthermore, a sinusoidal modulation with a periodicity of 180° is clearly present down to d=7% and is even faintly visible in the averaged run data for d=3%. Two of the 17 individuals tested under d=3% actually responded strongly (for an example, see Fig. 5); their runs even satisfied the strict criteria of positive motivation controls (see Materials and methods).

Clouds

Besides terrestrial objects, clouds can also obstruct parts of the celestial polarization pattern (Fig. 6A). In contrast to an opaque obstacle such as a tree, a cloud is often translucent. However, light passing through or reflected by a cloud is partly or totally unpolarized (Können, 1985). Together with the polarized light coming from areas of blue sky or from the air column between a cloud and the observer (Brines and Gould, 1982; Pomozi et al., 2001; Stockhammer, 1959), this results in a decrease of the overall degree of skylight polarization. We simulated such a situation by presenting a large ($2r$=92°) zenithal stimulus consisting of a strongly polarized centre (d=100%) and an unpolarized periphery (d=0%). By varying the ratio of the two components, we changed the mean degree of polarization ($\bar{d}$).

Results from 12 individuals are shown in Fig. 6B. Test data ($\bar{d}$=1% to 74%, number of runs N=17–19) are indicated by black, motivation controls ($\bar{d}$=100%, N=162) by gray, and zero controls ($\bar{d}$=0%, N=17) by white. The relative strength of the polarotactic response (S/S_{mot}; mean ± s.d.) is plotted against the mean degree of polarization for all conditions investigated. A reduction of $\bar{d}$ to 49% did not impair the polarotactic response of the crickets significantly (P=0.83). Below 17% polarization, response values declined (P<0.01). However, a significant difference to the zero control (white square) was present at least down to $\bar{d}$=10% (P<0.01). At $\bar{d}$=5% the polarotactic response was lost (P=0.30).

Fig. 7 compares the data of the two experiments in which the degree of polarization was gradually reduced; the relative strength of the polarotactic response (S/S_{mot}, mean ± s.d.) is plotted against the degree of linear polarization for the uniform stimulus simulating haze (black diamonds) and the compound stimulus simulating clouds (white squares). The results of the two experiments basically agree, indicating that the cricket polarization vision system is insensitive to the spatial structure of a polarized stimulus. In both cases, the mean strength of the orientation response to polarized light is a nonlinear function of d, with decreasing slope, closely resembling a root function (root index=2.75; R^2=0.92 for Haze and 0.86 for Clouds).

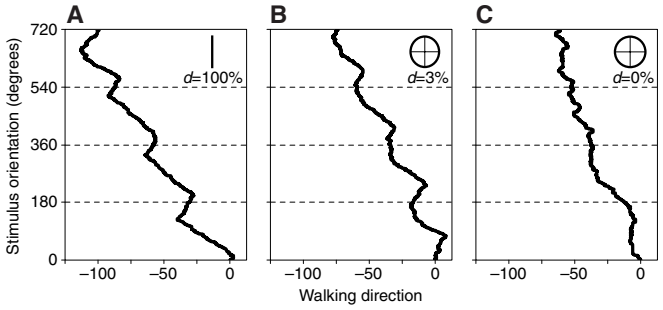

Fig. 5. Polarotactic behavior of an especially sensitive cricket under uniform stimuli of different degrees of polarization (d). (A–C) Rotational movements with d=100%, 3% and 0%, respectively (see polarization ellipses in the diagrams). Abscissa: walking direction (rotational component of the run) given by the number of dots on the ball that passed the detector; positive and negative values indicate right and left turns, respectively. Ordinate: stimulus orientation. Note that the periodic modulation of walking direction is almost as strong for 3% as for 100% polarization.

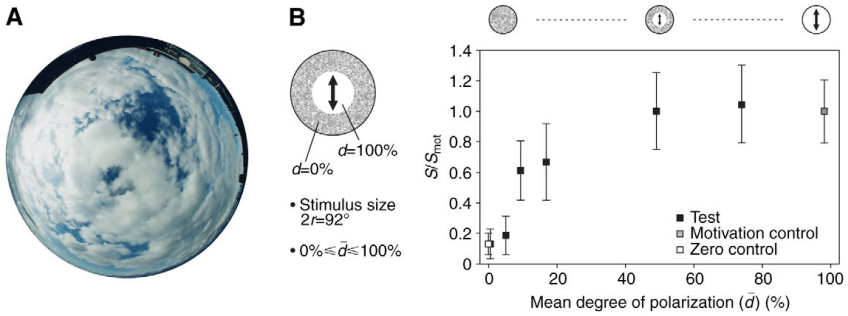

Fig. 6. Clouds experiment. (A) 180° fisheye view of the celestial hemisphere on a cloudy day. The mean degree of polarization is reduced since polarized light from patches of blue sky mixes with partly or totally unpolarized light from clouded sky regions. (B) Polarotactic response as a function of the mean degree of polarization ($\bar{d}$) for a compound stimulus. For a wide (92°) zenithal stimulus, $\bar{d}$ was reduced from 100% to 0% by changing the proportion of polarized to unpolarized light. Data are from 12 individuals. Tests are indicated by black symbols ($\bar{d}$=1% to 74%, N=17–19), motivation controls by gray symbols ($\bar{d}$=100%, N=162) and zero controls by white symbols ($\bar{d}$=0%, N=17). Note: a reduction in polarization to $\bar{d}$=49% did not impair the polarotactic response. With lower degrees of polarization, response values declined, but the orientation to polarized light was statistically significant at least down to a $\bar{d}$-level of 10% (P<0.01).

Discussion

Stimulus size

We have shown that field crickets clearly respond to a strongly polarized light stimulus in the zenith even if its size is reduced to just 1°. In the compound eye of adult field crickets, the DRA comprises ~600 upward-directed ommatidia and is 13–17 rows wide (Blum and Labhart, 2000; Brunner and Labhart, 1987; Labhart, 1988). The sampling frequency of the DRA is about one ommatidium per degree, the ommatidia have large acceptance angles of approximately 20° (Blum and Labhart, 2000), and both on- and off-axial polarization sensitivities are strong (Labhart et al., 1984). On the basis of these properties, we estimate that a 1° stimulus in the zenith stimulates at least one-third of all DRA ommatidia.

In our experiment, light intensity decreased with stimulus size. For a single photoreceptor in the cricket DRA, the threshold intensity for a reliable response to polarized light is in the order of 10^{10} quanta cm^{-2} s^{-1} (Labhart et al., 2001), which is about 10 times lower than the irradiance of our 1° stimulus. However, because of neural integration and polarization antagonism, POL neurons in the optic lobe show significant (half-maximal) responses at 10^{7} quanta cm^{-2} s^{-1} already (Labhart et al., 2001). Behavioral experiments yielded a similar threshold (Herzmann and Labhart, 1989). The intensity of our 1° stimulus was therefore approximately 10^{4} times higher than the threshold intensity of the cricket e-vector detection system.

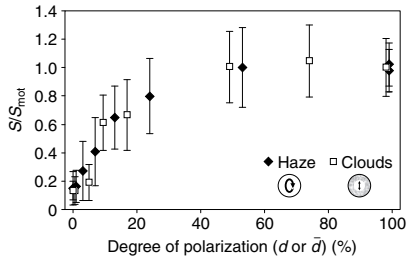

Fig. 7. Comparison between the Haze and Clouds experiments. The relative strength of the polarotactic response (S/S_{mot}; mean ± s.d.) is plotted against the degree of linear polarization (d or $\bar{d}$) for a uniform (black diamonds) and a compound stimulus (white squares). Note: the results are basically the same under both stimulus conditions.

For crickets walking in a meadow, the view of the sky is restricted by grass blades and other leaves. Could unpolarized light transmitted by leaves interfere with polarized skylight? Since chlorophyll strongly absorbs in the blue spectral range, the vegetation will appear dark against the blue sky for the blue-sensitive photoreceptors in the cricket DRA, and light stimulating the DRA will mostly be skylight. Hence, our experimental situation compares well with field conditions. Our data suggest that crickets are able to exploit even a minute patch of sky visible through dense vegetation given that the degree of polarization in this particular celestial spot is high enough.

There are but a few systematic studies on the minimum visual angle necessary for polarization vision in other insects. Data that are directly comparable to ours only exist for honey bees (*Apis mellifera*) (Edrich and von Helversen, 1976). The spatial threshold of polarization vision was tested by observing the waggle dances of foragers indicating the direction of a previously visited feeding site to hive mates on a horizontal comb. A strongly polarized light spot of variable size was presented at the zenith. Taking the scatter in the direction of waggle dances as an inverse measure for the degree of orientation, the conclusion was that the bees were able to orient by means of a polarized light stimulus of less than 1°. However, in contrast to crickets, the performance of the bees markedly decreased with stimulus size. Edrich and von Helversen suggested that the decreasing performance of the bees was primarily due to the decline in light intensity and was not caused by the small size of the stimulus (Edrich and von Helversen,

1976). The polarization vision system of the strictly day-flying honey bees is 10^3–10^4 times less sensitive than that of field crickets (Herzmann and Labhart, 1989; von Helversen and Edrich, 1974), insects that are active by day and by night (Rost and Honegger, 1987). Furthermore, there is an essential difference in the dioptric design of the eye; as in crickets, the optics of the honey bee DRA is degraded. Although the corneal lenses are clear in the centre, they contain light-scattering pore canals at the margins (Meyer and Labhart, 1981). As a consequence, the angular sensitivity functions of the photoreceptors show a relatively narrow peak in the centre (average half-width ~5.5°) and a wide, flat brim in the periphery in which light sensitivity decreases only slowly (Labhart, 1980). The e-vector sensitivity of the UV receptors (mediating polarization vision in bees) is high even 20–30° off axis (Labhart, 1980). Assuming an inter-ommatidial angle of about 3° (Edrich and von Helversen, 1976), we conclude that at adequate light intensities a polarized 1° stimulus at the zenith stimulates a large fraction of the approximately 140 DRA ommatidia of the bee (Sommer, 1979). However, the light sensitivity of the DRA photoreceptors decreases sharply within a few degrees from the optical axis. For small stimuli, which tend to produce weak irradiances at the eye, the number of ommatidia delivering reliable information is therefore considerably reduced. In *Megalopta genalis*, a nocturnal bee featuring a DRA with corneal structures similar to those of the honey bee, angular sensitivity functions of photoreceptors are much broader (average half-width ~13.8°) probably due to the 6–7 times wider diameter of the rhabdom (Greiner et al., 2007).

Other studies on the influence of stimulus size on polarized light orientation in honey bees and desert ants (*Cataglyphis bicolor*) were designed to assess the size requirements for correct celestial e-vector navigation rather than the threshold for e-vector detection. Bees or ants were trained to a food source under the unrestricted natural sky and were tested under small windows admitting either skylight or artificially polarized light (Duelli, 1975; von Frisch, 1965; Zolotov and Frantsevich, 1973). In contrast to the previous bee study (Edrich and von Helversen, 1976), the performance of the animal was not measured by the degree of orientation but by the deviation of the observed dance or walking direction from the trained direction. The minimal extension of the celestial e-vector pattern necessary for compass navigation was 10–15° for honey bees (von Frisch, 1965; Zolotov and Frantsevich, 1973) and ~10° for desert ants (Duelli, 1975). It is difficult to compare these results to ours for the following reasons: The position of the stimulus in the visual field, its degree of polarization and its e-vector composition changed in the experiments. Studies on the rules applied by navigating insects have revealed that bees and ants rely on a rather generalized representation of the e-vector pattern in the sky (Brines and Gould, 1979; Fent, 1986; Rossel et al., 1978). This can cause navigational errors if the view on the celestial hemisphere differs for training and test situations. Under natural conditions, a dramatic change of sky visibility between an outgoing and an incoming run of a foraging desert ant will hardly ever occur. For the recruitment dances of honey bees, modifications do not matter as long as all workers interpret mistakes consistently. The results of the navigation studies mentioned above do therefore neither specify the lower limit of e-vector detection nor do they necessarily give the relevant spatial threshold in nature.

A systematic investigation on the minimal visual angle necessary for polarization vision would be particularly desirable for ants. In none of the ants investigated so far was the optics of the DRA degraded (Labhart and Meyer, 1999); in *C. bicolor* the acceptance angle (5.5°) (Labhart, 1986) is slightly smaller than the interommatidial angle (6°) (Zollikofer, 1981; Zollikofer et al., 1995), meaning that the visual fields are relatively narrow and separate. A 1° stimulus will thus stimulate just a few ommatidia. Therefore, spatial integration by POL neurons in the optic lobe of *Cataglyphis* must be based on neural integration alone (Labhart, 2000), and stimulus size may play an important role in *Cataglyphis* ants.

Haze and clouds

We have investigated the influence of the degree of polarization (d) on the polarotactic behavior of field crickets under two conditions: a uniform and a compound light stimulus presented at the zenith simulating a hazy and a cloudy sky, respectively. For both experiments, we obtained basically the same results (see Fig. 7). Considering the strong spatial integration by the e-vector detection system of the cricket, this is not surprising; since the celestial polarization signal is averaged by optical and neural mechanisms over a large area of sky (Labhart et al., 2001), it is irrelevant if a certain degree of polarization results from a mixture of polarized and unpolarized light as under a partly clouded sky or from an overall reduced degree of polarization as under a uniform haze cover.

Our data show that a zenithal stimulus with an astonishingly low d-value suffices for a field cricket to orient. Statistically, the behavioral threshold is located between 5% and 7% polarization, but two individuals even responded at 3% polarization (see Fig. 5). Electrophysiological recordings have demonstrated that POL neurons can signal e-vector information down to d-levels of ~5% (Labhart, 1996), which corresponds fairly well to the behavioral threshold. As previously noticed for the intensity threshold of polarization vision (Herzmann and Labhart, 1989; Petzold and Labhart, 1993), there is a close correlation between the absolute sensitivity of the POL neurons and the one for the whole organism.

Due to a presumed feedback mechanism, the response strength of polarization-sensitive neurons in the central complex of crickets is independent of d, at least down to d=18% (M. Sakura, personal communication). The same is true for the polarotactic behavior of crickets but only down to 50% polarization. Between 50% and 20% polarization, the behavioral response decreases only slightly although to a statistically significant degree. The slight divergence between electrophysiology and behavior may be explained by the following argument: while the signaling intensity remains constant, the signaling precision of central complex neurons at low d-values may be reduced, explaining the reduction in the behavioral performance.

In the field, crickets are frequently facing low degrees of polarization. Although under optimal conditions the degree of polarization measured in small patches of sky can reach 75% in the blue range of the spectrum (Coulson, 1988), spatial

integration by the POL neurons over a large area of sky results in a considerably lower maximally experienced *d*-level (Labhart, 1999). This is because both e-vector orientation and degree of polarization vary across the sky (Coulson, 1988). Mean degrees of polarization in a celestial window similar in size to the visual field of cricket POL neurons reach 51–60% at most (Horváth and Wehner, 1999; Labhart, 1999; Lambrinos et al., 1997). Due to haze and clouds, and for high solar elevations, *d*-levels are often further reduced (Brines and Gould, 1982; Labhart, 1999; Pomozi et al., 2001). Measurements with an opto-electronic model of a cricket POL neuron under a variety of celestial conditions yielded *d*-levels of only 13% and 28% (medians) in the solar and anti-solar part of the sky, respectively (Labhart, 1999). Thus, the low detection threshold of the cricket polarization vision system is certainly justified. To be useful, weak celestial polarization signals must contain reliable directional information, i.e. they should indicate the same e-vector orientation as in clear skies. Measurements with the opto-electronic POL neuron model revealed that the precision of the directional signal in the sky was indeed high even under strong disturbances by clouds as long as the *d*-level was $\geq$5% (Labhart, 1999).

Concerning other insect species, the minimal *d*-level for polarization vision has only been investigated systematically in honey bees. By qualitative observations of dancing bees under a patch of blue sky, von Frisch determined a behavioral threshold of *d*~10% with a 'transition range' between 7% and 15% polarization (von Frisch, 1965). Quantitative measurements by Edrich and von Helversen under a zenithal polarized stimulus confirmed that bees can orient by a 10% stimulus (Edrich and von Helversen, 1987): lower *d*-values were not tested. However, it seems doubtful that honey bees, with their elaborate navigation system, are less polarization sensitive than crickets. We rather assume that differences in the testing procedure and evaluation method are responsible for the slightly higher threshold determined in bees.

Conclusions

Polarization vision in field crickets is an extremely sensitive and robust sensory system. It can deal with very low light intensities (Herzmann and Labhart, 1989; Labhart et al., 2001), low degrees of polarization (present study) and very small stimulus sizes (present study). Previous experiments have shown that crickets respond to polarized light at intensities that are even lower than the effective quantum flux under the clear, moonless night sky (Herzmann and Labhart, 1989). Here, we provide evidence that crickets exploit polarized stimuli down to *d*<7%, which implies that skylight is useful for e-vector orientation even under unfavorable meteorological conditions or at high solar elevations (Pomozi et al., 2001). We also demonstrate that crickets are able to rely on a tiny spot of polarized light simulating a minute patch of sky visible through dense vegetation. In fact, our data suggest that, as a result of spatial integration (Labhart et al., 2001), there is no threshold concerning stimulus size at all, provided that the light intensity and the degree of polarization are high enough.

Crickets sitting in a meadow may often experience a combination of unfavorable stimulus conditions, such as a restricted view of the sky along with a low *d*-level. How does this affect the orientation performance? We believe that the minimal *d*-level for e-vector detection does not depend on stimulus size since a reduced stimulus size in itself does not make e-vector detection more difficult for a cricket (Fig. 3). The following findings support this view: although stimulus size in the Haze (25°) and Clouds (92°) experiments differed considerably, the strength of the polarotactic response was basically the same for a given degree of polarization, including the threshold level. This seems to be true for honey bees as well. When tested under a stimulus of 4.7° (Edrich and von Helversen, 1987), the bees did not show a higher threshold for the degree of polarization than under a 15° stimulus (von Frisch, 1965). In another study, the polarotactic orientation of bees under a variety of stimulus sizes did not improve noticeably if the degree of polarization was increased from 30–40% to 90% (Zolotov and Frantsevich, 1973). Thus, at least in crickets and bees, stimulus size and *d*-level do not seem to interfere with each other.

A reduction in stimulus size is usually accompanied by a decline in light intensity. However, the polarotactic response of crickets was previously found to be intensity independent above a critical light level (Herzmann and Labhart, 1989). This is based on the polarization-opponent properties of the POL neurons in the optic lobe (Labhart, 1988), by which information on light intensity is filtered out. We therefore propose that, above a critical level, light intensity has no influence on the threshold of the degree of polarization.

When haze, clouds or terrestrial obstacles reduce sky visibility, orientation by polarized skylight outplays orientation by the sun. Such situations might have driven the evolution of sensory systems for detecting skylight polarization and it therefore makes sense that the e-vector detection system of crickets can deal with low *d*-levels and spatially restricted stimuli.

List of abbreviations

d	degree of polarization (%), polarization level
$\bar{d}$	mean degree of polarization (%), polarization level
DRA	dorsal rim area
e-vector	electric vector of light
FFT	fast Fourier transform
N	number of runs
r	radius
S	strength of behavioral response to polarized light
S_{mot}	mean strength of response in motivation controls
POL neuron	polarization-sensitive neuron in the cricket optic lobe

We thank Franziska Baumann for assistance with the crickets, Hansjörg Baumann and Helmut Heise for technical support, Dr Stefan Schuster for advice on the evaluation method, Drs Lorenz Gygax and Adrian Roellin for statistical consulting and Dr Midori Sakura, Tobias Seidl and Martin Kohler for valuable discussions throughout the project. This research was supported by a grant of the 'Studienstiftung des Deutschen Volkes' to M.J.H.

References

Barta, A. and Horváth, G. (2004). Why is it advantageous for animals to detect celestial polarization in the ultraviolet? Skylight polarization under clouds and canopies is strongest in the UV. *J. Theor. Biol.* **226**, 429-437.

Beugnon, G. and Campan, R. (1989). Homing in the field cricket, *Gryllus campestris*. *J. Insect Behav.* **2**, 187-198.

Blum, M. and Labhart, T. (2000). Photoreceptor visual fields, ommatidial array, and receptor axon projections in the polarisation-sensitive dorsal rim area of the cricket compound eye. *J. Comp. Physiol. A* **186**, 119-128.

Brines, M. L. and Gould, J. L. (1979). Bees have rules. *Science* **206**, 571-573.

Brines, M. L. and Gould, J. L. (1982). Skylight polarization patterns and animal orientation. *J. Exp. Biol.* **96**, 69-91.

Brunner, D. and Labhart, T. (1987). Behavioural evidence for polarization vision in crickets. *Physiol. Entomol.* **12**, 1-10.

Burghause, F. M. H. R. (1979). Die strukturelle Spezialisierung des dorsalen Augenteils der Grillen (Orthoptera, Grylloidea). *Zool. Jb. Physiol.* **83**, 502-525.

Coulson, K. L. (1988). *Polarization and Intensity of Light in the Atmosphere*. Hampton: A. Deepak Publishing.

Cronin, T. W., Warrant, E. J. and Greiner, B. (2006). Celestial polarization patterns during twilight. *Appl. Opt.* **45**, 5582-5589.

Duelli, P. (1975). A fovea for e-vector orientation in the eye of *Cataglyphis bicolor* (Formicidae, Hymenoptera). *J. Comp. Physiol.* **102**, 43-56.

Edrich, W. and von Helversen, O. (1976). Polarized light orientation of the honey bee: the minimum visual angle. *J. Comp. Physiol. A* **109**, 309-314.

Edrich, W. and von Helversen, O. (1987). Polarized light orientation in honey bees: is time a component in sampling? *Biol. Cybern.* **56**, 89-96.

Fent, K. (1986). Polarized skylight orientation in the desert ant *Cataglyphis*. *J. Comp. Physiol. A* **158**, 145-150.

Gál, J., Horváth, G., Barta, A. and Wehner, R. (2001). Polarization of the moonlit clear night sky measured by full-sky imaging polarimetry at full moon: comparison of the polarization of moonlit and sunlit skies. *J. Geophys. Res. D* **106**, 22647-22653.

Greiner, B., Cronin, T. W., Ribi, W. A., Wcislo, W. T. and Warrant, E. J. (2007). Anatomical and physiological evidence for polarisation vision in the nocturnal bee *Megalopta genalis*. *J. Comp. Physiol. A* **193**, 591-600.

Herzmann, D. and Labhart, T. (1989). Spectral sensitivity and absolute threshold of polarization vision in crickets: a behavioral study. *J. Comp. Physiol. A* **165**, 315-319.

Horváth, G. and Wehner, R. (1999). Skylight polarization as perceived by desert ants and measured by video polarimetry. *J. Comp. Physiol. A* **184**, 1-7.

Können, G. P. (1985). *Polarized Light in Nature*. Cambridge: Cambridge University Press.

Labhart, T. (1980). Specialized photoreceptors at the dorsal rim of the honeybee's compound eye: polarizational and angular sensitivity. *J. Comp. Physiol. A* **141**, 19-30.

Labhart, T. (1986). The electrophysiology of photoreceptors in different eye regions of the desert ant, *Cataglyphis bicolor*. *J. Comp. Physiol. A* **158**, 1-7.

Labhart, T. (1988). Polarization-opponent interneurons in the insect visual system. *Nature* **331**, 435-437.

Labhart, T. (1996). How polarization-sensitive interneurones of crickets perform at low degrees of polarization. *J. Exp. Biol.* **199**, 1467-1475.

Labhart, T. (1999). How polarization-sensitive interneurones of crickets see the polarization pattern of the sky: a field study with an opto-electronic model neurone. *J. Exp. Biol.* **202**, 757-770.

Labhart, T. (2000). Polarization-sensitive interneurons in the optic lobe of the desert ant *Cataglyphis bicolor*. *Naturwissenschaften* **87**, 133-136.

Labhart, T. and Meyer, E. (1999). Detectors for polarized skylight in insects: a survey of ommatidial specializations in the dorsal rim area of the compound eye. *Microsc. Res. Tech.* **47**, 368-379.

Labhart, T. and Meyer, E. (2002). Neural mechanisms in insect navigation: polarization compass and odometer. *Curr. Opin. Neurobiol.* **12**, 707-714.

Labhart, T., Hodel, B. and Valenzuela, I. (1984). The physiology of the cricket's compound eye with particular reference to the anatomically specialized dorsal rim area. *J. Comp. Physiol. A* **155**, 289-296.

Labhart, T., Petzold, J. and Helbling, H. (2001). Spatial integration in polarization-sensitive interneurones of crickets: a survey of evidence, mechanisms and benefits. *J. Exp. Biol.* **204**, 2423-2430.

Lambrinos, D., Maris, M., Kobayashi, H., Labhart, T., Pfeifer, R. and Wehner, R. (1997). An autonomous agent navigating with a polarized light compass. *Adapt. Behav.* **6**, 131-161.

Mappes, M. and Homberg, U. (2004). Behavioral analysis of polarization vision in tethered flying locusts. *J. Comp. Physiol. A* **190**, 61-68.

Mappes, M. and Homberg, U. (2007). Surgical lesion of the anterior optic tract abolishes polarotaxis in tethered flying locusts, *Schistocerca gregaria*. *J. Comp. Physiol. A* **193**, 43-50.

Meyer, E. P. and Labhart, T. (1981). Pore canals in the cornea of a functionally specialized area of the honey bee's compound eye. *Cell Tissue Res.* **216**, 491-501.

Nilsson, D.-E., Labhart, T. and Meyer, E. (1987). Photoreceptor design and optical properties affecting polarization sensitivity in ants and crickets. *J. Comp. Physiol. A* **161**, 645-658.

Petzold, J. (2001). Polarisationsempfindliche Neuronen im Sehsystem der Feldgrille *Gryllus campestris*: Elektrophysiologie, Anatomie und Modellrechnungen. PhD thesis, University of Zürich, Switzerland.

Petzold, J. and Labhart, T. (1993). Polarisation-opponent interneurons of crickets: absolute threshold, visual field properties and response to low degrees of polarization. In *Proceedings of the Neurobiology Conference Göttingen 21* (ed. N. Elsner and M. Heisenberg), p. 371. Stuttgart, New York: Thieme Verlag.

Pomozi, I., Horváth, G. and Wehner, R. (2001). How the clear-sky angle of polarization pattern continues underneath clouds: full-sky measurements and implications for animal orientation. *J. Exp. Biol.* **204**, 2933-2942.

Rossel, S., Wehner, R. and Lindauer, M. (1978). E-vector orientation in bees. *J. Comp. Physiol. A* **125**, 1-12.

Rost, R. and Honegger, H. W. (1987). The timing of premating and mating behavior in a field population of the cricket *Gryllus campestris* L. *Behav. Ecol. Sociobiol.* **21**, 279-289.

Sommer, E. W. (1979). Untersuchungen zur topografischen Anatomie der Retina und zur Sehfeldtopologie im Auge der Honigbiene, *Apis mellifera* (Hymenoptera). PhD thesis, University of Zürich, Switzerland.

Stockhammer, K. (1959). Die Orientierung nach der Schwingungsrichtung linear polarisierten Lichtes und ihre sinnesphysiologischen Grundlagen. *Ergeb. Biol.* **21**, 23-56.

Strutt, J. (Lord Rayleigh) (1871). On the light from the sky, its polarization and colour. *Philos. Mag.* **41**, 107-120.

Ukhanov, K. Y., Leertouwer, H. L., Gribakin, F. G. and Stavenga, D. G. (1996). Dioptrics of the facet lenses in the dorsal rim area of the cricket *Gryllus bimaculatus*. *J. Comp. Physiol. A* **179**, 545-552.

von Frisch, K. (1965). Die Orientierung nach polarisiertem Licht. In *Tanzsprache und Orientierung der Bienen*, pp. 384-447. Berlin, Heidelberg, New York: Springer-Verlag.

von Helversen, O. and Edrich, W. (1974). The spectral sensitivity of polarized light orientation in the honeybee. *J. Comp. Physiol.* **94**, 33-47.

von Philipsborn, A. and Labhart, T. (1990). A behavioural study of polarization vision in the fly, *Musca domestica*. *J. Comp. Physiol. A* **167**, 737-743.

Zahradník, J. (2002). *Der Kosmos Insektenführer*. Stuttgart: Franckh-Kosmos Verlags-GmbH.

Zollikofer, C. (1981). Optische Sehfeldvermessungen am Komplexauge von *Cataglyphis bicolor* und *Cataglyphis albicans* (Formicidae, Hymenoptera). Diploma-thesis, University of Zürich, Switzerland.

Zollikofer, C. P. E., Wehner, R. and Fukushi, T. (1995). Optical scaling in conspecific *Cataglyphis* ants. *J. Exp. Biol.* **198**, 1637-1646.

Zolotov, V. and Frantsevich, L. (1973). Orientation of bees by the polarized light of a limited area of the sky. *J. Comp. Physiol.* **85**, 25-36.

Zufall, F., Schmitt, M. and Menzel, R. (1989). Spectral and polarized light sensitivity of photoreceptors in the compound eye of the cricket (*Gryllus bimaculatus*). *J. Comp. Physiol. A* **164**, 597-608.

A small fly under the open sky: How *Drosophila* views the celestial polarization pattern

Miriam J. Henze[1,2,*], Christiane Bleul[3], Franziska Baumann[1], Thomas Labhart[1]

[1]Institute of Zoology, University of Zürich, Zürich, Switzerland, [2]Department of Cell and Organism Biology, Lund, Sweden, [3]Brain Research Institute, University of Zürich, Switzerland

*Author for correspondence (e-mail: miriam.henze@cob.lu.se)

I

II

III

IV

Manuscript to be published

Author contributions statement

MJH coordinated the experiments, collected part of the optical, light and electron microscopic data, carried out all data analyses, implemented and ran the model and wrote the manuscript

CB performed most of the optical experiments and produced part of the light and electron microscopic sections,

FB collected most of the light and electron microscopic data,

TL supervised the project, drafted the introduction and revised the manuscript.

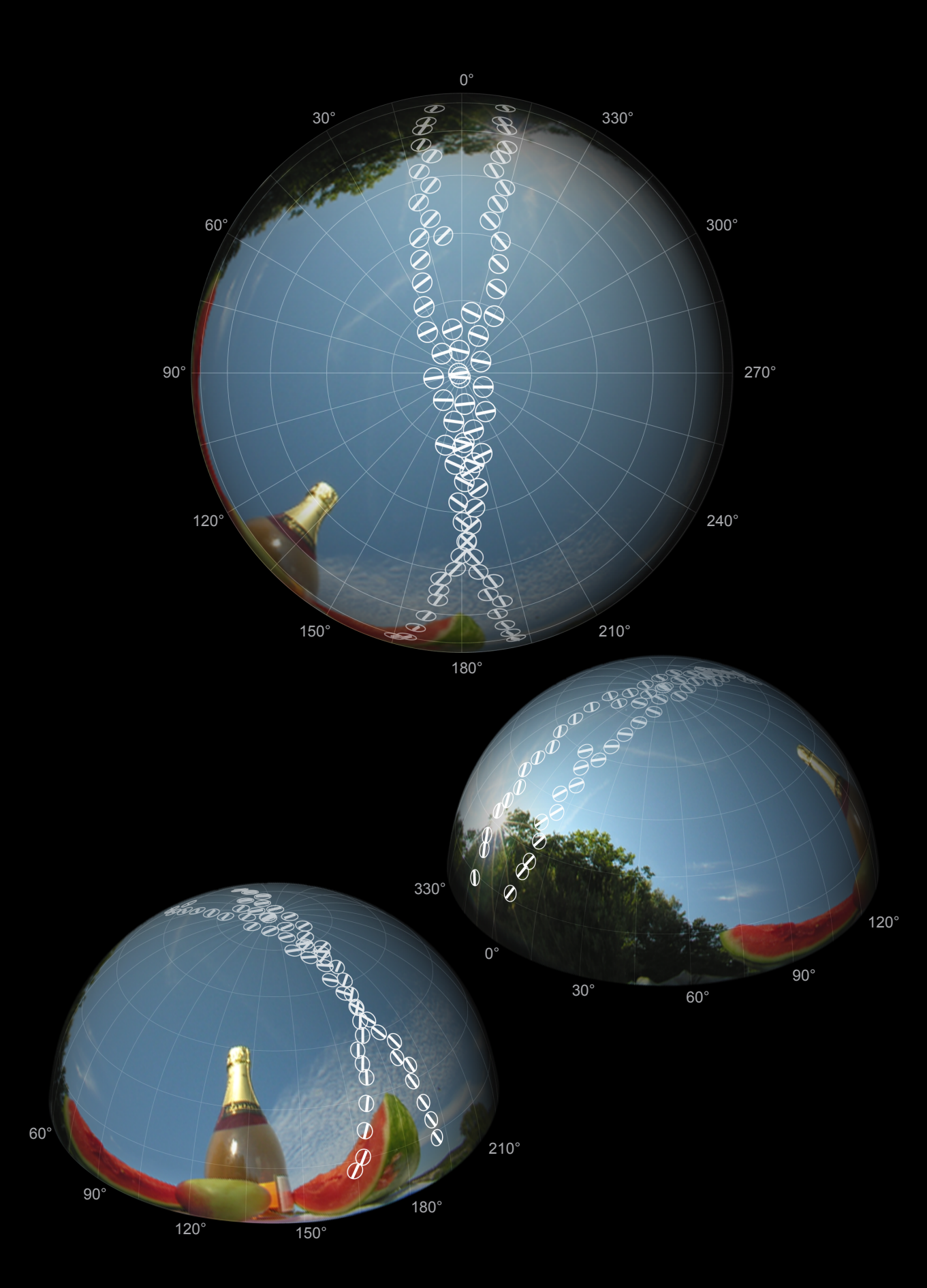
0°
30°
330°
60°
300°
90°
270°
120°
240°
150°
210°
180°
330°
120°
0°
90°
30°
60°
60°
210°
90°
180°
120°
150°

Cover picture. A fruit fly (*Drosophila melanogaster*) heading away from a slice of watermelon served on a picnic table can orient itself by skylight polarization. While this is a common ability among insects, the polarized light sensors of *Drosophila* (bars = axes of maximal polarization sensitivity of photoreceptors R7), which are arranged along the margin of the dorsal eye half, differ in two respects from those of other species. They have small visual fields (circles = half width of angular sensitivity) and are directed at vastly different parts of the sky including the zenith and areas near the horizon. By modeling photoreceptor input to the polarization vision system, M. J. Henze, C. Bleul, F. Baumann and T. Labhart (pp. 41-55) show the consequences of this sensor arrangement for neuronal coding of orientation. Picture composed by Martin Kohler.

Manuscript to be published

A small fly under the open sky: How *Drosophila* views the celestial polarization pattern

Miriam J. Henze[1,2,*], Christiane Bleul[3], Franziska Baumann[1], Thomas Labhart[1]

[1]*Institute of Zoology, University of Zürich, Zürich, Switzerland,* [2]*Department of Cell and Organism Biology, Lund, Sweden,* [3]*Brain Research Institute, University of Zürich, Switzerland*

*Author for correspondence (e-mail: miriam.henze@cob.lu.se)

Summary

Among insects, the ability to exploit skylight polarization for orientation is widespread. Photoreceptors in the dorsal rim area (DRA) of the compound eye are specialized to be strongly sensitive to the electric vector (*e*-vector) of linearly polarized light. In all species studied so far celestial *e*-vector detection is mediated by the DRA, and the ommatidia are functionally comparable. However, the geometry and optics of the DRA and thus the sensory input to the polarization vision system differ considerably. In crickets (*Gryllus sp.*), the DRA is restricted to the dorsalmost part of the eye and is many ommatidia wide. Spatial resolution is lost due to the large and overlapping visual fields of the photoreceptors. By contrast, the DRA ommatidia of fruit flies (*Drosophila melanogaster*) are located in just one or two rows along the entire dorsal eye margin and have small angular sensitivities of few degrees. This results in an arc-shaped DRA in which the caudal, dorsal and frontal sections receive input from different parts of the sky including the zenith and areas near the horizon. Current knowledge on sensory processing in the polarization vision pathway of insects is based on data from species like the cricket in which all DRA ommatidia collect light from roughly the same, zenithal sky region. To understand the implications of different DRA designs, we have modeled a typical *Drosophila* DRA and calculated the responses of the polarization-sensitive photoreceptors to the celestial polarization pattern. Simulations of the first few processing stages in the fly brain reveal that body orientation at a peripheral level cannot be coded in the same way as in crickets. We still assume that the functions of both polarization vision systems are alike and suggest that the design of the *Drosophila* DRA is a consequence of the small head size of the fly.

Key words: visual orientation, polarized skylight, insect navigation, polarization vision, dorsal rim area (DRA), polarization-sensitive neurons (POL neurons), model, Diptera, fruit fly (*Drosophila melanogaster*).

Introduction

Sunlight is linearly polarized by scattering processes in the atmosphere: At any point of the sky a particular orientation of the electric field component (*e*-vector) of light waves dominates. The resultant *e*-vector pattern forms concentric circles around the sun with the degree of polarization (proportion of light waves oscillating in the prevailing orientation) being highest and the intensity of light being lowest for a scattering angle of 90° (Coulson, 1988; Strutt, 1871).

Many arthropods use the celestial *e*-vector pattern as a reference for visual orientation (for reviews see (Horváth and Varjú, 2004; Wehner and Labhart, 2006)). Their rhabdomeric photoreceptors are inherently polarization-sensitive since the photosensitive part is formed by microvilli that extend at right angles to the optical axis and contain dichroic visual pigments. As a result of both, the tubular shape of the microvillus and a directional anchorage of the pigment molecules in the membrane, photon absorption is maximal for light with an *e*-vector parallel to the microvillar axis (Goldsmith and Wehner, 1977; Israelachvili and Wilson, 1976; Land, 1991; Moody and Parriss, 1961). If all microvilli are sufficiently aligned, avoiding randomizing effects, and the rhabdomere is reasonably short, preventing self-screening, the polarization-sensitivity is available to the whole cell (Nilsson et al., 1987; Wehner et al., 1975). The microvillar orientation can then be used as a convenient indicator for the *e*-vector tuning of the photoreceptor.

In all insect species studied so far, the receptors mediating celestial *e*-vector detection are confined to a small part of the compound eye, the so-called dorsal rim area (DRA). DRA ommatidia show a number of characteristic features (Labhart and Meyer, 1999): (1) They are directed towards the sky. (2) The microvilli forming the rhabdomere of each photoreceptor are well aligned. (3) Each ommatidium contains two sets of photoreceptors with mutually orthogonal microvilli orientations but (4) with the same spectral sensitivity. (5) The rhabdoms are comparatively short and have large cross-sectional areas. Together, these functional adaptations provide the basis for a color-blind and intensity-independent visual system that is highly sensitive to the *e*-vector orientation of linearly polarized light from above.

Despite common properties, there are also considerable differences between the DRAs of insect species. The disparities concern for instance the arrangement and the optical specializations of the DRA ommatidia. In some cases, the polarization-sensitive area is restricted to the dorsalmost part of the eye and is many ommatidia wide (field cricket (Blum and Labhart, 2000); locust (Homberg and Paech, 2002); cockchafer (Labhart et al., 1992); dung beetle (Dacke et al., 2003; Dacke et al., 2002)). In others, it extends all the way from the caudal to the frontal eye rim, but comprises only one or two ommatidial rows (dragonflies (Meyer and Labhart, 1993), fruit fly (Tomlinson, 2003; Wernet et al., 2003)). Several insects take an intermediate position, with a DRA that is relatively short and rather narrow (desert ant (Wehner, 1982; Herrling, 1976), honey bee (Wehner, 1982), halactid bee (Greiner et al., 2007), monarch butterfly (Labhart et al., 2009; Stalleicken et al., 2006)). In many cases, the optics of DRA ommatidia is degraded in ways that significantly increase the visual field (for a review see (Labhart and Meyer, 1999)). In other species such adaptations are missing (ants (Aepli et al., 1985; Labhart and Meyer, 1999; Wehner, 1982), monarch butterfly (Labhart et al., 2009; Stalleicken et al., 2006), some flies (review (Labhart and Meyer, 1999))). These differences have not received much attention so far, even though they strongly affect the sensory input to the polarization vision system and possibly have a functional basis. The arrangement and optics of DRA ommatidia define direction and size of the visual fields and thus ultimately determining which parts of the celestial polarization pattern are exploited.

Current knowledge on sensory processing of celestial *e*-vector information in the insect brain is mainly based on studies of two orthopteran species, the cricket (*Gryllus sp.*) and the locust (*Schistocerca gregaria*) (for reviews see (Homberg, 2004; Labhart and Meyer, 2002), both of which have DRAs with degraded optics which are confined to the dorsalmost part of the eye and many ommatidia wide. On a peripheral level, it is the cricket system that has been studied most extensively. Polarization-sensitive neurons (POL neurons) in the optic lobe are thought to represent the first processing layer. Several morphological types of POL neurons have been identified, but the POL1 neurons are the ones that are characterized best. They have dendritic aborizations in the dorsal medulla and send axonal processes to the contralateral optic lobe (Labhart and Petzold, 1993; Petzold, 2001). It has therefore been proposed that they play a role in bilateral signal exchange (Homberg, 2004). POL1 neurons receive input from the ipsilateral eye and their receptive fields are directed to the contralateral, upper part of the sky. The spiking activity of POL1 neurons is a sinusoidal function of *e*-vector orientation with alternating parts of excitation and inhibition and a 180° period. This suggests that the two sets of homochromatic photoreceptors with orthogonal microvilli orientations present in each DRA ommatidium give antagonistic input to the POL1 neurons, a mechanism that enhances the polarization contrast and makes the signal independent of fluctuations in ambient light intensity. Physiologically, three types of POL1 neurons can be distinguished which are most sensitive to *e*-vector orientations of 10°, 60° or 130° relative to the longitudinal body axis of the animal. Within their common, wide (>60°) receptive fields, the respective *e*-vector tuning axis remains constant (Labhart, 1988; Labhart and Petzold, 1993; Labhart et al., 2001; Petzold, 2001). These properties have the following structural basis: (1) Due to the absence of corneal facetting, missing screening pigment and wide rhabdoms, the visual fields of DRA ommatidia are substantially increased and strongly overlapping (half-width of average angular sensitivity ~20°) (Blum and Labhart, 2000; Burghause, 1979; Labhart et al., 1984; Ukhanov et al., 1996). (2) Each section of the DRA contains photoreceptors of all different microvillar orientations (Blum and Labhart, 2000) and (3) each POL1 neuron receives input from about 200 ommatidia of appropriate orientation from different sections of the DRA (Labhart, 1988; Labhart and Meyer, 2002; Labhart et al., 2001). The spatial integration increases the absolute light sensitivity and causes the neurons to respond to the mean *e*-vector within their receptive field rather than to structural details of the polarization pattern (Labhart, 1988; Labhart and Meyer, 2002; Labhart and Petzold, 1993; Labhart et al., 2001; Petzold, 2001). Thus, the three POL1 neurons could code the average *e*-vector orientation in their visual field by a triplet code - analogous to a trichromatic color vision system, in which color is conveyed by the signals of three spectral types of photoreceptors (Bernard and Wehner, 1977; Lambrinos et al., 1997; Lambrinos et al., 2000). Bilateral pooling of the signals of (unilateral) POL1 neurons with similar tuning axes can correct for visual field excentricities resulting in a zenith-centered system that reads the average *e*-vector in the upper part of the sky (Labhart and Meyer, 2002).

In the present study we ask how celestial *e*-vector information might be analyzed in fruit flies (*Drosophila melanogaster*). Both the arrangement and the optical specializations of DRA ommatidia differ considerably between *Drosophila* and the cricket. We have therefore assessed the visual field and the polarization properties of the *Drosophila* DRA in detail. Based on these data we have modeled the responses of the polarization-sensitive photoreceptors to the celestial polarization pattern and simulated the first processing stages by putative monocular and binocular POL neurons.

Materials and methods

I) Measurements

In a first step to model polarization vision in *Drosophila*, the *e*-vector tuning axes of the polarization-sensitive photoreceptors were projected on the visual sphere. For this purpose, we measured the natural head posture of the flies, the optical axes of the dorsal rim ommatidia and the microvilli orientation of photoreceptor R7 in the DRA.

Animals: Data were collected from adult fruit flies (*Drosophila melanogaster*, Meigen). To determine the ommatidial orientation in relation to the eye rim *in vivo*, we used a p*rh1-eGFP* transgenic line (w⁻; CyO/Sp; rh1-GFP/TM2) kindly provided by M. Wernet. This transgene has been described previously (Pichaud and Desplan, 2001). In short, it contains the coding sequence of the enhanced green fluorescent protein (*eGFP*) under control

of a minimal *rh1* promoter (Mismer and Rubin, 1987), which generates a strong *eGFP* signal in the outer six photoreceptors. All other measurements were carried out on wild type flies.

Head posture: In order to determine the head posture of flies under different locomotor conditions, we evaluated side view photographs of sitting and flying *Drosophila* (Fig. 1A-E). A Canon EOS 350D camera was equipped with a water level and aligned horizontally. Sitting flies were photographed using a retro-converter combined with a Canon 18-55 mm wide-angle lens at a focal distance of 24 mm (aperture 22, exposure time 1/20 s, sensitivity ISO 200). Pictures of free-flying *Drosophila* were taken in a wind-tunnel from a distance of about 1 m with a Sigma 70-300 mm telephoto lens at maximum zoom (aperture 22, exposure time 1/4000 s, sensitivity ISO 1600). The wind-tunnel has been described in detail elsewhere (Fry et al., 2008). It provided a laminar airflow of 0.37 m/s or 0.79 m/s in a working section made of clear acrylic. The flies were released at the downwind end and spontaneously initiated upwind flight. They were photographed against a bright red homogeneous background which did not disturb them because of their low sensitivity to long wavelength light (Feiler et al., 1992; Feiler et al., 1988; Salcedo et al., 1999).

For sitting flies, we measured both the angle between the long axis of the compound eye (axis of maximum diameter) and the vertical (Fig. 1A), and the angle between the long axis of an ellipse fitted to the head silhouette and the vertical (Fig. 1B). For free-flying flies only the latter could be analyzed (Fig. 1C) and the angle between the vertical and the eye was inferred from the angle between head and eye in sitting flies.

Optical axes: We determined the optical axes of DRA ommatidia by observing corneal pseudopupils under orthodromic illumination. Flies were glued to the tip of a toothpick and mounted in the center of a three-dimensional goniometer-apparatus installed under a microscope. The goniometer consisted of two measuring wheels which were oriented perpendicular to each other. We aligned the head of the fly such that its sagittal plane was parallel to one of the wheels (no yaw deviation). This allowed us to adjust pitch and roll of the head by the goniometer. Because of the hexagonal shape of the facets, ommatidial rows originate at six fairly stable positions from the border of the compound eye which we termed 'origins' (Fig. 1J). We adopted the origins in the upper half of the eye as landmarks for our measurements. The fly in the goniometer was rotated until the pseudopupil was centered on an origin or between two neighboring origins - henceforth called 'inter-origins' (Fig. 1K). The angular deviations from the sagittal plane and from the long axis of the compound eye were then read as roll and pitch respectively. Both values together were used to define the point on the eye on which the pseudopupil was centered. Optical axes of single ommatidia were derived as follows: The change in pitch from one measuring point to the next was divided by the average number of ommatidia in between. This yielded an interommatidial angle which allowed us to calculate the pitch values of the optical axes for single DRA ommatidia. The respective roll values were inferred from the measured data points by cubic spline interpolation. All data were finally corrected for the natural head posture of the fly (see above) and transformed to conventional spherical coordinates for modeling (frontal direction: azimuth $\theta = 0°$, elevation $\varphi = 0°$; lateral: $\theta = \pm 90°$, $\varphi = 0°$; zenith: $\varphi = 90°$).

To investigate whether there was a difference between the optical results from male and female flies, we used a mixed model approach to the analyses of repeated measures (MIXED procedure in SAS 9.1.3, SAS Institute Inc., Cary, NC, USA). The covariance parameter *fly* was treated as a random effect, while the variable *sex* and the two repeated variables *eye* and *position* were introduced as fixed effects. Based on REML (restricted maximum likelihood) information criteria (Wolfinger, 1993), we chose unstructured and first-order auto-regressive covariance structures for *eye* and *position*, respectively (Wolfinger, 1996). The denominator degrees of freedom for the tests of the fixed effects were computed by the Kenward-Roger method (Schaalje et al., 2002).

Microvilli orientation: The microvilli orientation of R7 was first measured in electron microscopic sections and then related to the course of the eye rim by determining the ommatidial orientation in light microscopic sections and in live p*rh1-eGFP* transgenic flies.

For transmission light and electron microscopy, the eyes were fixed with 2% glutaraldehyde in 0.05 M Na-cacodylate buffer (pH 7.2 - 7.4) at 4°C overnight and post-fixed at room temperature for 2 hours with 2% OsO_4 in distilled H_20. After dehydration with 2,2-dimethoxypropane for 20 minutes and with pure acetone for 45 minutes, the tissue was embedded in Epon 812 and processed on an Ultracut microtome (Leica Microsystems, Wetzlar, Germany) using a diamond knife. We cut semi-thin (1 µm) and ultra-thin (80-90 nm) tangential sections of the DRA. Semi-thin sections were stained with methylene blue and viewed under bright-field illumination in an BX61 microscope equipped with a Color view IIIu camera (both: Olympus, Tokyo, Japan), whereas ultra-thin sections were treated with uranyl acetate and lead citrate and photographed under a Philips transmission electron microscope (CM100, FEI, Hillsboro, Oregon, USA) with a Gatan digital camera (Pleasanton, CA, USA). GFP expression in the outer photoreceptors of live transgenic flies was visualized under a fluorescent microscope (BX61, Olympus, Tokyo, Japan) by neutralizing the cornea using water immersion (Pichaud and Desplan, 2001). In order to view different areas of the DRA from straight above, we glued the flies in appropriate positions on the wax bottom of a Petri dish before submerging them. Photographs were taken by an Olympus digital camera (F-View II). All pictures were adjusted for brightness and contrast in Adobe® Photoshop (Adobe Systems Incorporated, San Jose, CA, USA) prior to further analysis.

We measured the angle between the microvilli of R7 and an axis through the rhabdomeres of R1-R3 in electron microscopic sections (Fig. 1G). The same ommatidia were analyzed in light microscopic sections, in which we determined the orientation of R1-R3 with respect to the eye rim at the center of an origin

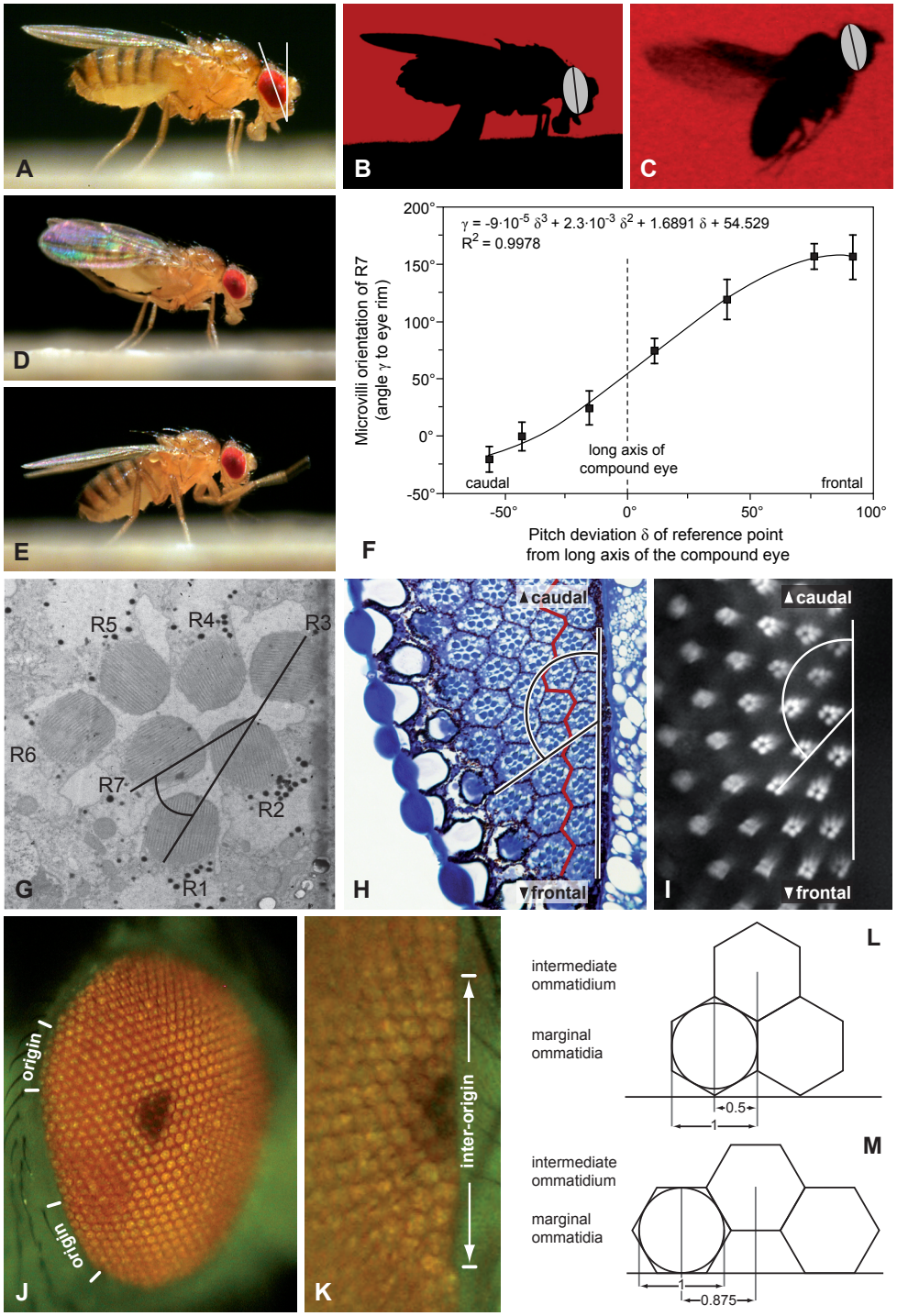
A
B
C
D
E
F
γ = -9·10-5 δ3 + 2.3·10-3 δ2 + 1.6891 δ + 54.529
R2 = 0.9978
Microvilli orientation of R7
(angle γ to eye rim)
200°
150°
100°
50°
0°
-50°
caudal
long axis of
compound eye
frontal
-50°
0°
50°
100°
Pitch deviation δ of reference point
from long axis of the compound eye
G
R5
R4
R3
R6
R7
R2
R1
H
caudal
frontal
I
caudal
frontal
J
origin
origin
K
inter-origin
L
intermediate
ommatidium
marginal
ommatidia
0.5
1
M
intermediate
ommatidium
marginal
ommatidia
1
0.875

Fig. 1. Optical, histological and posture analysis. (A-E) Head posture of flies under different locomotor conditions. In flies sitting on a horizontal surface (A, B) and grooming themselves with their hind (D) or front legs (E) we measured both the angle between the long axis of the compound eye and the vertical (A) and the angle between the long axis of an ellipse fitted on the head silhouette and the vertical (B). For free-flying individuals only the latter could be determined (C) and the angle between the vertical and the eye was inferred from the angle between head and eye in sitting flies. (F-I) Microvilli orientation of photoreceptor R7 in the DRA. (F) Angle γ between the microvilli orientation of R7 and the eye rim (average ± standard deviation) plotted against the pitch deviation δ of the respective reference point (see J,K) from the long axis of the compound eye. The data are well fitted by a 3rd degree polynomial (R^2 = coefficient of determination). (G) We determined the angle between the microvilli of R7 and an axis through the rhabdomeres of R1-R3 in electron microscopic sections. (H) For the same ommatidia, the angle between R1-R3 and the eye rim was measured in light microscopic sections (red line: border between DRA and remainder of the eye). (I) These angles were confirmed in live p*rh1-e*GFP transgenic flies under a fluorescent microscope using water immersion to neutralize the cornea. (J,K) Reference points on the eye. Ommatidial rows originate at six fairly stable positions from the border of the compound eye which we termed 'origins' (J). To measure the optical axes of DRA ommatidia, the fly was mounted in a goniometer and rotated until the corneal pseudopupil was centered on an origin or, as shown in (K), between two neighboring origins ('inter-origins'). The same reference points were employed in (F-I). (L,M) Spacing of DRA ommatidia along the eye rim. Ommatidial cross-sections form quasi-regular hexagons which adjoin the border of the compound eye with a vertex at an origin and with a side at inter-origins. Thus, the distance between a marginal and an intermediate ommatidium along the eye rim is 0.5 and 0.875 times the diameter of the circle inscribed in the hexagon at origins (L) and inter-origins (M), respectively

or an inter-origin (Fig. 1H). To confirm that our results were consistent with the conditions in the live insect, we repeated these measurements *in vivo* in p*rh1-eGFP* transgenic flies (Fig 1I).

Ommatidial cross-sections in *Drosophila* form quasi-regular (equilateral and equiangular) hexagons which adjoin the border of the compound eye with a vertex at an origin and with a side at inter-origins. Concerning the distance between a marginal and an intermediate ommatidium along the eye rim, this leads to a value of 0.5 times the diameter of the circle inscribed in the hexagon at origins (Fig. 1L) and 0.875 times this length at inter-origins (Fig. 1M). Based on the spacing factors, we assigned positional values to DRA ommatidia. The center of an origin or inter-origin was defined as zero, whereas the caudal and the frontal direction were denoted as minus and plus respectively. We included only ommatidia with positional values $<|3|$ in our analysis and made sure that the sum of positional values was close to zero ($<|0.4|$) for each center in order to get a symmetric input from both sides. In addition, the very first DRA ommatidium both frontally and caudally were evaluated.

For all these reference points, we calculated the average angle (γ) between the microvilli-orientation of R7 and the eye rim and plotted it against the pitch deviation (δ) from the long axis of the compound eye (Fig. 1F). The data could be fitted well by a 3rd degree polynomial, which was subsequently used to infer the microvillar orientation of R7 in each DRA ommatidium ($\gamma = -9{\cdot}10^{-5}\ \delta^3 + 2.3{\cdot}10^{-3}\ \delta^2 + 1.6891\ \delta + 54.529$; coefficient of determination $R^2 = 0.9978$).

Arrangement and plotting of DRA ommatidia: The number and distribution of DRA ommatidia was assessed in 55 light microscopic sections, covering every eye region 4 to 15 times. According to these results, we projected a typical *Drosophila* DRA on the visual sphere. Each polarization-sensitive photoreceptor R7 was defined by its optical axis, the microvilli orientation (i.e. its *e*-vector tuning axis) and the half width of angular sensitivity ρ_0 (Fig. 4).

II) Modeling

We simulated the celestial polarization pattern for different solar elevations and calculated the responses of model R7 and R8 DRA photoreceptors to the virtual stimulus for a full rotation of the fly about its yaw axis (Fig. 5A,B). The signals were processed by operations mimicking neural networks in order to determine the activity of polarization-sensitive neurones (POL neurones) in the brain. All models were realized by custom-made programs in Matlab® (The MathWorks, Natick, MA, USA).

Sky parameters: Based on the Rayleigh-Model of single scattering processes in an isotropic atmosphere, the parameters of an idealized celestial polarization pattern were calculated by the following formulas (Beran, 1978):

$$\vec{e} = \frac{\hat{r} \times \hat{s}}{|\hat{r} \times \hat{s}|}$$

with $\vec{e}$ = electric vector of light, $\hat{s}$ = direction of the sun, $\hat{r}$ = scattering direction of light.

$$d = \frac{1 - \cos^2 \kappa}{1 + \cos^2 \kappa} \cdot 0.65$$

with d = degree of polarization, κ = angle between the direction of the sun ($\hat{s}$) and the scattering direction of light ($\hat{r}$).

A factor of 0.65 was included in the formula to account for the polarization maximum measured in the natural sky at 345 nm (Coulson, 1988), the wavelength of peak absorbance for the opsin Rh3 (Feiler et al., 1992) which is expressed by both inner photoreceptors of the DRA (Fortini and Rubin, 1990).

$$I = 0.75 \cdot (1 + \cos^2 \kappa)$$

with I = relative light intensity and κ = angle between the direction of the sun ($\hat{s}$) and the scattering direction of light ($\hat{r}$).

The intensity values in an isotropic atmosphere are the product of solar impact, atmospheric refraction characteristics and phase function (Beran, 1978). However, for a specific wavelength, solar impact and refraction characteristics are constant. Given the fact that R7 and R8 both express the same opsin in the DRA (Feiler et al., 1992; Fortini and Rubin, 1990), relative light intensities can simply be calculated by the phase function which describes the dependence of the light intensity from the scattering direction of light.

Photoreceptors: In our model, the rhabdomere of each DRA

photoreceptor consists of one microvillus. Such a simplification is acceptable for the following reasons: (1) The absolute response levels of R7 and R8 are irrelevant in the present context. (2) The rhabdomeres of both receptors have approximately the same cross-sectional area and length (Baumann, unpublished data). (3) As shown for the DRA of larger flies (Hardie, 1984), screening effects of the distally positioned R7 on R8 are negligible.

The absorption of an incident ray by one microvillus of R7 or R8 was calculated using the equation given below (modified after (Schlecht and Täuber, 1975) and (Petzold, 2001)):

$$A = I\cdot\left(d\cdot(k_1\cdot\sin^2\beta + k_2\cdot\cos^2\beta\cdot\sin^2\alpha + k_1\cdot\cos^2\beta\cdot\cos^2\alpha) + (1-d)\cdot\left(k_1 + \frac{k_2\cdot\sin^2\alpha}{2}\right)\right)\cdot 0.5^{\left(\frac{2\cdot\rho}{\rho_0}\right)^2}$$

with

$$\alpha = \arccos(\vec{i}\circ\vec{m}), \quad \beta = \arccos\left(\frac{\vec{e}\circ\vec{m}'}{|\vec{e}|\cdot|\vec{m}'|}\right), \quad \rho = \arccos(\vec{i}\circ\vec{a}),$$

$$\vec{m}' = \vec{m} - (\vec{i}\circ\vec{m})\cdot\vec{i}, \qquad |\vec{i}| = 1, \quad |\vec{m}| = 1, \quad |\vec{a}| = 1$$

$\vec{i}$ = incident ray, $\vec{e}$ = electric vector of light, $\vec{a}$ = optical axis of ommatidium, $\vec{m}$ = longitudinal axis of microvillus, $\vec{m}'$ = projection of $\vec{m}$ into a plane orthogonal to $\vec{i}$, A = light absorption, I = light intensity, d = degree of polarization, β = angle between $\vec{e}$ and $\vec{m}'$, α = angle between $\vec{i}$ and $\vec{m}$, ρ = angle between $\vec{a}$ and $\vec{i}$, ρ_0 = half width of angular sensitivity function, k_2/k_1 = polarization sensitivity (*PS*) of the microvillus for rays of axial incidence. For the definition of vectors and angles see also Fig. 2.

Some of the photoreceptor properties in the *Drosophila* DRA have not been investigated yet and had to be estimated for applying the formula: (1) The rhabdomeres of R7 and R8 are tiered and

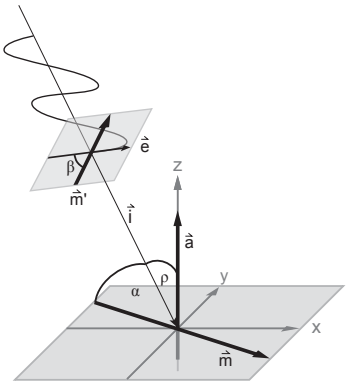

Fig. 2. Modeling rhabdomeric photoreceptors. Definition of parameters used to calculate light absorption by a microvillus. The designations are as follows: $\hat{i}$ incident ray, $\hat{e}$ electric vector of light, $\hat{a}$ optical axis of ommatidium, $\hat{m}$ longitudinal axis of microvillus, $\hat{m}'$ projection of $\hat{m}$ into a plane orthogonal to $\hat{i}$, β angle between $\hat{e}$ and $\hat{m}'$, α angle between $\hat{i}$ and $\hat{m}$, ρ angle between $\hat{a}$ and $\hat{i}$. A sinusoidal line indicates the oscillation of the predominant *e*-vector of a linearly polarized light ray.

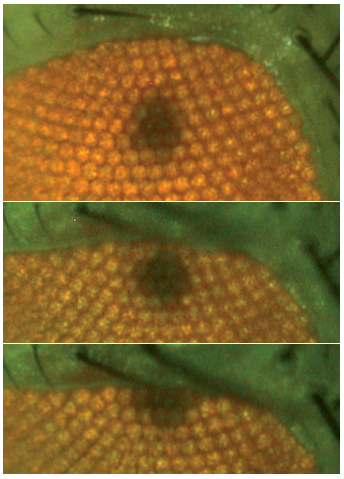

Fig. 3. No evidence for optical specializations of DRA ommatidia. The orthodromic pseudopupil does not change its appearance when it is gradually moved to the dorsal eye rim (top to bottom).

were thus assumed to have identical optical axes. (2) We suppose that the microvilli of R7 and R8 are oriented orthogonal to each other as shown in larger fly species (Hardie, 1984; Wunderer and Smola, 1982). (3) From optomotor responses, which are presumably driven by the outer photoreceptors, Götz (Götz, 1964) derived a half width of angular sensitivity ρ_0 of 3.5° in fruit flies. Calculations by Stavenga (Stavenga, 2003) yielded 4.2° for R1-6 and 2.8° for R7 and R8 in the main retina. Since we have found no evidence of optical specializations in the DRA of *Drosophila* (Figs. 1H and 3) except that the diameter of the inner photoreceptors is increased to the size of the outer ones (Wernet et al., 2003) (see also Fig. 1G), we used 4.2° as a conservative estimate for ρ_0. (4) For the polarization sensitivity ($PS = k_2/k_1$) of R7 and R8 in the DRA, we have employed an average of 10 as measured in *Musca* and *Calliphora* (Hardie, 1984). The absolute values of the constants k_1 and k_2 are irrelevant in this study. We have therefore chosen them such that unpolarized light of axial incidence with an intensity 1 has an absorption of 1 ($k_1 = 1/6$ and $k_2 = 10/6$).

The absorption values of each photoreceptor were determined with a sampling density of 1° for incident light rays up to an angle of incidence of $\rho = 10°$. For $\rho > 10°$, a ray accounts for $\leq 10^{-7}$ of axial absorption ($\rho = 0°$) and is thus negligible.

The relationship between the photoreceptor response R and the intensity I is log-linear over a wide range of intensities (Laughlin et al., 1987; Laughlin, 1981; Laughlin, 1989). Since the absorption A changes linearly with I (see above), R was calculated as:

$$R = \log_{10}(A)$$

with R = photoreceptor response and A = light absorption

Neural processing: Electrophysiological data suggest that POL neurons in the peripheral visual system (optic lobe) receive antagonistic input from photoreceptors with orthogonal microvilli orientations (Labhart, 1988; Labhart, 2000). We have

thus calculated the activity of local interneurons by subtracting the response of R8 from the one of R7 in the same ommatidium. Signals from several local interneurons were pooled to assess the activity of monocular POL neurones. The responses of binocular POL neurones were modeled by interactions between monocular POL neurons of both eyes (for details see Results).

Results

I) The DRA of the fruit fly and its projection to the celestial hemisphere

Position and extent of the DRA: The compound eye of Drosophila is dorsoventrally divided by a line of mirror symmetry of photoreceptor orientation which is called the equator. We found that the DRA started on average with the third ommatidium (SD = ±1) above the equator frontally (n = 6) as well as caudally (n = 5). At both ends, DRA ommatidia were interspersed with normal ommatidia and occurred only directly adjacent to the border of the eye. Towards the centre of the DRA, they formed a continuous marginal line which reached a maximal width of up to two ommatidial rows dorsally. Altogether, the DRA in one compound eye of Drosophila melanogaster comprised 39 ommatida (mean value derived from the evaluation of 55 light microscopic sections covering every region of the DRA 4 to 15 times).

Visual field of the DRA: Flies standing on a horizontal surface kept their head posture stable even when grooming themselves with their front or hind legs (Fig. 1D,E). The average angle between the long axis of the compound eye and the vertical was 21° (SD = ± 3°, n = 8). Under these conditions, the optical axes of DRA ommatidia, projected on the visual sphere, form a long, narrow band (Fig. 4) reaching down to about the same elevation both in the back (elevation φ = 11°) and in the front (φ = 16°). At its caudal end, the DRA of each eye is directed 12° ipsilaterally. It crosses the midline dorso-caudally (φ = 54°), reaches a maximal contralateral direction of 9° dorso-frontally (φ = 41°) and ends 9° contralaterally in the front. The optical data described here are averaged from measurements on both eyes of 11 male fruit flies. Results for females (n = 12) were not significantly different ($F_{1,20.6} = 0.37$; P = 0.55 for the divergence from the sagittal plane; $F_{1,20.3} = 3.52$; P = 0.08 for the elevation φ), although there was a trend towards a slightly more caudal position of the DRA in females.

In free flying Drosophila the head posture was more variable and the head was slightly pitched backwards compared to sitting flies (compare Figs. 1B and C). For a laminar air flow of 37 cm/s in the wind tunnel, the average angle between the long axis of the compound eye and the vertical was 29° (SD = ± 8°, n = 12). A few measurements taken at 79 cm/s gave similar values (31° ± 8°, n = 4).

Microvilli orientation of R7 and R8: The microvilli orientation of photoreceptor R7 changes across the DRA in a fan-like manner. Frontally and caudally the microvilli run almost parallel to the eye rim, whereas they are approximately orthogonal to it at the vertex of the head. Thus, the *e*-vector analyzers formed by R7 are more sensitive to light polarized parallel to the longitudinal body axis of the animal at sky regions close to the horizon and more sensitive to light polarized orthogonal to that axis at the zenith (Fig. 4). For R8 the opposite is the case since its microvilli-orientation is about perpendicular to the one of R7 in each DRA ommatidium. This has been shown in larger flies (Hardie, 1984; Wunderer and Smola, 1982) and is supported by preliminary data from Drosophila melanogaster (Baumann, unpublished observations).

Angular sensitivity of R7 and R8: Angular sensitivity of R7 and R8: In light microscopic sections, differences in the dioptric elements or in the distribution of screening pigment between the DRA and the main retina were not observed. Nor did the orthodromic pseudopupil change its appearance at the dorsal eye rim (Fig. 3). This obvious lack of adaptations to increase the visual field of the ommatidia allowed us to infer the angular sensitivity of DRA photoreceptors from values determined for the main retina. The half width of angular sensitivity ρ_0 of the outer photoreceptors was calculated as 3.5° (Götz, 1964) and 4.2° (Stavenga, 2003) by different methods and authors. Since the cross-sectional area of the inner photoreceptors in the DRA approximates the one of the outer ones (Wernet et al., 2003), we used 4.2° as a conservative estimate for ρ_0. As demonstrated by the projections of ρ_0 in Fig. 4, the visual fields of R7 and R8 in the DRA are rather small and discrete.

II) Polarization-sensitive neurons and coding of body orientation

We simulated the celestial polarization pattern for different solar elevations and calculated the responses of model photoreceptors to the virtual stimulus for a full rotation of the fly about its yaw axis (Fig. 5A,B). This was done for all R7 and R8 cells in the DRA of both eyes.

Local POL neurons: In ants and crickets, electrophysiological data suggest that photoreceptors with orthogonal microvilli orientations provide antagonistic excitatory and inhibitory input to POL neurons in the optic lobe (Labhart, 1988; Labhart, 2000). Many polarization-sensitive neurons of the locust brain also show polarization-opponency (Heinze and Homberg, 2007; Heinze and Homberg, 2009; Pfeiffer and Homberg, 2007; Pfeiffer et al., 2005; Vitzthum et al., 2002). In addition, the demonstration of two sets of photoreceptors with mutually orthogonal microvilli orientations in the DRAs of a large number of insect species (Labhart and Meyer, 1999) indicates that polarization antagonism is a crucial principle in skylight polarization vision in general. We have therefore calculated the activity of interneurons, henceforth called local POL neurons, by subtracting the response of R8 from the one of its R7 counterpart in the same ommatidium (Fig. 5C). For a full rotation of the fly about its yaw axis, this produces a function describing the firing rate of a local POL neuron for specific body orientations (Fig. 5D). Because of the differential, polarization-opponent input, the signal modulation of local POL neurons is larger

than the one of the photoreceptors, increasing the polarization contrast. Furthermore, within the operational range of the photoreceptors, local POL neuron activity becomes independent of light intensity.

Monocular POL neurons: How is sensory information on skylight polarization further processed by the nervous system? In the optic lobe of crickets, there are three types of POL1 neurons with different *e*-vector tuning axes selectively receiving input from DRA ommatidia with microvilli orientations that are alike (Labhart et al., 2001). Adopting this principle in *Drosophila*, we integrated the signals of roughly equal numbers of local POL neurons (12 to 13) of each eye with similar *e*-vector tuning axes in order to assess the activity of putative monocular POL neurons in the fly. These neurons have different tuning axes and respond maximally to *e*-vector orientations of 30°, 80° or 140° relative to the longitudinal body axis (Fig. 6). Because of the fan-array of microvilli orientations in the *Drosophila* DRA, local POL neurons with similar *e*-vector tuning axes receive input from ommatidia that are grouped in the caudal, dorsal and frontal part of the DRA. The photoreceptors have small angular sensitivities and the ommatidia in the three pooling areas of the DRA vastly diverging optical axes (Fig. 6). As a result, the putative monocular POL neurons of the fly possess discrete, elongated visual fields that are either directed frontally, dorsally or caudally.

Binocular POL neurons: Cricket POL1 neurons receive input from the ipsilateral eye and have large receptive fields that are slightly excentric with respect to the zenith (Labhart et al., 2001; Petzold, 2001). Interestingly, each of the three tuning types of POL1 neurons has a counterpart in the contralateral optic lobe with a similar *e*-vector tuning axis (Labhart and Petzold, 1993; Petzold, 2001). Thus, bilateral pooling of the signals of POL1 neurons with corresponding tuning axes would result in a zenith-centered system that reads the average *e*-vector orientation in the upper part of the sky (Labhart, 1999; Labhart and Meyer, 2002). There is evidence that such pooling actually occurs. The axons of POL1 neurons in the cricket run all the way from one optic lobe to the other (Labhart and Petzold, 1993; Petzold, 2001) which suggests that the two sides of the polarization vision system cooperate. Direct evidence for bilateral pooling

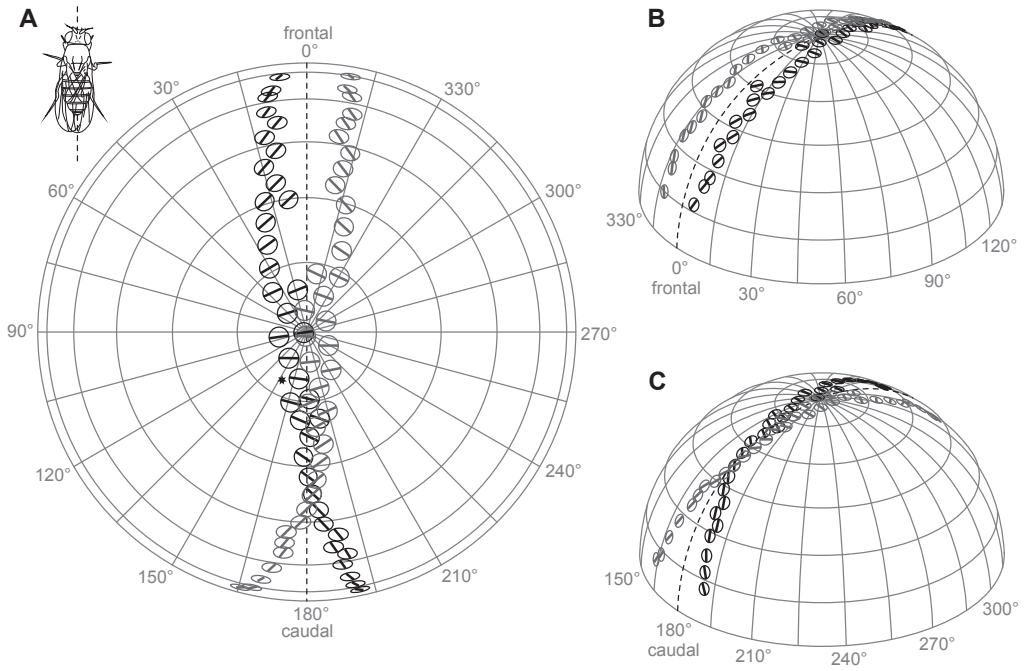

Fig. 4. Properties of R7 photoreceptors of a typical Drosophila DRA projected on the upper visual hemisphere according to the head posture of a fly sitting on a horizontal surface. The broken line indicates the longitudinal body axis. Azimuth 0° and elevation 0° denote the frontal direction. Black and grey symbols represent the DRA of the right and left eye, respectively. The receptors are arranged in a line of one to two ommatidia along the margin of the dorsal eye half. They have small visual fields (circles: half width of angular sensitivity ρ_0) and are directed at vastly different parts of the sky including the zenith and areas near the horizon. The microvilli orientations of photoreceptors R7 (bars) are frontally and caudally approximately parallel to the eye rim and dorsally orthogonal to it. In each DRA ommatidium, R8 has the same optical axis and visual field as R7 but an orthogonal microvilli orientation (not shown). (A) Zenithal projection. (B,C) View on the frontal (B) and caudal part (C) of the DRA respectively. For the asterisk in (A) see Fig. 5.

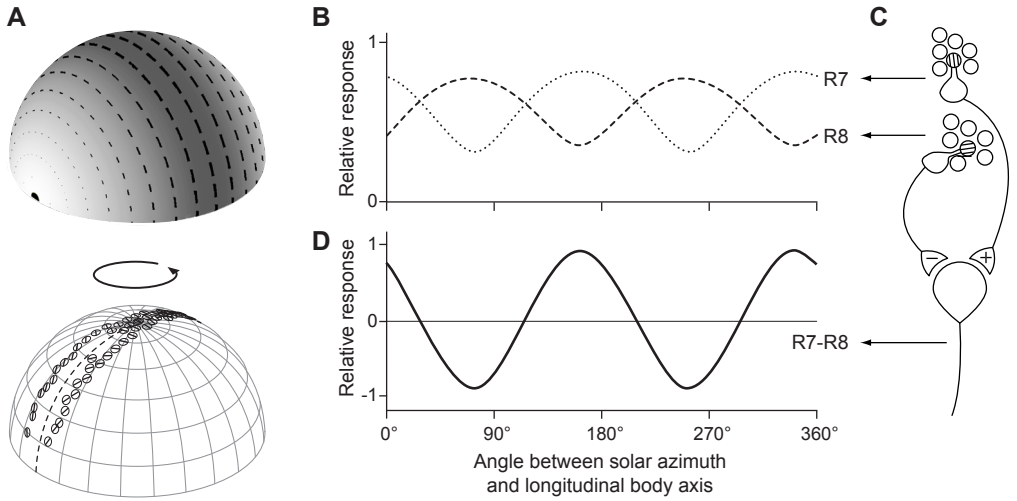

Fig. 5. (A) Top: Three-dimensional representation of the celestial polarization pattern for an elevation of the sun (black hemi-disk) of 0°. Tilt and size of the bars denote the prevailing *e*-vector orientation and the degree of polarization, respectively. The gray shading depicts the gradient of light intensity in the sky. Bottom: Responses of model DRA photoreceptors to a simulated polarization pattern were calculated for a full rotation of the fly about its yaw axis. The broken line indicates the longitudinal body axis. At 0° and 360°, the animal faces the sun. (B) Modeled response curves of two receptors for a solar elevation of 0°. The data shown here originate from receptor R7 marked by an asterisk in Fig. 4 and its R8 counterpart in the same ommatidium. (C) R7 and R8 have mutually orthogonal microvilli orientations, i.e. perpendicular *e*-vector tuning axes, and act antagonistically on a local POL neuron. (D) Modeled response curve of the local POL neuron describing its firing rate as a function of body orientation. Because of the differential, polarization-opponent input from the photoreceptors, the amplitude of the signal is increased and, above threshold level, intensity independent.

is available for another orthopteran insect, the locust. Most types of polarization-sensitive neurons in the central complex seem to receive binocular input with the same *e*-vector tuning axes for ipsi- and contralateral stimulation (el Jundi et al., 2009; Homberg and Heinze, 2009).

Pooling the signals of monocular POL neurons of both eyes with similar *e*-vector tuning axes in our *Drosophila* model results in three binocular POL neurons. Corresponding to their maximal *e*-vector sensitivity relative to the longitudinal body axis of the fly, they are termed POL30, POL80 and POL140. Whereas POL80 has a continuous, dorsal field of view that is symmetrical to the longitudinal body axis of the animal, the visual fields of POL30 and POL140 are divided and lateralized. They receive input from the caudal and frontal regions of either the right (POL30) or the left visual hemisphere (POL140). Fig. 7A shows the response functions of these three neurons to the celestial polarization pattern for a full rotation of the fly about its yaw axis. When the sun is at the horizon (first column), all curves are roughly sinusoidal with a 180° period, but differ in phase and amplitude. Although the response functions for sitting and flying individuals have similar shapes (upper and lower row), the amplitude of POL80 changes strongly. At higher solar elevations (second and third column) the sinusoidal signal modulation is gradually lost for one of the two 180° periods of a full rotation. This is particular obvious for POL30 and POL140, which sample information from lower elevations of the celestial hemisphere where the degree of polarization is higher at high solar elevations than in the zenith.

Apart from combining the signals of monocular POL neurons with similar *e*-vector tuning axes, we also analyzed all other possible pooling combinations. However, the response functions of the respective binocular POL neurons were as variable as the ones of POL30, POL80 and POL140 under the different conditions investigated (data not shown). More promising results were obtained for single POL neurons receiving global input from the DRA.

Fig. 7B depicts the response functions of a binocular POL neuron which pools the signals of POL30, POL80 and POL140. For a solar elevation of 0° (first column), the curve is sinusoidal. Minima occur when the fly is oriented towards or away from the sun, maxima when the animal is aligned with the prevailing *e*-vector orientation in the sky, i.e. for angles of 90° and 270° between solar azimuth and longitudinal body axis. The position of the extrema is almost the same for sitting and flying flies (upper and lower row) and for different altitudes of the sun (columns). However, with increasing solar elevation (second and third column) the sinusoidal signal modulation is gradually lost in the 180° period in which the fly faces the solar half of the celestial hemisphere.

Since the *e*-vector tuning axes in the frontal and caudal sections of the DRA are approximately orthogonal to the ones in the dorsal part, we modeled a binocular POL neuron receiving

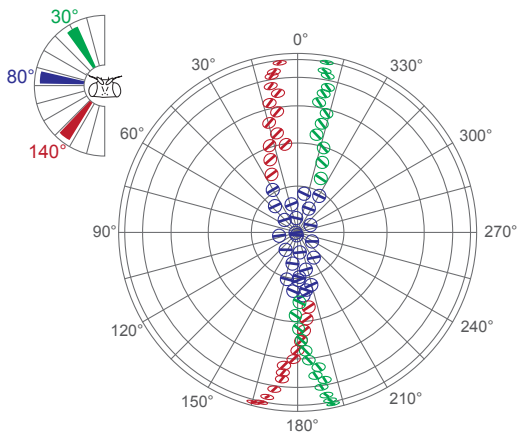

Fig. 6. Tuning axes of three putative monocular POL neurons of Drosophila. In our model, monocular POL neurons receive antagonistic input from R7 and R8 photoreceptors of the DRA via local POL neurons. They integrate the signals of receptor populations with similar microvilli orientations indicated by red, blue and green symbols in the diagram to the right (for a detailed description see Fig. 4). As a result, monocular POL neurons have different tuning axes and respond maximally to *e*-vector orientations of 30°, 80° or 140° relative to the longitudinal body axis of the animal (diagram to the upper left).

antagonistic input from these two analyzer populations, i.e. we subtracted the signals of POL30 and POL140 from the ones of POL80. As shown in Fig. 7C, the response curves of such a neuron are sinusoidal with maxima when the fly is oriented approximately towards or away from the sun and with minima about 90° in between. For solar elevations above 0° (second and third column) the amplitudes in the two 180° periods differ slightly. Nevertheless, a sinusoidal modulation remains present in both periods up to solar altitudes of at least 70° (data not shown). Thus, the shape of the curves is almost the same at different solar elevations and for sitting and flying, although the amplitude of the response changes considerably

Discussion

Possible reasons for an arch-shaped DRA in Drosophila

The cricket DRA with its upwards-directed, large and overlapping visual fields averages the upper, circumzenithal part of the celestial polarization pattern for azimuthal orientation. Due to its arch shape and the small angular sensitivities of the photoreceptors, the *Drosophila* DRA, in contrast, samples discrete information from almost all elevations of the celestial hemisphere. One could therefore assume that the DRA of the fly detects changes in head pitch for flight stabilization. However, the celestial polarization pattern does not provide appropriate cues for pitch determination. This is especially obvious when the sun is at the horizon and the whole sky is polarized orthogonal to the solar and antisolar azimuth (Fig. 5A). Whereas *e*-vector orientation in relation to the fly changes if the animal rotates about its yaw axis, it stays constant for different pitch angles. Even at higher solar elevations, the *e*-vector orientation in the sky hardly changes along the meridians, i.e. for different pitch angles of the animal. Exceptions are the regions close to the sun and the anti-sun. There, however, low degrees of polarization impair *e*-vector detection.

Why does *Drosophila* then include areas near the horizon for analyzing celestial polarization? Is an arch-shaped DRA an adaptation for orientation at high solar elevations, when the degree of polarization in the upper part of the sky is too low and the light intensity too high for *e*-vector detection? Considering the large number of insects with mainly dorsally-directed DRAs (Blum and Labhart, 2000; Dacke et al., 2003; Dacke et al., 2002; Greiner et al., 2007; Homberg and Paech, 2002; Labhart et al., 2009; Labhart et al., 1992; Stalleicken et al., 2006; Wehner, 1982), this seems improbable.

Could the specific design of the *Drosophila* DRA be an adaptation to the small head size of the fly? If the DRA was limited to the dorsalmost region of the compound eye, *e*-vector information would only be sampled in a very restricted part of the celestial hemisphere. This poses a certain risk of losing the orientation cue in situations in which terrestrial objects or clouds reduce sky visibility. Crickets have solved the problem by enlarging the visual fields of their DRA photoreceptors, allowing polarized skylight orientation even if most of the celestial hemisphere is covered (Blum and Labhart, 2000; Henze and Labhart, 2007; Labhart et al., 1984). In *Drosophila*, sampling *e*-vector information in a narrow arch across the sky might serve the same purpose. It is probably the most effective way to compensate for the small visual fields of the DRA photoreceptors while keeping as many ommatidia as possible for color vision, the function that the inner photoreceptors R7 and R8 fulfill in the main retina (Heisenberg and Buchner, 1977; Hérnandez de Salomon and Spatz, 1983; Menne and Spatz, 1977; Yamaguchi et al., 2008). In the DRA, these receptors are transformed to polarization sensors (Wernet et al., 2003), whereas the six outer retinula cells do not show any adaptations for *e*-vector detection. Due to the intact optics of the DRA ommatidia, they remain available for motion vision and shape

Fig. 7. Modeled response functions of binocular POL neurons to the celestial polarization pattern. The firing rate (relative response) of binocular POL neurons is plotted against the body orientation (angle between solar azimuth and longitudinal body axis) for a full rotation of a fly about its yaw axis. At 0° and 360° the animal faces the sun. Columns show the results for different solar elevations, and the upper and lower rows in (A-C) consider the head posture of sitting and flying individuals, respectively. In our model, signals of binocular POL neurons were assessed by interactions between monocolar POL neurons of both eyes. (A) Three binocular POL neurons each receiving input from one pair of monocular POL neurons with similar *e*-vector tuning axes (POL30, POL80 and POL140, for color coding see Fig. 6). (B) One bincolular POL neuron pooling the signals of the three binocular POL neurons described in (A), i.e. POL30 + POL80 + POL140. (D) One binocular POL neuron receiving antagonistic input from the dorsal center of the DRA and its frontal and caudal ends, i.e. POL80 – (POL30 + POL140)

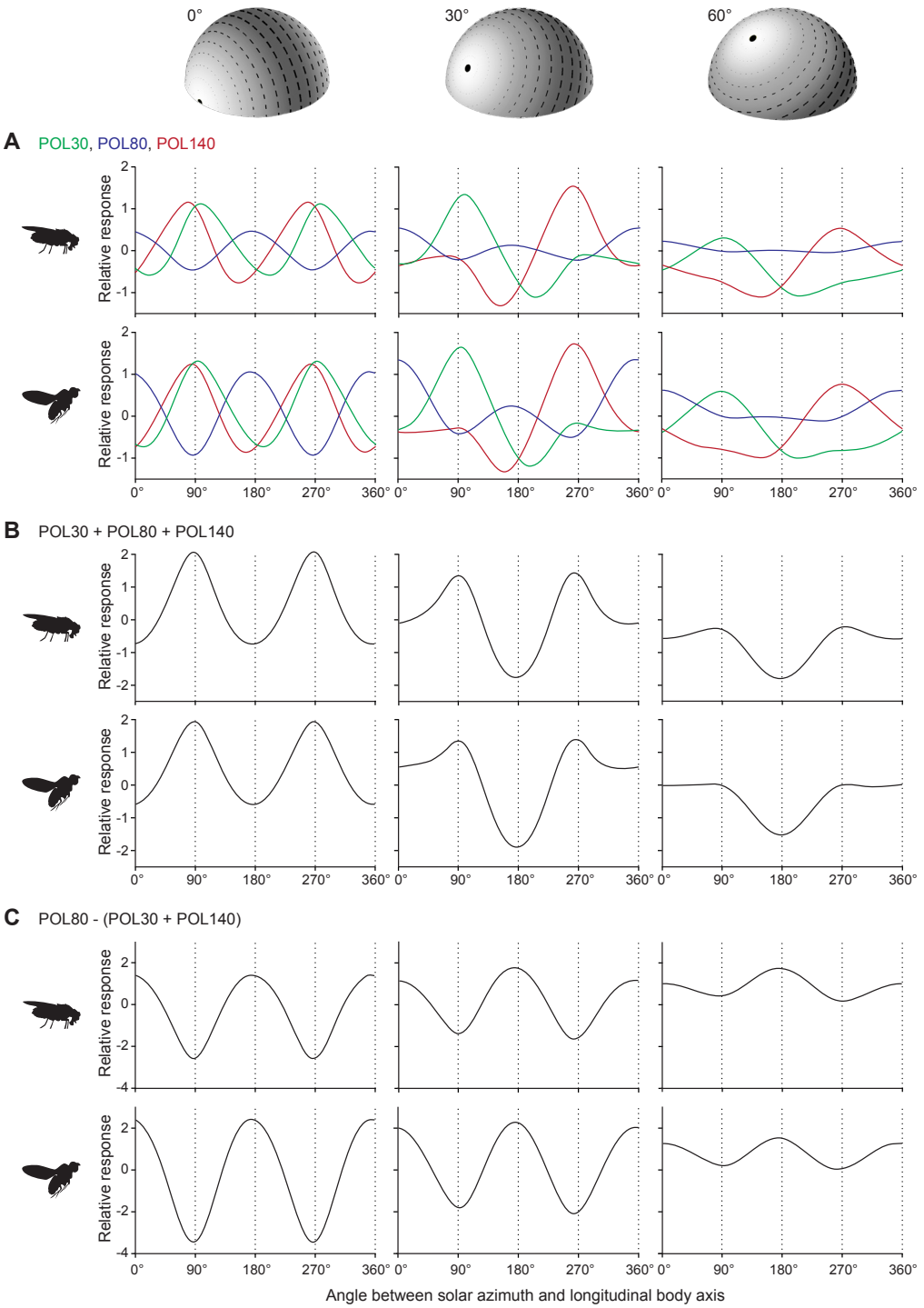
0°
30°
60°
A
POL30, POL80, POL140
Relative response
B
POL30 + POL80 + POL140
Relative response
C
POL80 - (POL30 + POL140)
Relative response
0°
90°
180°
270°
360°
Angle between solar azimuth and longitudinal body axis

analysis as in the rest of the eye (Heisenberg and Buchner, 1977; Yamaguchi et al., 2008). Probably, *Drosophila* cannot afford a DRA completely specialized for the detection of polarized light. The limited head space of the tiny fly puts severe constraints on the construction of its compound eyes. On the one hand the size of the ommatidia has reached the limit for a working neural superposition eye and the facets cannot be made any smaller, on the other hand the eyes already occupy a larger fraction of the head than in bigger flies (Stavenga, 2003). Thus the usage of all receptors has to be economical. The significantly larger crickets, in contrast, seem to be able to dedicate a number of ommatidia to polarization vision alone. All functional DRA photoreceptors except for the small, proximal R8 cell express the same visual pigment and have extended visual fields prohibiting any color, shape or motion analysis (Blum and Labhart, 2000; Henze et al., 2009; Labhart et al., 1984; Zufall et al., 1989).

Modeling the DRA of Drosophila

In order to understand the impact of the DRA design in *Drosophila* on neuronal coding of body orientation with respect to the celestial *e*-vector pattern, we have modeled the sensory input to the polarization vision system of the fly and simulated the first few processing stages. An idealized celestial polarization pattern calculated for single scattering processes in an isotropic atmosphere (Rayleigh-scattering) (Strutt, 1871) was employed as a virtual stimulus. Even though natural sky conditions are more complex, the Rayleigh model describes the celestial *e*-vector pattern quite well - in particular for shorter wavelengths (Suhai and Horváth, 2004). These are crucial for *e*-vector detection in *Drosophila* since the polarization-sensitive retinula cells in the DRA of the fly are ultraviolet-sensitive (Feiler et al., 1992; Fortini and Rubin, 1990).

To model light absorption by the photoreceptors, we measured the microvilli-orientation and the optical axis of R7 in the DRA. Other photoreceptor properties such as polarization sensitivity (*PS*), the half width of angular sensitivity (ρ_0) and the angle between the microvilli orientation of R7 and R8 were estimated. These evaluations are based on data from larger fly species (Hardie, 1984; Wunderer and Smola, 1982) or from the main retina of *Drosophila* (Götz, 1964; Stavenga, 2003) in combination with our own observations on the *Drosophila* DRA (e.g. Figs. 1G,H and 3).

Coding azimuthal body orientation by POL neurons

Because of their common visual field (Labhart et al., 2001; Petzold, 2001), the three *e*-vector tuning types of cricket POL1 neurons could in principle code *e*-vector orientation by a triplet code, i.e. in the same way as color is coded by the signals of three spectral types of photoreceptors in a trichromatic color vision system (Bernard and Wehner, 1977; Lambrinos et al., 1997; Lambrinos et al., 2000). The large receptive fields of the POL1 neurons are slightly excentric with respect to the zenith (Labhart et al., 2001; Petzold, 2001). However, bilateral pooling of the signals of POL1 neurons with similar tuning axes results in a zenith-centered system that reads the average *e*-vector orientation in the upper part of the sky (Labhart, 1999; Labhart and Meyer, 2002). Due to the mirror symmetry of the celestial polarization pattern, this *e*-vector is always orthogonal to the solar and antisolar azimuth, i.e. the cricket system could indicate body orientation in relation to the polarization pattern without being recalibrated during the course of the day.

Given the DRA design of *Drosophila*, binocular POL neurons with the same properties as bilaterally pooled cricket POL1 neurons could not be generated in our model. To obtain three neurons with *e*-vector tuning axes distinct from each other but constant across the visual field of each neuron, we integrated the signals of DRA ommatidia with similar microvilli orientations from different thirds of the DRA. The resulting binocular POL neurons, POL30, POL80 and POL140, do not have common visual fields. While one is directed dorsally, the other two receive input from the frontal and caudal regions of either the right or the left visual hemisphere. The response functions to the celestial polarization pattern change strongly with solar elevation and also slightly depending on whether the animal is sitting or flying (Fig. 7A). Since the relation of the three curves to each other varies, the system would have to be constantly recalibrated if it coded a specific body orientation with respect to the *e*-vector pattern by a triplet code over the course of the day and for different locomotor conditions. Without any further adjustments it could only be employed to keep a constant cruising course during a short foraging trip.

In principle, however, constant information on azimuthal body orientation with respect to the celestial polarization pattern is contained in the signals of the three binocular POL neurons mentioned above. This becomes obvious when the responses of a single POL neuron receiving global input from the DRAs of both eyes are calculated by interactions between POL30, POL80 and POL140 (Fig. 7B,C). A summation of all signals (Fig. 7B) results in a response function which changes its shape with solar elevation, but the position of the antisolar azimuth is always marked by a minimum. For a neuron that receives differential input from the center and the caudal and frontal sections of the DRA (Fig. 7C) the position of the extrema as well as the shape of the response curve stays approximately the same for all solar elevations and locomotor conditions, only the modulation amplitude changes.

POL neurons with alternative properties

So far, polarization-sensitive neurons have been demonstrated in the optic lobes of crickets (Labhart, 1988), locusts (Homberg and Würden, 1997), cockroaches (Loesel and Homberg, 2001) and desert ants (Labhart, 2000). Of these insect species, ants are the ones that are most closely related to flies. The photoreceptors in the DRA of the desert ant (*Cataglyphis bicolor*) possess small visual fields and show the same fan-like microvillar arrangement as in *Drosophila* (Aepli et al., 1985; Labhart, 1986; Labhart and Meyer, 1999; Wehner, 1982). One could therefore assume that the properties of ant and fly POL neurons are similar. POL neuons in desert ants receive polarization-opponent and monochromatic input (Labhart, 2000). Both are features that they share with the POL neurons of crickets. However, as tested in one cell, selective stimulation of the anterior and medioposterior section

of the ant DRA with small stimuli produced substantially different *e*-vector tuning axes of the POL neuron. For a large stimulus, the tuning axis was the resultant of the tuning axes determined for the small stimuli (Labhart, 2000). These data indicate that the POL neurons of *Cataglyphis* integrate signals from photoreceptors with distinct microvilli orientations from different sections of the DRA. However, all knowledge we currently have of POL neurons in *Cataglyphis* relies on very few recordings (9 individual cells) and does therefore not provide a solid basis for simulation experiments. We have therefore modeled *Drosophila* POL neurons according to the properties of the well-studied cricket POL1 neurons (Labhart, 1988; Labhart and Petzold, 1993; Labhart et al., 2001; Petzold, 2001), keeping the *e*-vector tuning axis (almost) constant within the whole receptive field

Conclusions

In insects, the visual systems to analyze celestial *e*-vector information share many functional properties. However, differences in the design of the DRA result in a spatially distinct sensory input, which might affect the neuronal processing stages in the brain. Since there is evidence that polarization vision evolved independently in several insect taxa (Labhart and Meyer, 1999), some variation in the polarization vision pathway is quite likely. One should therefore be careful to adopt the results from a small number of closely related species with similar DRAs as universal for all insect orders. Instead, it would be desirable to extend the current research to species with particularly different DRA designs. For those that are not amenable to electrophysiological experiments, a model based on the determination of the microvilli orientations, optical axes and visual fields of the polarization-sensitive photoreceptors in the DRA, like the one presented in this study, might be a feasible alternative.

Acknowledgments

We thank Vasco de Medici and Steven Fry for pictures of free-flying Drosophila and Martin Kohler for photographs of sitting flies. We are grateful to Mathias Wernet for providing transgenic Drosophila, to Florian Bachmann for advice on Matlab programming, to Stefan Sommer for help on statistics and to Emily Baird for proofreading part of the manuscript. M.J.H. was supported by the "Studienstiftung des deutschen Volkes".

List of abbreviations

α	optical axis of the ommatidium
A	light absorption
d	degree of polarization
DRA	dorsal rim area
$\vec{e}$, *e*-vector	electric vector of light
$\vec{i}$	incident ray
I	(relative) light intensity
k_2/k_1	polarization sensitivity (*PS*) of the microvillus for rays of axial incidence
$\vec{m}$	longitudinal axis of microvillus
$\vec{m}'$	projection of the longitudinal axis of the microvillus ($\vec{m}$) into a plane orthogonal to the incident ray ($\vec{i}$)
n	number of cases
POL neuron	polarization-sensitive neuron
POL30, POL80, POL140	binocular neurons maximally sensitive to *e*-vector orientations of 30°, 80° or 140° relative to the longitudinal body axis of the animal
PS	polarization sensitivity
$\vec{r}$	scattering direction of light
R	photoreceptor response
$\vec{s}$	direction of the sun
a	angle between the incident ray ($\vec{i}$) and the longitudinal axis of the microvillus ($\vec{m}$)
b	angle between *e*-vector ($\vec{e}$) and projection ($\vec{m}'$) of the longitudinal axis of the microvillus into the plane orthogonal to the incident ray ($\vec{i}$)
γ	average angle between the microvilli-orientation of R7 in the DRA and the eye rim
δ	angular deviation from the long axis (axis of maximal diameter) of the compound eye
λ	wavelength
θ	azimuth
κ	angle between the direction of the sun ($\vec{s}$) and the scattering direction of light ($\vec{r}$)
ρ	angle between optical axis (α) of the ommatidium and incident ray ($\vec{i}$)
ρ_0	half width of angular sensitivity function
φ	elevation
x	cross product
◦	dot product

References

Aepli, F., Labhart, T. and Meyer, E. P. (1985). Structural specializations of the cornea and retina at the dorsal rim of the compound eye in hymenopteran insects. *Cell Tissue Res.* **239**, 19-24.

Beran, D. (1978). Atmosphärische Rayleigh-Streuung im ultravioletten und sichtbaren Spektralbereich. *Deutsche Forschungs- und Versuchsanstalt für Luft- und Raumfahrt, Mitteilungen*, 78-103.

Bernard, G. D. and Wehner, R. (1977). Functional similarities between polarization vision and color-vision. *Vision Res.* **17**, 1019-1028.

Blum, M. and Labhart, T. (2000). Photoreceptor visual fields, ommatidial array, and receptor axon projections in the polarisation-sensitive dorsal rim area of the cricket compound eye. *J. Comp. Physiol. A* **186**, 119-128.

Burghause, F. M. H. R. (1979). Structural specialization in the dorso-frontal region of the cricket compound eye (Orthoptera, Grylloidea). *Zoologische Jahrbücher - Abteilung für allgemeine Zoologie und Physiologie der Tiere* **83**, 502-525.

Coulson, K. L. (1988). *Polarization and intensity of light in the atmosphere*. Hampton, Virginia USA: A. Deepak Publishing.

Dacke, M., Nordström, P. and Scholtz, C. (2003). Twilight orientation to polarised light in the crepuscular dung beetle Scarabaeus zambesianus. *J. Exp. Biol.* **206**, 1535-1543.

Dacke, M., Nordström, P., Scholtz, C. H. and Warrant, E. J. (2002). A specialized dorsal rim area for polarized light detection in the compound eye of the scarab beetle *Pachysoma striatum*. *J Comp Physiol* **188**, 211-216.

el Jundi, B., Heinze, S., Pfeiffer, K. and Homberg, U. (2009). Transformation of receptive field structure and ocular dominance

between different stages of the polarization vision pathway in the brain of the locust. In *Proceedings of the 8th Meeting of the German Neuroscience Society*, pp. T14-5A. Göttingen.

Feiler, R., Bjornson, R., Kirschfeld, K., Mismer, D., Rubin, G. M., Smith, D. P., Socolich, M. and Zuker, C. S. (1992). Ectopic expression of ultraviolet-rhodopsins in the blue photoreceptor cells of *Drosophila*: visual physiology and photochemistry of transgenic animals. *J. Neurosci.* **12**, 3862-3868.

Feiler, R., Harris, W. A., Kirschfeld, K., Wehrhahn, C. and Zuker, C. S. (1988). Targeted misexpression of a *Drosophila* opsin gene leads to altered visual function. *Nature* **333**, 737-741.

Fortini, M. E. and Rubin, G. M. (1990). Analysis of cis-acting requirements of the Rh3 and Rh4 genes reveals a bipartite organization to rhodopsin promoters in *Drosophila melanogaster*. *Genes Dev.* **4**, 444-463.

Fry, S. N., Rohrseitz, N., Straw, A. D. and Dickinson, M. H. (2008). TrackFly: virtual reality for a behavioral system analysis in free-flying fruit flies. *J. Neurosci. Methods* **171**, 110-117.

Goldsmith, T. H. and Wehner, R. (1977). Restrictions on rotational and translational diffusion of pigment in the membranes of a rhabdomeric photoreceptor. *J. Gen. Physiol.* **70**, 453-490.

Götz, K. G. (1964). Optomotorische Untersuchung des visuellen Systems einiger Augenmutanten der Fruchtfliege *Drosophila*. *Kybernetik* **2**, 77-92.

Greiner, B., Cronin, T. W., Ribi, W. A., Wcislo, W. T. and Warrant, E. J. (2007). Anatomical and physiological evidence for polarisation vision in the nocturnal bee *Megalopta genalis*. *J. Comp. Physiol. A* **193**, 591-600.

Hardie, R. C. (1984). Properties of photoreceptor-R7 and photoreceptor-R8 in dorsal marginal ommatidia in the compound eyes of *Musca* and *Calliphora*. *J. Comp. Physiol.* **154**, 157-165.

Heinze, S. and Homberg, U. (2007). Maplike representation of celestial e-vector orientations in the brain of an insect. *Science* **315**, 995-997.

Heinze, S. and Homberg, U. (2009). Linking the input to the output: new sets of neurons complement the polarization vision network in the locust central complex. *J. Neurosci.* **29**, 4911-4921.

Heisenberg, M. and Bucher, E. (1977). The role of retinula cell types in visual behavior of *Drosophila melanogaster*. *J. Comp. Physiol. A* **117**, 127-162.

Henze, M. J., Gesemann, M., Dannenhauer, K. and Labhart, T. (2009). Opsin divergence and retinal regionalization in the visual system of the cricket (*Gryllus bimaculatus*). In *Two Facets of Insect Vision: Polarization Sensitivity and Visual Pigments*, (ed. M. J. Henze), pp.73-86 Switzerland: PhD thesis, University of Zürich.

Henze, M. J. and Labhart, T. (2007). Haze, clouds and limited sky visibility: polarotactic orientation of crickets under difficult stimulus conditions. *J. Exp. Biol.* **219**, 3266-3276.

Hérnandez de Salomon, C. and Spatz, H.-C. (1983). Colour vision in *Drosophila melanogaster*: Wavelength Discrimination. *J. Comp. Physiol. A* **150**, 31-37.

Herrling, P. (1976). Regional distribution of three ultrastructural retinula types in retina of *Cataglyphis bicolor* Fabr. (Formicidae, Hymenoptera). *Cell Tissue Res*. **169**, 247-266.

Homberg, U. (2004). In search of the sky compass in the insect brain. *Naturwissenschaften* **91**, 199-208.

Homberg, U. and Heinze, S. (2009). Coding of celestial E-vector orientations in the central complex of the desert locust. In *Proceedings of the 8th Meeting of the German Neuroscience Society*, pp. S11-1. Göttingen.

Homberg, U. and Paech, A. (2002). Ultrastructure and orientation of ommatidia in the dorsal rim area of the locust compound eye. *Arth. Struct. Dev.* **30**, 271-280.

Homberg, U. and Würden, S. (1997). Movement-sensitive, polarization-sensitive, and light-sensitive neurons of the medulla and accessory medulla of the locust, *Schistocerca gregaria*. *J. Comp. Neurol.* **386**, 329-346.

Horváth, G. and Varjú, D. (2004). *Polarized Light in Animal Vision - Polarization Patterns in Nature.* Berlin, Heidelberg, New York: Springer-Verlag.

Israelachvili, J. N. and Wilson, M. (1976). Absorption characteristics of oriented photopigments in microvilli. *Biol. Cybern.* **21**, 9-15.

Labhart, T. (1986). The Electrophysiology of Photoreceptors in Different Eye Regions of the Desert Ant, *Cataglyphis-Bicolor*. *J. Comp. Physiol. A* **158**, 1-7.

Labhart, T. (1988). Polarization-opponent interneurones in the insect visual-system. *Nature* **331**, 435-437.

Labhart, T. (1999). How polarization-sensitive interneurones of crickets see the polarization pattern of the sky: A field study with an optoelectronic model neurone. *J. Exp. Biol.* **202**, 757-770.

Labhart, T. (2000). Polarization-sensitive interneurons in the optic lobe of the desert ant *Cataglyphis bicolor*. *Naturwissenschaften* **87**, 133-136.

Labhart, T., Baumann, F. and Bernard, G. D. (2009). Specialized ommatidia of the polarization-sensitive dorsal rim area in the eye of Monarch butterflies have non-functional reflecting tapeta. *Cell Tissue Res*., in press.

Labhart, T., Hodel, B. and Valenzuela, I. (1984). The physiology of the cricket's compound eye with particular reference to the anatomically specialized dorsal rim area. *J. Comp. Physiol.* **155**, 289-296.

Labhart, T. and Meyer, E. (1999). Detectors for polarized skylight in insects: A survey of ommatidial specializations in the dorsal rim area of the compound eye. *Microsc. Res. Tech.* **47**, 368-379.

Labhart, T. and Meyer, E. (2002). Neural mechanisms in insect navigation: polarization compass and odometer. *Curr. Opin. Neurobiol.* **12**, 707-714.

Labhart, T., Meyer, E. and Schenker, L. (1992). Specialized ommatidia for polarization vision in the compound eye of cockchafers, *Melolontha melolontha* (Coleoptera, Scarabaeidae). *Cell Tissue Res.* **268**, 419-429.

Labhart, T. and Petzold, J. (1993). Processing of polarized light information in the visual system of crickets. In *Sensory Systems of Arthropods* (ed. K. Wiese, F. G. Gribakin, A. V. Popov, G. Renninger), pp. 158-169. Basel: Birkhäuser Verlag.

Labhart, T., Petzold, J. and Helbling, H. (2001). Spatial integration in polarization-sensitive interneurones of crickets: A survey of evidence, mechanisms and benefits. *J. Exp. Biol.* **204**, 2423-2430.

Lambrinos, D., Maris, M., Kobayashi, H., Labhart, T., Pfeifer, R. and Wehner, R. (1997). An autonomous agent navigating with a polarized light compass. *Adapt. Behav.* **6**, 131-161.

Lambrinos, D., Moller, R., Labhart, T., Pfeifer, R. and Wehner, R. (2000). A mobile robot employing insect strategies for navigation. *Robot. Auton. Syst.* **30**, 39-64.

Land, M. F. (1991). Polarizing the world of fish. *Nature* **353**, 118-119.

Laughlin, S., Howard, J. and Blakeslee, B. (1987). Synaptic limitations to contrast coding in the retina of the blowfly *Calliphora*. *P. Roy. Soc. Lond. B Bio*. **231**, 437-467.

Laughlin, S. B. (1981). Peripheral visual systems of invertebrates. In *Handbook of Sensory Physiology* VII/6B, (ed. H. Autrum), pp. 135-280. Berlin, Heidelberg, New York: Springer.

Laughlin, S. B. (1989). The role of sensory adaptation in the retina. *J. Exp. Biol.* **146**, 39-62.

Loesel, R. and Homberg, U. (2001). Anatomy and physiology of neurons with processes in the accessory medulla of the cockroach *Leucophaea maderae*. *J. Comp. Neurol.* **439**, 193-207.

Menne, D. and Spatz, H.-C. (1977). Colour Vision in *Drosophila melanogaster*. *J. Comp. Physiol. A* **114**, 301-312.

Meyer, E. and Labhart, T. (1993). Morphological specializations of dorsal rim ommatidia in the compound eye of dragonflies and damselflies (Odanata). *Cell Tissue Res*. **272**, 17-22.

Mismer, D. and Rubin, G. M. (1987). Analysis of the promoter of the ninaE opsin gene in *Drosophila melanogaster*. *Genetics* **116**, 565-578.

Moody, M. F. and Parriss, J. R. (1961). The discrimination of polarized light by Octopus: a behavioural and morphological study. *Z. vgl. Physiol.* **44**, 268-291.

Nilsson, D.-E., Labhart, T. and Meyer, E. (1987). Photoreceptor design

and optical-properties affecting polarization sensitivity in ants and crickets. *J. Comp. Physiol. A* **161**, 645-658.

Petzold, J. (2001). Polarisationsempfindliche Neuronen im Sehsystem der Feldgrille *Gryllus campestris*: Elektrophysiologie, Anatomie und Modellrechnungen. In *Mathematisch-naturwissenschaftliche Fakultät*, vol. *PhD*, pp. 230. Zürich: Universität Zürich.

Pfeiffer, K. and Homberg, U. (2007). Coding of azimuthal directions via time-compensated combination of celestial compass cues. *Curr. Biol.* **17**, 960-965.

Pfeiffer, K., Kinoshita, M. and Homberg, U. (2005). Polarization-sensitive and light-sensitive neurons in two parallel pathways passing through the anterior optic tubercle in the locust brain. *J. Neurophysiol.* **94**, 3903-3915.

Pichaud, F. and Desplan, C. (2001). A new visualization approach for identifying mutations that affect differentiation and organization of the *Drosophila* ommatidia. *Development* **128**, 815-826.

Salcedo, E., Huber, A., Henrich, S., Chadwell, L. V., Chou, W. H., Paulsen, R. and Britt, S. G. (1999). Blue- and green-absorbing visual pigments of *Drosophila*: ectopic expression and physiological characterization of the R8 photoreceptor cell-specific Rh5 and Rh6 rhodopsins. *J. Neurosci.* **19**, 10716-10726.

Schaalje, G. B., McBride, J. B. and Fellingham, G. W. (2002). Adequacy of approximations to distributions of test statistics in complex mixed linear models. *J. Agric. Biol. Envir. Stat.* **7**, 512-524.

Schlecht, P. and Täuber, U. (1975). The photochemical equilibrium in rhabdomeres of *Eleodone* and its effect on dichroic absorption. In *Photoreceptor Optics*, (ed. A. W. Snyder), pp. 316-335. Berlin, Heidelberg, New York: Springer-Verlag.

Stalleicken, J., Labhart, T. and Mouritsen, H. (2006). Physiological characterization of the compound eye in monarch butterflies with focus on the dorsal rim area. *J. Comp. Physiol. A* **192**, 321-331.

Stavenga, D. G. (2003). Angular and spectral sensitivity of fly photoreceptors. II. Dependence on facet lens F-number and rhabdomere type in *Drosophila*. *J. Comp. Physiol. A* **189**, 189-202.

Strutt, J. (Lord Rayleigh) (1871). On the light from the sky, its polarization and colour. *Philos. Mag.* **41**, 107-120.

Suhai, B. and Horvath, G. (2004). How well does the Rayleigh model describe the E-vector distribution of skylight in clear and cloudy conditions? A full-sky polarimetric study. *J. Opt. Soc. Am. A* **21**, 1669-1676.

Tomlinson, A. (2003). Patterning the peripheral retina of the fly: decoding a gradient. *Dev. Cell* **5**, 799-809.

Ukhanov, K., Leertouwer, H., Gribakin, F. and Stavenga, D. (1996). Dioptrics of the facet lenses in the dorsal rim area of the cricket *Gryllus bimaculatus*. *J. Comp. Physiol. A* **179**, 545-552.

Vitzthum, H., Muller, M. and Homberg, U. (2002). Neurons of the central complex of the locust *Schistocerca gregaria* are sensitive to polarized light. *J. Neurosci.* **22**, 1114-1125.

Wehner, R. (1982). Himmelsnavigation bei Insekten. Neurophysiologie und Verhalten. In *Neujahrsbl. Naturforsch. Ges. Zürich*, vol. 184, pp. 1-132.

Wehner, R., Bernard, G. D. and Geiger, E. (1975). Twisted and non-twisted rhabdoms and their significance for polarization detection in the bee. *J. Comp. Physiol.* **104**, 225-245.

Wehner, R. and Labhart, T. (2006). Polarisation vision. In *Invertebrate Vision* (ed. E. Warrant and D.-E. Nilsson), pp. 291-348. Cambridge, New York, Melbourne, Madrid, Cape Town, Singapore, São Paulo: Cambridge University Press.

Wernet, M., Labhart, T., Baumann, F., Mazzoni, E., Pichaud, F. and Desplan, C. (2003). Homothorax switches function of *Drosophila* photoreceptors from color to polarized light sensors. *Cell* **115**, 267-279.

Wolfinger, R. (1993). Covariance structure selection in general mixed models. *Commun. Stat. Simulat.* **22**, 1079-1106.

Wolfinger, R. D. (1996). Heterogeneous variance-covariance structures for repeated measures. *J. Agric. Biol. Envir. Stat.* **1**, 205-230.

Wunderer, H. and Smola, U. (1982). Fine-structure of ommatidia at the dorsal eye margin of *Calliphora erythrocephala* Meigen (Diptera, Calliphoridae) - an eye region specialized for the detection of polarized-light. *Int. J. Insect Morphol.* **11**, 25-38.

Yamaguchi, S., Wolf, R., Desplan, C. and Heisenberg, M. (2008). Motion vision is independent of color in *Drosophila*. *Proc. Natl. Acad. Sci. USA* **105**, 4910-4915.

Zufall, F., Schmitt, M. and Menzel, R. (1989). Spectral and polarized-light sensitivity of photoreceptors in the compound eye of the cricket (*Gryllus bimaculatus*). *J. Comp. Physiol. A* **164**, 597-608.

Is there a common genetic program to specify polarization-sensitive photoreceptors in insects?

M. J. Henze[1,*], M. Wernet[2] and T. Labhart[1]

[1]*Zoologisches Institut, Universität Zürich, Winterthurerstr. 190, Zürich, Switzerland* and
[2]*Neurobiology Department, Stanford University, 299 W. Campus Drive, CA, USA*

*Author for correspondence (e-mail: miriam.henze@zool.uzh.ch)

I

II

Pilot study

III

IV

Author contributions statement
MJH conducted the experiments, analyzed the data, prepared the figures and wrote the manuscript.
MW designed the experiments and co-edited the manuscript.
TL co-edited the manuscript.

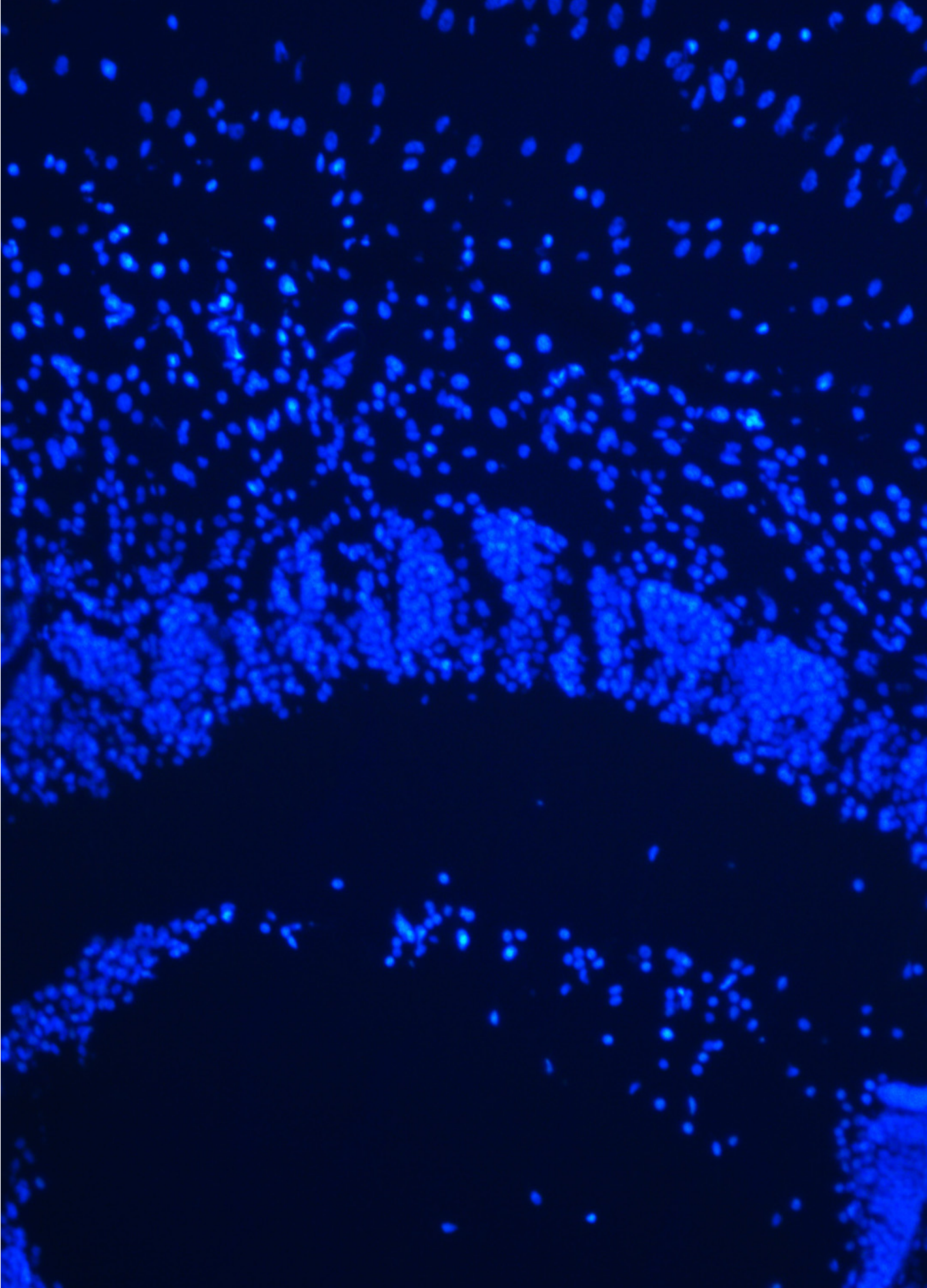

Cover picture. DAPI staining of a frozen section trough the optic lobe and the compound eye of the cricket *Gryllus bimaculatus* showing the arrangement of cell nuclei. Up in the picture corresponds to distal in reality. Photograph taken by Miriam Henze.

Is there a common genetic program to specify polarization-sensitive photoreceptors in insects?

M. J. Henze[1,*], M. Wernet[2], T. Labhart[1]

[1]*Zoologisches Institut, Universität Zürich, Winterthurerstr. 190, Zürich, Switzerland* and [2]*Neurobiology Department, Stanford University, 299 W. Campus Drive, CA, USA*

*Author for correspondence (email: miriam.henze@zool.uzh.ch)

Summary

The compound eyes of many insect species possess a so-called dorsal rim area (DRA), a skyward-directed region in which photoreceptors are specialized to detect polarized light. Group-specific differences in the morphology of DRA ommatidia have led to the assumption that polarization vision evolved independently in several insect taxa. However, developmental evidence from fruit flies and grasshoppers suggests that DRA formation during metamorphosis of the derived Diptera and during embryogenesis of the phylogenetically more primitive Orthoptera is initiated by homologous signaling pathways. A promising route to further address the question of DRA ancestry is to study downstream mediators of DRA specification in different taxa. The general employment of one selector gene would support a monophyletic origin while group-specific selector genes would favor polyphyly. So far homothorax (hth), the DRA selector gene in the fruit fly, could not be detected in the eye field of the embryonic grasshopper. Our pilot experiments failed to verify the expression of hth in the DRA of another orthopteran species, the cricket (*Gryllus bimaculatus*). Thus, polarization vision in insects might be a case of convergent evolution of morphological traits via the recruitment of homologous upstream signaling pathways.

Key words: polarization vision, dorsal rim area (DRA), development, wingless, Iroquois complex, homothorax, extradenticle, *Gryllus bimaculatus*.

Introduction

Among insects, the ability to exploit skylight polarization for spatial orientation is widespread (for reviews see (Horváth and Varjú, 2004; Labhart and Meyer, 1999; Wehner and Labhart, 2006)). Photoreceptors in an upward-directed region of the compound eye, the so-called dorsal rim area (DRA), are modified to be strongly sensitive to the electric vector of linearly polarized light. Specializations found in DRA ommatidia of vastly different species comprise two sets of homochromatic photoreceptors with strictly aligned and mutually orthogonal microvilli, an enlarged cross-sectional area of the rhabdom and in many cases degraded optics. Apart from these functional adaptations, however, group-specific fine-structural disparities in the design of DRA ommatidia suggest that polarization vision arose independently in several insect taxa (Labhart and Meyer, 1999). In addition to anatomical and physiological comparisons, developmental studies can provide evidence for evolutionary relationships. In the fruit fly (*Drosophila melanogaster*) some components of a signaling pathway that trigger the formation of the DRA during metamorphosis have been identified: The diffusible morphogen wingless (Wg) is expressed in the tissue circumscribing the differentiating pupal retina. In the presence of the Iroquois complex (Iro-C), which is confined to the dorsal half of the eye field, intermediate levels of Wg emanating from the future head capsule into the peripheral retina induce the expression of the selector gene homothorax (hth) in a subset of photoreceptors (Tomlinson, 2003; Wernet et al., 2003). Hth translocates its cofactor Extradenticle (Exd) into the nucleus (Jaw et al., 2000; Pai et al., 1998; Rieckhof et al., 1997) where they together presumably form transcriptional complexes with HOX proteins to execute the fate switch of the cell from color to polarized light sensitivity (Wernet et al., 2003). The described expression patterns persist into adulthood and can therefore also be detected in the imago (Tomlinson, 2003; Wernet et al., 2003).

In the embryonic grasshopper (*Schistocerca americana*), the only other insect species for which data on the molecular genetic control of DRA development exists so far, Wg is found in the presumptive head cuticle bordering the differentiating retina and Iro-C in the dorsal-most region of the eye field (Dong and Friedrich, 2005). There is a strong spatial correlation between the Iro-C expression in the embryo and the dorsally restricted outline of the DRA in the first instar nymph. Assuming that the expression patterns remain until later development, DRA formation in *Schistocerca* and *Drosophila* are very likely to be initiated by homologous signaling pathways.

Grasshoppers and flies are only distantly related, the former

belonging to the phylogenetically primitive order of the Orthoptera and the later being a member of the derived Diptera. It is therefore most parsimonious to assume that Wg and Iro-C are generally involved in insect DRA specification. This, however, does not necessarily challenge the concept that insect DRAs are polyphyletic. Homologous groups of transcription factors have previously been shown to be responsible for the formation of independently evolved morphological traits (e.g. (Gompel and Carroll, 2003; Sucena et al., 2003)). One possibility to investigate this hypothesis is to examine the expression of hth, the *Drosophila* downstream mediator of DRA specification (Wernet et al., 2003), in non-dipteran species. Shared employment of hth as a DRA selector gene would support the idea of homology while the absence of Hth would favor convergent evolution.

Using nuclear localization of Exd as a marker, no Hth expression could be detected in the eye field of the embryonic grasshopper head (Dong and Friedrich, 2005). This result suggests that the selector gene input for DRA development is not conserved between Diptera and Orthoptera. However, denser taxon sampling is required to address this question. We have therefore conducted a pilot study to investigate whether Hth functions as a downstream mediator of DRA specification in the cricket *Gryllus bimaculatus*, a close relative of the grasshopper for which a partial coding sequence of the hth gene has already been cloned (Inoue et al., 2002).

An elaborate comparison between *Drosophila* and *Gryllus* including embryonic as well as larval stages is promising because of marked differences in DRA design and development (Fig. 1): (1) Between holometabolous insects, such as fruit flies, and hemimetabolous insects, such as crickets, there are fundamental differences in the timing of eye development. In *Drosophila*, compound eyes start to develop in the eye-antennal imaginal disc of the last larval instar, i.e. at the onset of metamorphosis, and are completed when the adult fly emerges from the pupa (Wolff and Ready, 1993). Cricket nymphs, on the other hand, hatch with small compound eyes already equipped with a DRA. Throughout larval stages additional rows of ommatidia are recruited from a budding zone at the anterior margin of the eye, thereby expanding the DRA during every molt (Labhart and Keller, 1992; Pohl, 1988). (2) DRAs vary in shape among insect species. Compared to *Drosophila*, where polarization-sensitive photoreceptors are located in one to two rows of ommatidia along the entire dorsal eye margin (Fortini and Rubin, 1990; Tomlinson, 2003; Wernet et al., 2003), the DRA in *Gryllus* is wider and shorter and is restricted to the dorso-frontal region of the eye (Blum and Labhart, 2000; Burghause, 1979). (3) On closer inspection, several group-specific features of DRA ommatidia become evident that do not necessarily result from general disparities in eye design between the different taxa. In orthopteran species, the visual fields of DRA ommatidia are enlarged by degraded optics and reduced or missing screening pigment. Polarization vision is mediated by several blue receptors that together with ultraviolet sensitive cells form a closed rhabdom. The microvilli orientation of one of the blue receptors is orthogonal to those of all the others (Blum and Labhart, 2000; Burghause, 1979; Burghause, 1981; Egelhaaf and Dambach, 1983; Eggers and Gewecke, 1993; Henze et al., 2009; Herzmann and Labhart, 1989; Homberg and Paech, 2002; Labhart et al., 1984; Ukhanov et al., 1996; Zufall et al., 1989). In a typical dipteran fly, in contrast, DRA ommatidia do not show optical specializations and contain an open rhabdom with six green-sensitive outer and two tiered ultraviolet-sensitive inner photoreceptors. Only the ultraviolet receptors show high polarization sensitivity due to micovillar alignment and the micovilli of the distally located receptor 7 are orthogonal to those of the proximal photoreceptor 8 (Fortini and Rubin, 1990; Hardie, 1984; Hardie, 1985; Wunderer and Smola, 1982a; Wunderer and Smola, 1982b).

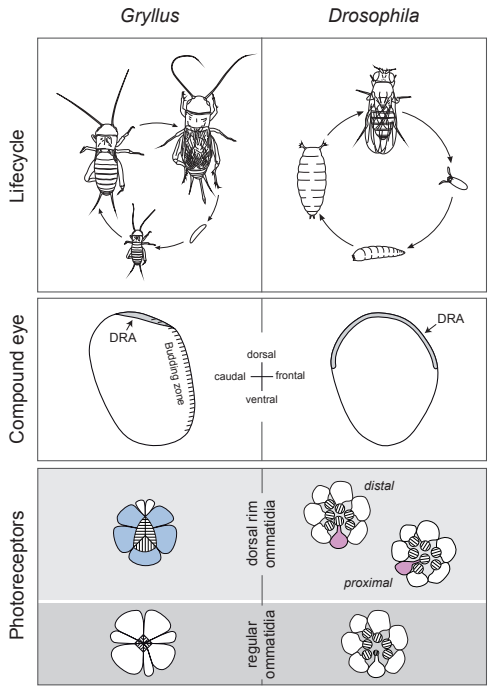

Fig. 1. Comparison between the DRA of *Gryllus* and *Drosophila*.
Development (first row): Cricket larvae hatch with small compound eyes already equipped with a DRA. Throughout larval stages additional ommatidia are recruited from a budding zone at the anterior margin of the eye (see second row). In *Drosophila*, compound eyes do not form until metamorphosis and are completed before the imago emerges from the pupa.
Shape (second row): Compared to *Drosophila*, where polarization-sensitive photoreceptors are located in a slender line along the entire dorsal eye margin, the DRA in *Gryllus* is wider, shorter and is restricted to the dorsal-most part of the eye.
Fine-structure (third row): As indicated in schematic cross-sections, DRA photoreceptors of crickets and fruit flies differ substantially in spectral (blue versus ultraviolet) and structural details (e.g. number of microvillar types of homochromatic receptors 4/1 versus 1/1).
Drawings are partly taken from (Labhart and Meyer, 1999).

Taken together, these points demonstrate important differences in temporal, spatial and fine-structural aspects of DRA development. It is therefore particularly interesting to investigate if and how this is reflected in the molecular genetic control of retinal patterning in *Gryllus* and *Drosophila*.

Materials and methods

Animals

This pilot study was carried out on two-spotted crickets (*Gryllus bimaculatus*, De Geer) and adult fruit flies (*Drosophila melanogaster*, Meigen) of the strains *Canton-S* and *w1118*. The red-eyed *Canton-S* and the white-eyed *w1118* flies are wild-type in every aspect except that the latter lack screening pigment in their compound eyes. All insects were obtained from laboratory stocks at the Hokkaido University (Sapporo, Japan).

Tissue preparation

Heads of adult flies and larval crickets as well as cricket brains and cricket embryos were fixed in phosphate buffered paraformaldehyde (2% or 4%) at room temperature for 45 minutes or at 4°C overnight. To prepare the tissue for cryosections, it was incubated in 20% sucrose in PBS (phosphate buffered saline) at 4°C for at least 12 hours, then embedded in freezing medium (OCT Cryocompound, Leica Microsystems, Wetzlar, Germany) and frozen in liquid nitrogen. We cut 10 to 20 µm sections on a cryostat (Leica CM1510S, Leica Microsystems, Wetzlar, Germany), mounted them on silane coated slides and dried them at room temperature for immunostaining or at 65°C for *in situ* hybridization. The slides were stored at -80°C.

Immunostaining

Primary antibodies used for immunohistochemistry were polyclonal anti-Hth guinea pig 1/2000, 1/500 or 1/200 (kindly provided by R. Mann, Columbia University, New York, NY, USA) and anti-ElaV mouse or rat monoclonals 1/10 (Developmental Studies Hybridoma Bank, University of Iowa, Iowa City, IA, USA) raised against the respective *Drosophila melanogaster* protein. As secondary antibodies we applied Alexa Fluor 555-conjugated rabbit anti-mouse (Molecular Probes, Eugene, OR,

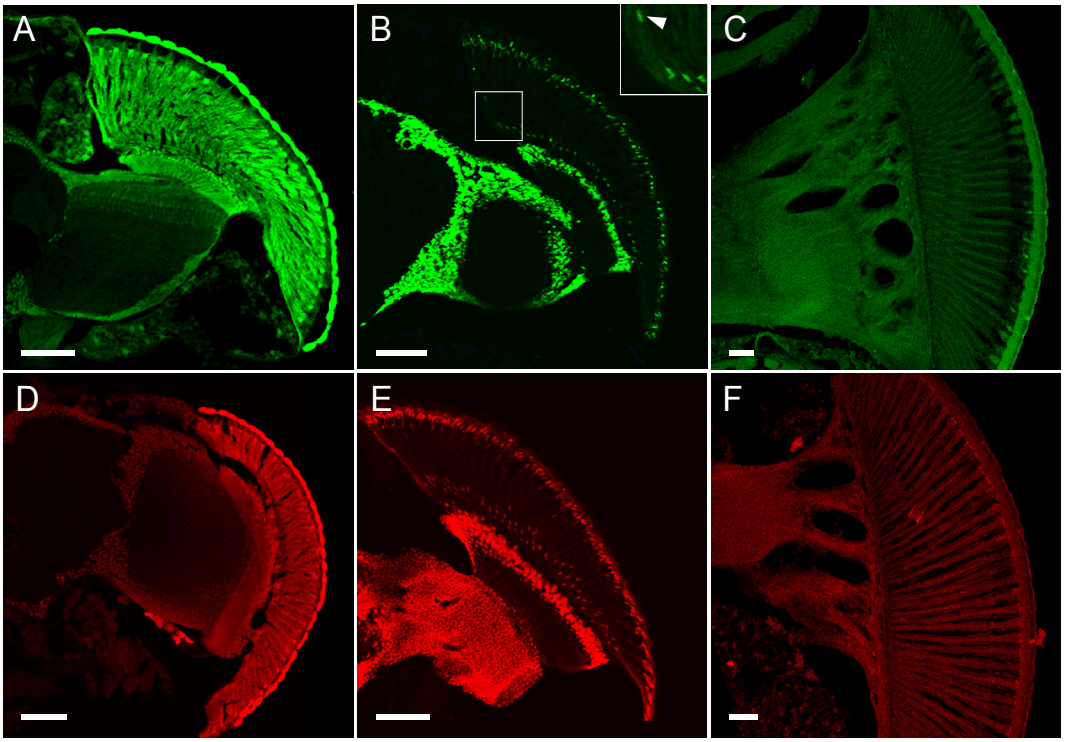

Fig. 2. Immunostaining for the neuronal marker Elav. Transverse frozen sections through compound eye and optic lobe treated with rat anti *Drosophila* Elav (A-C) or mouse anti *Drosophila* Elav (D-E) antibodies. (A, D) *Canton-S Drosophila*: Elav-positive cells are clearly visible in the optic lobe, but signals in the eye are masked by autofluorescent screening pigment. (B, E) *w1118 Drosophila*: Neuronal nuclei in the eye and optic lobe are labeled. The arrowhead indicates a distally displaced R8 nucleus typical of the DRA. (C, F) *Gryllus bimaculatus*: No specific cross-reactivity. Up corresponds to dorsal in all panels of this figure as well as in Figs. 3-5. Scalebars = 50 µm.

USA), Cy2-conjugated donkey anti-rat and Cy3-conjugated donkey anti-guinea pig (Jackson ImmunoResearch, West Grove, PA, USA) in a dilution of 1/200.

Whole-mounts and sections were washed in PBST (PBS containing 0.2% Triton X-100), blocked with 1% BSA (bovine serum albumin) in PBST for at least 30 minutes and incubated with the primary antibody in blocking solution (1% BSA in PBST) at 4°C up to five days. After washing with PBST, the tissue was treated with the secondary antibody in blocking solution up to three days at 4°C, washed with PBST and dehydrated in an ethanol series (70%, 90%, 100%). Whole-mounts and sections were cleared in methysalicylate and xylene respectively, and inspected under a confocal laser scanning microscope (FV300 or FV1000, both Olympus, Tokyo, Japan). Images were processed in Adobe® Photoshop (Adobe Systems Incorporated, San Jose, CA, USA).

In situ hybridization

Sense and antisense digoxigenin (DIG) labeled RNA probes for *in situ* hybridization were transcribed by a DIG RNA labeling kit (Roche Diagnostics, Rotkreuz, Switzerland) from linearized plasmids containing a 400 to 700 bp coding fragment of the *Gryllus bimaculatus* extradenticle (exd), homothorax (hth) or wingless (wg) gene (kindly provided by S. Noji, University of Tokushima, Tokushima City, Japan). After synthesis, the riboprobes were precipitated with 4 mol/l LiCl and 100% ethanol. They were used for *in situ* hybridization only if sufficient amounts of transcript could be detected in a control gel.

Cryosections were postfixed in 4% phosphate buffered paraformaldehyde for 30 minutes. After an acetylation and several washing steps, the tissue was equilibrated in hybridization buffer (50% formamide, 5% Denhardt's solution, 750 mmol/l NaCl, 75 mmol/l trisodium citrate dihydrate, 0.5 mg/ml herring sperm DNA, 0.25 mg/ml torula yeast RNA) for 3 hours and incubated with the probe diluted in hybridization buffer at 58°C overnight. Further washing steps were followed by equilibration in blocking solution (3% skim milk powder) and detection with an alkaline phosphatase-coupled anti-Dig Fab-fragment (Roche Diagnostics, Mannheim, Germany) in blocking solution. The signal was developed by a colorimetric reaction with the two substrates nitro blue tetrazolium (NBT) and 5-bromo-4-chloro-3-indolyl phosphate (BCIP) in alkaline phosphatase solution containing 50 mmol/l $MgCl_2$ and 1 mmol/l levamisole. Images were produced by a Color view IIIu camera mounted on a BX61 microscope (both: Olympus, Tokyo, Japan). Brightness and contrast were adjusted using Adobe® Photoshop (Adobe Systems Incorporated, San Jose, CA, USA).

Results

No cross-reaction of anti Drosophila Hth in larval crickets

Drosophila DRA photoreceptors 7 and 8 are characterized by Hth expression (Wernet et al., 2003). In a first approach to identify molecular downstream factors that control DRA development in *Gryllus bimaculatus*, we tested whether Hth can be detected in the DRA of crickets by anti *Drosophila* Hth. To discriminate photoreceptors from other cells in the compound eye by immunolabeling, we studied whether one of the available anti *Drosophila* Elav monoclonals is suited as a neuronal marker in *Gryllus bimaculatus*. None of these antibodies showed specific cross-reactivity when applied on frozen sections through the compound eye and the optic lobe of crickets (Fig. 2 C, F and Fig. 3 B). The same result was obtained for whole-mount cricket brains (not shown).

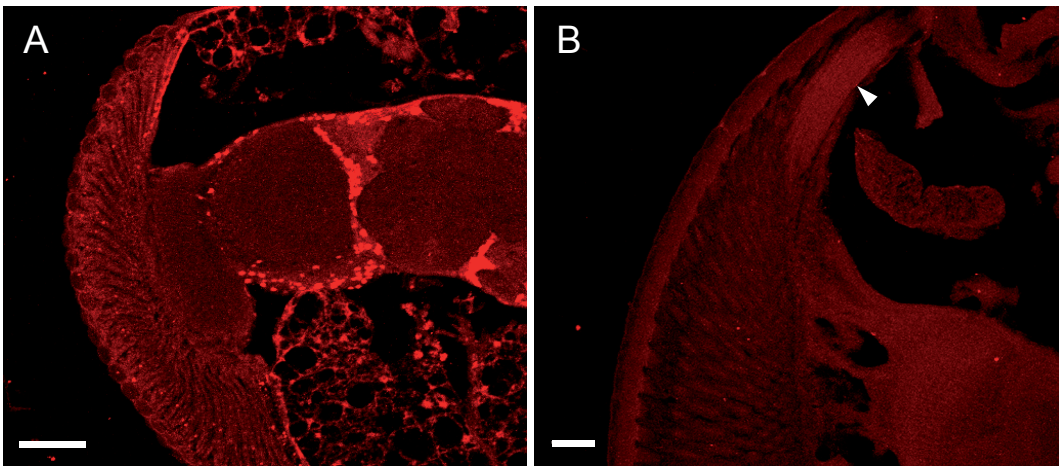

Fig. 3. Immunostaining for the DRA marker Hth. Transverse frozen sections through compound eye and optic lobe incubated with guinea pig anti *Drosophila* Hth antibody. (A) *w1118 Drosophila*: Corresponding to its multiple functions in developmental processes, Hth expression is not only detected in photoreceptor nuclei of the DRA but also in the brain and in other parts of the head. (B) *Gryllus bimaculatus*: No specific cross-reactivity. Note the slightly stronger autofluorescence of the DRA (arrowhead) compared to the rest of the eye. Scalebars = 100 µm.

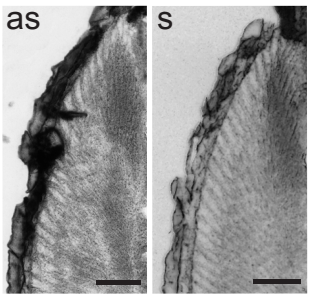

Fig. 4. *In situ* hybridization for the DRA marker Exd. Dorsal half of a longitudinal section through the compound eye of *Gryllus bimaculatus* incubated with antisense (as) and sense (s) probe for cricket exd mRNA. We did not observe a specific labeling but often a darker background staining in the DRA than in the rest of the eye. Scalebars = 100 µm.

In parallel to *Gryllus* preparations, we processed sections and whole-mounts of *Drosophila* heads as positive controls. Since the red screening pigment in the compound eye of the wild-type *Canton-S* strain masks signals in both the red and the green channel by strong autofluorescence (Fig. 2 A, D), we also examined white-eyed *w1118* flies. A specific signal was observed for all antibodies. On sections, rat and mouse anti Elav antibodies labeled neuronal nuclei in the brain and in the compound eye (Fig. 2 B, E) including those of DRA photoreceptors (Fig. 2 B, inset). Hth expression was detected in photoreceptor nuclei in the DRA as well as in the brain and in several other parts of the head (Fig. 3 A). This is consistent with the multiple roles Hth plays in developmental patterning processes. Results for whole-mounts were essentially the same (not shown).

No hth, exd and wg transcripts in the compound eye of larval crickets?

Since the available anti *Drosophila* antibodies did not cross-react in *Gryllus bimaculatus*, we investigated the expression of molecular components that are potentially involved in the control of DRA development in the cricket by *in situ* hybridization. In *Drosophila*, a graded Wg signal in the presence of Iro-C induces the expression of hth in the inner photoreceptors (Tomlinson, 2003; Wernet et al., 2003). Hth translocates Exd into the nucleus where they presumably form transcriptional complexes with HOX proteins to execute the fate switch from color to polarized light sensitivity (Wernet et al., 2003). We applied *in situ* probes for the *Gryllus bimaculatus* orthologs of *Drosophila* wg, hth and exd to frozen sections through the compound eyes of larval crickets. Despite testing several protocols, various hybridization temperatures and high probe concentrations, we could not find any evidence of wg, hth or exd expression in the DRA (Fig. 4) nor in any other part of the eye nor in the adjacent area of the head. We also processed sections through the brain and through embryos, neither of which produced a positive result (not shown). A two-step reverse transcription polymerase chain reaction (RT-PCR) for relative quantification of transcripts in the upper and lower part of the compound eye using β-actin as an internal control failed to amplify wg and yielded only little product for hth, which was slightly more abundant ventrally than dorsally (not shown).

Special tissue properties of the DRA

In dried sections through the compound eye, the DRA can easily be localized since it is the only unpigmented eye region (Fig. 5 A). During *in situ* hybridization the brownish screening pigment in the other parts of the eye is gradually rinsed out (Fig. 5 B) and therefore cannot serve as a negative marker to identify the DRA. However, in processed sections totally devoid of screening pigment the DRA shows a stronger blue-induced green autofluorescence than the rest of the eye (Fig. 5 C). The same phenomenon can be observed to a lesser extent in the red spectral range as a result of green excitation (Fig. 5 D, see also Fig. 3 B). After signal development the DRA was also frequently marked by a dark background staining (Fig. 4).

Discussion

Molecular genetic control of DRA development

In order to shed light on the evolution of skylight polarization vision in insects we have investigated whether homologous signaling pathways (wg) and / or selector genes (hth) induce DRA formation in both flies and crickets. We used two alternative approaches to analyze the pattern of hth expression during DRA development in the cricket: localization of Hth protein by immunocytochemistry and detection of hth mRNA by *in situ* hybridization.

Neither immunostainings with anti *Drosophila* Hth nor with anti *Drosophila* Elav were successful in the cricket. Previous experiments have shown that the Hth antibody we used cross-reacts in the house fly, *Musca domestica* (Wernet, 2004), but not in the monarch butterfly, *Danaus plexippus* (J. Stalleicken, personal communication). We have also observed that the anti *Drosophila* Elav raised in the rat works in *Musca*, whereas the one generated in the mouse does not (M. Wernet, unpublished). Our results are therefore not unexpected. However, since antigenic relatedness does not necessarily correspond to species relatedness, it might still be worth testing other Hth antibodies that are available. Alternatively, one could try to raise an antibody specifically against *Gryllus* Hth. In any case, an immunohistochemical approach would be advisable as it is essential to verify that translation of mRNA takes place and especially valuable if rare transcripts correlate with more abundant protein. If all attempts to label Hth fail, one should at least try to detect it indirectly by nuclear accumulation of its cofactor Exd. An Exd antibody whose cross-reactivity has been verified in *Gryllus bimacultaus* is available (Inoue et al., 2002).

Even though we used a probe specifically designed for *Gryllus bimaculatus*, we were unable to provide evidence for hth transcripts in the compound eye of larval crickets by *in situ* hybridization. There are several possibilities to interpret this result. Expression might only be present in the embryo and not in the nymphs, or may only be found in the budding

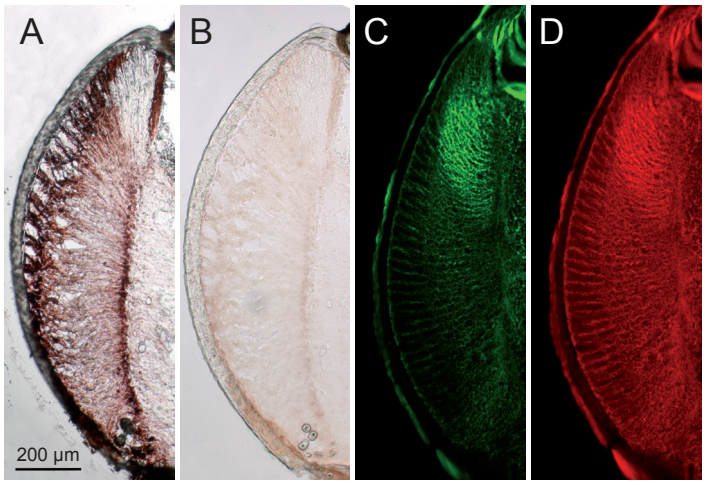

Fig. 5. Tissue properties of the cricket DRA. Longitudinal frozen sections through the compound eye of *Gryllus bimaculatus* at different stages of the *in situ* hybridization protocol. (A) After drying: The DRA is the only area in the compound eye that is devoid of screening pigment. (B) After first washing: Most of the screening pigment has been rinsed out. (C, D) Before signal development: The DRA shows a stronger autofluorescence than the rest of the eye, both in the green and in the red spectral range.

zone of the larval DRA at certain times prior to ecdysis. Such a spatially and temporally restricted signal might have been overlooked. However, we ensured that we examined larvae that were close to molting as indicated by a double-layered cuticle. We have collected sections of the whole head including the budding zone and the brain and we have also processed embryos without any positive result. In *Drosophila*, Hth is not an eye-specific transcriptional regulator but plays multiple roles in developmental patterning processes, such as segment specification, central nervous system formation and leg morphogenesis. Therefore, even if absent from the DRA, it is likely to be expressed elsewhere in the cricket. In fact, hth transcripts have previously been detected in *Gryllus bimaculatus* in the proximal region of the developing embryonic leg bud by the same *in situ* probe that we used in our experiments (Inoue et al., 2002). This gives reason to believe that our negative findings have procedural causes rather than proving the absence of hth expression. We can rule out a principal failure of our protocol since we have applied other probes in parallel that produced a specific staining. However, this concerned retinal opsins for which a high-copy transcript was to be expected. As for hth, probes for the transcription factors wg and exd (Fig. 4) similarly yielded no positive results. Therefore it could be that the sensitivity of our technique has to be improved in order to assess less abundant mRNA.

A powerful technique to detect rare messages is PCR. We have run a two-step RT-PCR for relative quantification of hth and wg transcripts in the lower and upper part of the compound eye. Our results are not meaningful, though, since it was impossible to identify an exponential phase condition for the endogenous standard at which the gene of interest could be verified. Hence, we recommend repeating the experiments either with a detection method of higher sensitivity than ethidium bromide staining of agarose gels or with a competitive assay in which the signal of the internal control is attenuated by the presence of a certain amount of modified primers that cannot be extended (Competimer™ Technology, Ambion, Austin, TX, USA).

A spatial and temporal correlation between the expression of a transcription factor and DRA formation does not prove causality. For this purpose functional analyses are needed. In a more extensive study, one should therefore conduct molecular genetic manipulation experiments alongside with *in situ* hybridizations and immunostainings. One option would be the application of lithium, which is a potent activator of the wg signaling pathway across species (Davies et al., 2000; Dong and Friedrich, 2005; Stambolic et al., 1996). Apart from that, the cricket is amenable to RNA interference (RNAi) techniques. The effect of RNAi mediated knockdown of hth and exd on appendage formation and body segmentation in *Gryllus bimaculatus* has recently been shown (Mito et al., 2008; Ronco et al., 2008). Silencing of wg expression by RNAi has also been tried (Miyawaki et al., 2004). However, the results were ambiguous. Even though the amount of wg mRNA was reduced in treated embryos, a phenotype with regard to segmentation could not be observed. This suggests the presence of functionally redundant pathways which might be constituted by members of the Wnt gene family other than wg. Possibly for the same reason, an ectopic activation of the wg pathway in the presence of Iro-C induces DRA formation in the fruit fly, but reception of the Wg signal is not required for normal DRA development (Wernet et al., 2003).

Autofluorescence of the DRA

In sections through the compound eye of the cricket, the DRA showed a prominent blue-induced green autofluorescence. The

same has previously been reported in the live animal (Stavenga, 1989). It was attributed to the fact that the screening pigment masks the autofluorescence of the visual pigments in the rest of the eye. However, in our sections the screening pigment had been rinsed out completely. We have also observed that the DRA of living white-eyed crickets fluoresces stronger than the rest of the eye (T. Labhart and M. Henze, unpublished). Thus, the phenomenon is likely due to the blue-sensitive visual pigment which is heavily expressed in the DRA (Henze et al., 2009; Labhart et al., 1984; Zufall et al., 1989).

Acknowledgments

We are most grateful to H. Aonuma for the opportunity to work in his laboratory, and to him and M. Sakura for excellent organizational support. We thank R. Mann, S. Noji and the Hybridoma bank for reagents, H. Aonuma, D. Hatakeyama, T. Watanabe, T. Hiraguchi, M. Sakura, M. Kikuchi, A. Bohnert and M. Kohler for technical assistance, T. Allison for a stimulating discussion and R. Tourle for proofreading the manuscript. This study was supported by a 3 month research fellowship from the Hokkaido University to M.J.H..

References

Blum, M. and Labhart, T. (2000). Photoreceptor visual fields, ommatidial array, and receptor axon projections in the polarisation-sensitive dorsal rim area of the cricket compound eye. *J. Comp. Physiol. A* **186**, 119-128.

Burghause, F. M. H. R. (1979). Die strukturelle Spezialisierung des dorsalen Augenteils der Grillen (Orthoptera, Grylloidea). *Zool. Jb. Physiol.* **83**, 502-525.

Burghause, F. M. H. R. (1981). Die Struktur der Komplexaugen von der Gewächshausschrecke, *Tachycines asynamorus*. *Zool. Beitr. NF* **27**, 185-197.

Davies, S. P., Reddy, H., Caivano, M. and Cohen, P. (2000). Specificity and mechanism of action of some commonly used protein kinase inhibitors. *Biochem. J.* **351**, 95-105.

Dong, Y. and Friedrich, M. (2005). Comparative analysis of Wingless patterning in the embryonic grasshopper eye. *Dev. Genes. Evol.* **215**, 177-197.

Egelhaaf, A. and Dambach, M. (1983). Giant rhabdomes in a specialized region of the compound eye of a cricket - *Cycloptiloides canariensis* (Insecta, Gryllidae). *Zoomorphology* **102**, 65-77.

Eggers, A. and Gewecke, M. (1993). The dorsal rim area of the compound eye and polarization vision in the desert locust (*Schistocerca gregaria*). In *Sensory Systems of Arthropods* (ed. K. Wiese, F. G. Gribakin, A. V. Popov, G. Renninger), pp. 101-109. Basel: Birkhäuser Verlag.

Fortini, M. E. and Rubin, G. M. (1990). Analysis of cis-acting requirements of the Rh3 and Rh4 genes reveals a bipartite organization to rhodopsin promoters in *Drosophila melanogaster. Genes. Dev.* **4**, 444-463.

Gompel, N. and Carroll, S. B. (2003). Genetic mechanisms and constraints governing the evolution of correlated traits in drosophilid flies. *Nature* **424**, 931-935.

Hardie, R. C. (1984). Properties of photoreceptors R7 and R8 in dorsal marginal ommatidia in the compound eyes of *Musca* and *Calliphora*. *J. Comp. Physiol*. **154**, 157-165.

Hardie, R. C. (1985). Functional organization of the fly retina. In *Progress in Sensory Physiology*, vol. 5 (ed. H. Autrum, D. Ottoson, E. R. Perl, R. F. Schmidt, H. Shimazu and W. D. Willis), pp. 1-79. Berlin: Springer-Verlag.

Henze, M. J., Gesemann, M., Dannenhauer, K. and Labhart, T. (2009). Opsin divergence and retinal regionalization in the visual system of the cricket (*Gryllus bimaculatus*). In *Two Facets of Insect Vision: Polarization Sensitivity and Visual Pigments* (ed. M. J. Henze), pp. 69-86. PhD thesis, University of Zürich, Switzerland.

Herzmann, D. and Labhart, T. (1989). Spectral sensitivity and absolute threshold of polarization vision in crickets - a behavioral study. *J. Comp. Physiol. A* **165**, 315-319.

Homberg, U. and Paech, A. (2002). Ultrastructure and orientation of ommatidia in the dorsal rim area of the locust compound eye. *Arthropod. Struct. Dev.* **30**, 271-280.

Horváth, G. and Varjú, D. (2004). Polarized light in animal vision - polarization patterns in nature. Berlin: Springer-Verlag.

Inoue, Y., Mito, T., Miyawaki, K., Matsushima, K., Shinmyo, Y., Heanue, T., Mardon, G., Ohuchi, H. and Noji, S. (2002). Correlation of expression patterns of homothorax, dachshund, and Distal-less with the proximodistal segmentation of the cricket leg bud. *Mech. Develop*. **113**, 141-148.

Jaw, T. J., You, L. R., Knoepfler, P. S., Yao, L. C., Pai, C. Y., Tang, C. Y., Chang, L. P., Berthelsen, J., Blasi, F., Kamps, M. P. et al. (2000). Direct interaction of two homeoproteins, Homothorax and Extradenticle, is essential for EXD nuclear localization and function. *Mech. Develop*. **91**, 279-291.

Labhart, T., Hodel, B. and Valenzuela, I. (1984). The physiology of the cricket's compound eye with particular reference to the anatomically specialized dorsal rim area. *J. Comp. Physiol*. **155**, 289-296.

Labhart, T. and Keller, K. (1992). Fine-structure and growth of the polarization-sensitive dorsal rim area in the compound eye of larval crickets. *Naturwissenschaften* **79**, 527-529.

Labhart, T. and Meyer, E. (1999). Detectors for polarized skylight in insects: A survey of ommatidial specializations in the dorsal rim area of the compound eye. *Microsc. Res. Techniq.* **47**, 368-379.

Mito, T., Ronco, M., Uda, T., Nakamura, T., Ohuchi, H. and Noji, S. (2008). Divergent and conserved roles of extradenticle in body segmentation and appendage formation, respectively, in the cricket *Gryllus bimaculatus*. *Dev. Biol.* **313**, 67-79.

Miyawaki, K., Mito, T., Sarashina, I., Zhang, H., Shinmyo, Y., Ohuchi, H. and Noji, S. (2004). Involvement of Wingless/Armadillo signaling in the posterior sequential segmentation in the cricket, *Gryllus bimaculatus* (Orthoptera), as revealed by RNAi analysis. *Mech. Dev*. **121**, 119-130.

Pai, C. Y., Kuo, T. S., Jaw, T. J., Kurant, E., Chen, C. T., Bessarab, D. A., Salzberg, A. and Sun, Y. H. (1998). The Homothorax homeoprotein activates the nuclear localization of another homeoprotein, Extradenticle, and suppresses eye development in *Drosophila*. *Gene. Dev*. **12**, 435-446.

Pohl, R. (1988). Das postembryonale Wachstum der Retina und die Anatomie von Lamina und Medulla bei *Gryllus bimaculatus* De Geer 1773, Teil I: Einleitung; Material und Methoden; Differenzierungszone. *Zool. Jb. Anat*. **117**, 353-393.

Rieckhof, G. E., Casares, F., Ryoo, H. D., AbuShaar, M. and Mann, R. S. (1997). Nuclear translocation of Extradenticle requires homothorax, which encodes an Extradenticle-related homeodomain protein. *Cell* **91**, 171-183.

Ronco, M., Uda, T., Mito, T., Minelli, A., Noji, S. and Klingler, M. (2008). Antenna and all gnathal appendages are similarly transformed by homothorax knock-down in the cricket *Gryllus bimaculatus*. *Dev. Biol*. **313**, 80-92.

Stambolic, V., Ruel, L. and Woodgett, J. R. (1996). Lithium inhibits glycogen synthase kinase-3 activity and mimics Wingless signalling in intact cells. *Curr. Biol*. **6**, 1664-1668.

Stavenga, D. G. (1989). Pigments in compound eyes. In *Facets of vision* (ed. D. G. Stavenga and R. C. Hardie), pp. 152-172. Berlin: Springer-Verlag.

Sucena, E., Delon, I., Jones, I., Payre, F. and Stern, D. L. (2003). Regulatory evolution of shavenbaby/ovo underlies multiple cases of morphological parallelism. *Nature* **424**, 935-938.

Tomlinson, A. (2003). Patterning the peripheral retina of the fly: decoding a gradient. *Dev. Cell*. **5**, 799-809.

Ukhanov, K., Leertouwer, H., Gribakin, F. and Stavenga, D. (1996). Dioptrics of the facet lenses in the dorsal rim area of the cricket *Gryllus bimaculatus*. *J. Comp. Physiol. A* **179**, 545-552.

Wehner, R. and Labhart, T. (2006). Polarisation vision. In *Invertebrate vision* (ed. E. Warrant and D. E. Nilsson), pp. 291-348. New York: Cambridge University Press.

Wernet, M., Labhart, T., Baumann, F., Mazzoni, E., Pichaud, F. and Desplan, C. (2003). Homothorax switches function of *Drosophila* photoreceptors from color to polarized light sensors. *Cell* **115**, 267-279.

Wernet, M. F. (2004). Patterning the retina of *Drosophila melanogaster* for color and polarized light vision. *PhD thesis*, Universität Köln, Germany.

Wolff, T. and Ready, D. F. (1993). Pattern formation in the *Drosophila* retina. In *The development of Drosophila melanogaster*, vol. 2 (ed. M. Bate and A. Martinez Arias), pp. 1277-1325. Plainview, NY: Cold Spring Harbor Laboratory Press.

Wunderer, H. and Smola, U. (1982)a. Morphological differentiation of the central visual cells R7/8 in various regions of the blowfly eye. *Tissue Cell* **14**, 341-358.

Wunderer, H. and Smola, U. (1982)b. Fine structure of ommatidia at the dorsal eye margin of *Calliphora erythrocephala* Meigen (Diptera, Calliphoridae): an eye region specialized for the detection of polarized light. *Int. J. Insect Morphol.* **11**, 25-38.

Zufall, F., Schmitt, M. and Menzel, R. (1989). Spectral and polarized light sensitivity of photoreceptors in the compound eye of the cricket (*Gryllus bimaculatus*). *J. Comp. Physiol. A* **164**, 597-608.

Opsin divergence and retinal regionalization in the visual system of the cricket (*Gryllus bimaculatus*)

Miriam J. Henze[1,2]*, Matthias Gesemann[1], Kerstin Dannenhauer[1] and Thomas Labhart[1]

[1] *Institute of Zoology, University of Zürich, Zürich, Switzerland,* [2] *Department of Cell and Organism Biology, Lund, Sweden*

*Author for correspondence (e-mail: miriam.henze@cob.lu.se)

I

II

III

IV

Manuscript to be published

Author contributions statement

MJH cloned the opsin genes, carried out in-situ hybridizations and electroretinogram recordings, analyzed the data, prepared the figures and wrote the manuscript,
MG supervised the molecular part of the project, designed the primers and performed manual annotations of the opsin genes,
KD carried out in-situ hybridizations,
TL supervised the electrophysiological part of the project and edited the manuscript.

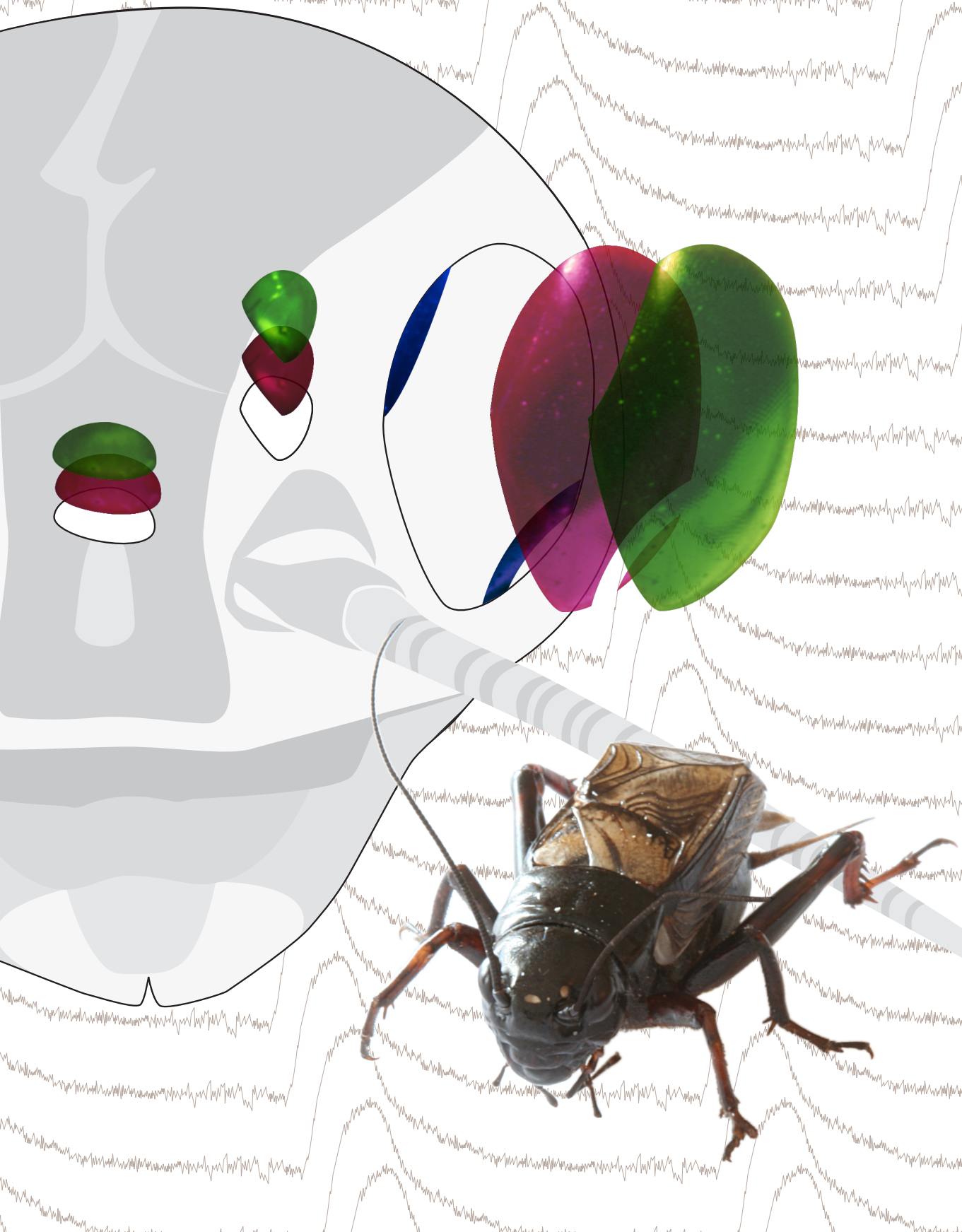

Cover picture. Most adult insects possess two kinds of visual organs: a pair of lateral compound eyes and three dorsal ocelli. M. J. Henze, M. Gesemann, K. Dannenhauer and T. Labhart (pp. 73-86) provide electrophysiological and molecular evidence for different green- and ultraviolet (UV)-sensitive visual pigments in both eye types of the cricket (*Gryllus bimaculatus*). They also show that the retina of the cricket compound eye is spectrally divided into three parts: the polarization-sensitive dorsal rim area expresses blue- and UV-opsin, a newly-discovered ventral area (position marked in the drawing is presumptive) expresses blue- and green-opsin, and the remainder of the compound eye UV- and green-opsin. This spectral heterogeneity may reflect specific functions of the two eye types and of the different regions of the compound eye. Picture composed by Martin Kohler.

Manuscript to be published

Opsin divergence and retinal regionalization in the visual system of the cricket (*Gryllus bimaculatus*)

Miriam J. Henze[1,2,*], Matthias Gesemann[1], Kerstin Dannenhauer[1] and Thomas Labhart[1]

[1]*Institute of Zoology, University of Zürich, Zürich, Switzerland,* [2]*Department of Cell and Organism Biology, Lund, Sweden*

*Author for correspondence (e-mail: miriam.henze@cob.lu.se)

Summary

Most adult insects possess two eye types: three ocelli and a pair of compound eyes. The concomitance of different kinds of visual organs in one organism makes insects an interesting model for visual pigment evolution. Whereas spectral sensitivities have been investigated in many insect taxa, studies on the sequence and expression pattern of opsin genes have concentrated on a few, highly derived, holometabolous insect orders. Spectral sensitivities do not necessarily mirror phylogenetic relationships and, based on the limited molecular data set available so far, general conclusions on the evolution of insect opsins are questionable. We have therefore investigated retinal opsins in the cricket *Gryllus bimaculatus*, a comparatively primitive, hemimetabolous insect. Combining electrophysiological and molecular methods, we provide evidence for two ocellar photopigments, a green- (λ_{max} = 511 nm) and an ultraviolet (UV)-sensitive one (λ_{max} = 350 nm). In the compound eyes, three spectral classes of photoreceptors with peak absorbances in the green (515 nm), blue (445 nm) and UV (332 nm) range have previously been identified. We show that the respective opsins differ from those found in the ocelli. According to the opsin expression pattern, the retina of the compound eyes can be divided into three parts: (1) the so-called dorsal rim area, which is specialized to detect skylight polarization, with blue- and UV-opsin, (2) a newly-discovered ventral area of unknown function with blue- and green-opsin and (3) the remainder of the compound eye with UV- and green-opsin. These results indicate that regionalization in the visual system of the cricket is more complex than assumed earlier.

Key words: opsin, visual pigment, spectral sensitivity, photoreceptor, ocellus, compound eye, retinal heterogeneity, regionalization, *Gryllus bimaculatus* (Orthoptera).

Introduction

Many adult insects possess two kinds of visual organs: a pair of lateral compound eyes (facetted eyes) and up to three dorsal ocelli (single lens eyes). Both eye types were probably present in the first euarthropods already (Bitsch and Bitsch, 2005; Paulus, 1979; Paulus, 2000), which indicates that their evolutionary divergence dates back at least to the early Cambrian, more than 500 million years ago (Waloszek, 2003). Ocelli are cup-shaped, isolated camera-type eyes that were inherited from arthropod predecessors (Bitsch and Bitsch, 2005; Mayer, 2006; Paulus, 2000). Compound eyes, on the other hand, represent an autapomorphy (novel acquisition) of euarthropods (Bitsch and Bitsch, 2005; Nilsson and Kelber, 2007; Paulus, 1979; Paulus, 2000). They consist of replicated subunits, the ommatidia, which are basically identical but can be modified in some respects to create retinal heterogeneity and regionalization (Nilsson and Kelber, 2007; Stavenga, 1992; Stavenga et al., 2001). The concomitance of different kinds of eyes in one organism makes insects an interesting model to study visual pigment evolution. Visual pigments are crucial in the sensory process of vision and one would expect that their fate is related to the function as well as to the history of the eyes.

A possibility to characterize visual pigments is their absorption spectrum. Spectral sensitivities of photoreceptors, which have been investigated in many insect taxa, are to a major extent determined by the visual pigments they contain. The ocelli of most species show absorption maxima in both the ultraviolet (UV) and the blue-green spectral range (dragonflies (Chappell and DeVoe, 1975; Ruck, 1965), mantis (Sontag, 1971), locust (Wilson, 1978), bumblebee (Meyer-Rochow, 1980), honey bee (Goldsmith and Ruck, 1958), moths (Eaton, 1976; Pappas and Eaton, 1977)). Exceptions are the dragonfly *Anax junius* with potentially three visual pigments (UV, blue and blue-green (Chappell and DeVoe, 1975)) and a few cases in which only one of the two typical peak sensitivities was found (UV in the desert ant *Cataglyphis bicolor* (Mote and Wehner, 1980); blue-green in the cockroach *Periplaneta americana* (Goldsmith and Ruck, 1958) and the cricket *Gryllus firmus* (Lall and Trouth, 1989)). Flies possess a single receptor type in their ocelli which

is unusual in two respects: it has a long-wavelength sensitivity maximum shifted towards blue-violet and it achieves UV-sensitivity by a sensitizing pigment (*Musca* (Kirschfeld et al., 1988); *Calliphora* (Kirschfeld et al., 1988; Kirschfeld and Lutz, 1977); *Drosophila* (Feiler et al., 1988; Hu et al., 1978)).

Insect compound eyes typically contain three spectral classes of receptors: UV, blue and green (Briscoe and Chittka, 2001). In some species blue receptors are missing (e.g. in the cockroach *Periplaneta americana* (Mote and Goldsmith, 1970), the red flour beetle *Tribolium castaneum* (Jackowska et al., 2007; Richards et al., 2008) and the desert ant *Cataglyphis bicolor* (Labhart, 1986)), in others additional red receptors are present (e.g. in the dragonfly *Hemicordulia tau* (Yang and Osorio, 1991), some butterflies (Bernard and Stavenga, 1979) and hymenopterans (Peitsch et al., 1992)). However, these features seem to be the result of convergent evolution. From the spectral sensitivity data superimposed on the phylogeny of Insecta, it was concluded that the Devonian ancestor of all winged (pterygote) insects possessed UV, blue and green receptors (Briscoe and Chittka, 2001). Spectral sensitivity data do not necessarily mirror phylogenetic relationships and it would therefore be desirable to compare the amino acid sequences of the opsins, the apoproteins that together with a chromophore constitute visual pigments.

Up to now, molecular studies have concentrated on Hymenoptera, Diptera, Lepidoptera and Coleoptera, all of which are highly derived, holometabolous insect orders. Based on such a restricted data set, general conclusions on the evolution of insect opsins are questionable. In particular, the relationship between the visual pigments in the ocelli and the compound eyes has not received much attention so far. We have therefore cloned retinal opsins of the cricket *Gryllus bimaculatus*, a comparatively primitive, hemimetabolous insect, and investigated the phylogenetic origin as well as the spatial expression pattern of the identified opsin paralogues.

The compound eyes of crickets are of the apposition type. Each ommatidium is composed of a corneal lens, two primary and several secondary pigment cells, four crystalline cone cells and eight receptor cells. The rhabdomeres of the photoceptors fuse to form a closed rhabdom which is directly connected to the crystalline cone (Burghause, 1979). Despite this uniform *bauplan*, the fine structure of the ommatidia varies. A specialized region at the dorsofrontal margin of the compound eye, the so called dorsal rim area (DRA), is easily detectable even in the live insect because of its pale appearance. The ommatidia that constitute the DRA lack corneal faceting and screening pigment and the pigment cells are vestigial (Burghause, 1979; Nilsson et al., 1987; Ukhanov et al., 1996). As shown by anatomical, electrophysiological and behavioral experiments, this eye region is dedicated to polarization vision (Blum and Labhart, 2000; Brunner and Labhart, 1987; Burghause, 1979; Labhart et al., 1984; Zufall et al., 1989). Intracellular recordings revealed three spectral classes of photoreceptors with maximal sensitivities at 332 nm (UV), 445 nm (blue) and 515 nm (green) in the compound eyes of *Gryllus bimaculatus*. Blue receptors were only found in the DRA, UV cells in the dorsal region of the pigmented part of the eye and green receptors everywhere outside the DRA (Zufall et al., 1989).

The cricket ocellus has a single lens consisting of transparent cuticle. A clear zone is located between it and the following photoreceptor layer which comprises a large number of closely packed retinula cells in an irregular arrangement (Chapman, 1998). We have determined the spectral sensitivities of the ocelli in *G. bimaculatus* by electroretinogram (ERG) recordings since no such data was available so far.

Crickets belong to the order of the Orthoptera, whose ancestors diverged about 350 million years ago from the phylogenetic branch that gave rise to holometabolous insects (Grimaldi and Engel, 2005). The results of this study can thus facilitate comparisons of opsin diversification and serve as a link to even more distant comparisons as to crustaceans and chelicerates.

Material and methods

Animals

Two-spotted crickets (*Gryllus bimaculatus,* De Geer*)* were collected in 2004 at different field locations in Tunisia and were subsequently maintained and bred in the laboratory under a 14/10 hours light-dark cycle (L20W/10S daylight lamps; Osram, Munich, Germany) at 26°C and 60% relative humidity.

Cloning

Crickets were rapidly frozen in liquid nitrogen. We extracted total RNA from the head or, in case of the short-wavelength (SW) opsin, from the non-DRA region of the compound eye using the RNeasy® kit (QIAGEN, Hombrechtikon, Switzerland). cDNA was synthesized by means of the SuperScript™ First-Strand Synthesis System for RT-PCR (Invitrogen, Basel, Switzerland). To detect *Gryllus bimaculatus* (*Gb*) opsins, we designed three sets of degenerate primers based on conserved amino acid sequences of the following visual pigments:

(1) the long-wavelength (LW) opsins of the desert locust *Schistocerca gregaria* (Lo1, GenBank accession number X80071), the praying mantis *Sphodromantis sp.* (X71665), the tobacco hornworm *Maduca sexta* (Manop1, L78080) and the honey bee *Apis mellifera* (AmLop1, U26026),

(2) the middle-wavelength (MW) opsins of the band-legged ground cricket *Dianemobius nigrofasciatus* (AB291232), the desert locust *Schistocerca gregaria* (Lo2, X80072), the tobacco hornworm *Maduca sexta* (Manop3, AD001674), the monarch butterfly *Danaus plexippus* (AY605544) and the honey bee *Apis mellifera* (AmBLop, AF004168) and

(3) the SW opsins of the tobacco hornworm *Manduca sexta* (Manop2, L78081), the monarch butterfly *Danaus plexippus* (AY605546), the honey bee *Apis mellifera* (AmUVop, AF004169) and the fruit fly *Drosophila melanogaster* (Rh3, M17718).

We amplified opsin-like sequences from the *Gb* cDNA by polymerase chain reaction (PCR), ligated the PCR products into the pCR®II vector (Invitrogen, Basel, Switzerland) and screened plasmids by EcoRI digestion for inserts of the correct size. Promising clones were sequenced and assembled in the SeqMan module of Lasergene (DNASTAR, Madison, WI, USA). Based

on these results, we designed gene-specific primers and carried out a 5' and a 3' RACE.

Phylogenetic analysis

Insect and chelicerate opsin genes were downloaded from GenBank (http://www.ncbi.nlm.nih.gov/Genbank/). Accession numbers are as follows: horseshoe crab *Limulus polyphemus* (opsin1, L03781; opsin2, L03782), Adanson's house jumper *Hasarius adansoni* (Rh1, AB251846; Rh2, AB251847; Rh3, AB251848), pantropical jumper *Plexippus paykulli* (Rh1, AB251849; Rh2, AB251850; Rh3, AB251851), honey bee *Apis mellifera* (AmLop1, U26026; AmLop2, BK005515; AmBLop, AF004168; AmUVop, AF004169; pteropsin, BK005510), fruit fly *Drosophila melanogaster* (Rh1, K02315; Rh2, M12896; Rh3, M17718; Rh4, M17730; Rh5, U67905; Rh6, Z86118, Rh7, NM_079311), painted lady *Vanessa cardui* (VanG, AY613986; VanB, AY613987; VanUV, AF414074), red flour beetle *Tribolium castaneum* (Green, XM_968054; UV, XM_965251, pteropsin-like1, XM_001816394; pteropsin-like2, DQ060238), band-legged ground cricket *Dianemobius nigrofasciatus* (AB291232), desert locust *Schistocerca gregaria* (Lo1, X80071; Lo2, X80072), praying mantis *Sphodromantis sp.* (X71665). The translated full-length amino acid sequences were aligned with the four *Gb* opsins in ClustalX (http://www.clustal.org/) using a Gonnet 250 protein weight matrix. A phylogeny was reconstructed by the neighbor-joining method. The reliability of the groupings was estimated with 10 000 bootstrap replicates. We designated honey bee pteropsin and the pteropsin-like sequences of the red flour beetle aa outgroups and used TreeView (http://taxonomy.zoology.gla.ac.uk/rod/treeview.html) to display the rooted tree.

Information on gene expression and on the wavelength of peak sensitivity (λ_{max}) of the opsins is stated wherever available. The respective references are as follows: *Limulus polyphemus* (Chapman and Lall, 1967; Dalal et al., 2003; Lall, 1970; Smith et al., 1993), *Hasarius adansoni* and *Plexippus paykulli* (Koyanagi et al., 2008), *Apis mellifera* (Goldsmith and Ruck, 1958; Menzel and Blakers, 1976; Peitsch et al., 1992; Townson et al., 1998; Velarde et al., 2005; Wakakuwa et al., 2005), *Drosophila melanogaster* (Bernard and Stavenga, 1979; Chou et al., 1996; Feiler et al., 1992; Feiler et al., 1988; Fortini and Rubin, 1990; Fryxell and Meyerowitz, 1987; Huber et al., 1997; Mazzoni et al., 2008; Montell et al., 1987; Papatsenko et al., 1997; Pollock and Benzer, 1988; Salcedo et al., 1999; Zuker et al., 1987), *Vanessa cardui* (Briscoe et al., 2003), *Tribolium castaneum* (Jackowska et al., 2007) and *Gryllus bimaculatus* (Zufall et al., 1989).

In situ hybridization

Sense and antisense digoxigenin (DIG) labeled RNA probes were transcribed by a DIG RNA labeling kit (Roche Diagnostics, Rotkreuz, Switzerland) from linearized plasmids containing a 300 to 720 bp coding fragment of the respective *Gb* opsin gene. The synthesized riboprobes were used for *in situ* hybridization only if sufficient amounts of transcript could be detected in a control gel.

Cricket heads were fixed in 4% phosphate buffered paraformaldehyde at room temperature for 45 minutes. They were embedded in freezing medium (Tissue-Tek O.C.T. Compound, Sakura Finetek Europe B.V., Zoeterwoude, the Netherlands) and frozen in liquid nitrogen. We cut 15 to 20 µm sections on a cryostat (Microm HM 550, Thermo Fisher Scientific Inc., Waltham, MA, USA), mounted them on silane coated slides and dried them at 65°C. The tissue was postfixed in 4% phosphate buffered paraformaldehyde for 30 minutes. After acetylation and several washing steps, it was equilibrated in hybridization buffer (50% formamide, 5% Denhardt's solution, 750 mmol/l NaCl, 75 mmol/l trisodium citrate dihydrate, 0.5 mg/ml herring sperm DNA, 0.25 mg/ml torula yeast RNA) for 3 hours and incubated with the probe at 58°C overnight. Further washing steps were followed by equilibration in blocking solution (3% skim milk powder) and detection with an alkaline phosphatase-coupled anti-Dig Fab-fragment (Roche Diagnostics, Mannheim, Germany). The signal was developed by a colorimetric reaction with the two substrates nitro blue tetrazolium (NBT) and 5-bromo-4-chloro-3-indolyl phosphate (BCIP) in alkaline phosphatase solution containing 50 mmol/l $MgCl_2$ and 1 mmol/l levamisole.

We collected images of the processed sections by a Color view IIIu camera mounted on a BX61 microscope (both: Olympus, Tokyo, Japan) and used Adobe® Photoshop (Adobe Systems Incorporated, San Jose, CA, USA) to adjust brightness and contrast.

Electroretinogram

Adult crickets were mounted in a tight plastic tube on a holder in such a way that only the head was exposed. Head and antennae were firmly glued to the tube with wax and the compound eyes were covered with opaque black emulsion paint (Herbol GmbH, Cologne, Germany). The animals were transferred to a Faraday cage and an electrolytically sharpened tungsten electrode was inserted into the margin of the median or the left lateral ocellus, while the reference electrode was positioned in the dorso-caudal part of the head capsule. Electroretinogram (ERG) signals were recorded with a P15 amplifier (bandwidth 0.3-100 Hz, Grass Technologies, West Warwick, Rhode Island, USA) and monitored on the screen of a storage oscilloscope.

For each ocellus, measurements were performed under two conditions: (1) dark-adaptation and (2) light-adaptation with bright long-wavelength illumination ($\lambda > 545$ nm, edge filter, Schott AG, Mainz, Germany).

We stimulated the ocellus by 100 ms flashes of quasi-monochromatic light. The light of a 450 W xenon arc lamp was passed through one of thirteen narrowband interference filters ranging from 318 to 664 nm (Filtrop AG, Balzers, Liechtenstein). It was focused into a flexible UV-transmitting light guide whose far end was positioned in the Faraday cage where it provided a 28° stimulus centered on the ocellus under investigation.

We varied the intensity of the stimulus by neutral density filters (Filtrop AG, Balzers, Liechtenstein) such that the amplitude of the ERG response was the same at all wavelengths. Spectral sensitivities were provided by the reciprocal values of

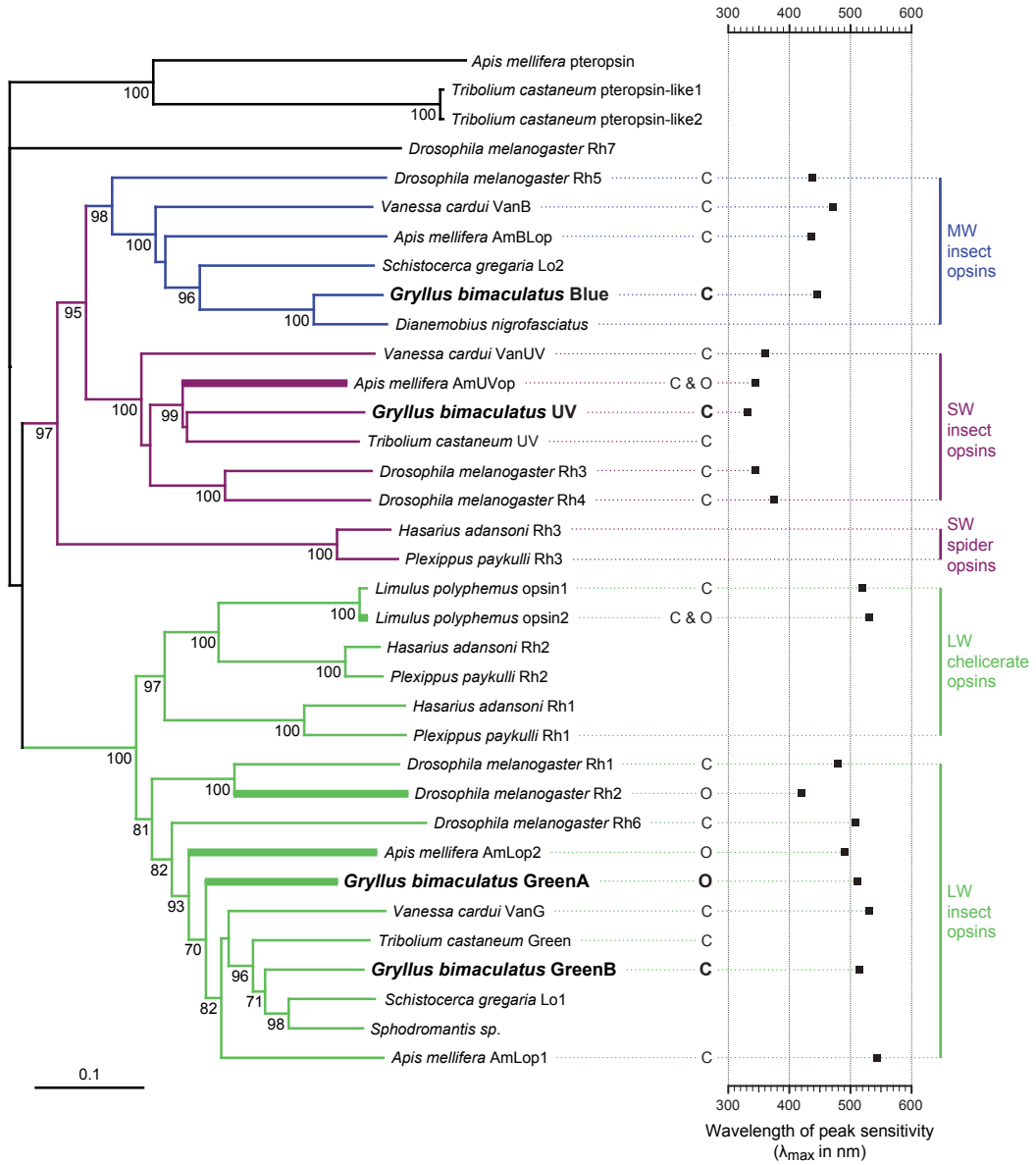

Fig. 1. Evolutionary origin of cricket opsins. The phylogenetic tree is based upon a neighbor-joining analysis of aligned, full-length amino acid sequences with honey bee pteropsin and the pteropsin-like proteins of the red flour beetle as an outgroup. Support for the branches is indicated as percentage of 10 000 bootstrap replicates below the nodes. Only values ≥ 70% are shown. *Gryllus bimaculatus* sequences are highlighted in bold. The different opsin lineages are colored in purple (SW = short-wavelength clade), blue (MW = middle-wavelength clade) and green (LW = long-wavelength clade) and are labeled to the right. If known, the wavelength of peak sensitivity (λ_{max}) is given. The location of opsin expression is indicated by C for the compound eyes, and O and bold branches for the ocelli. For references on sequences, expression data and λ_{max}-values see Materials and Methods. The scale bar represents 0.1 amino acid substitutions per site.

the stimulus intensities and were normalized to the maximal spectral sensitivity determined for each ocellus under the respective adaptation condition.

Statistics and models

ERG recordings were performed on both the median and the left lateral ocellus of 12 crickets, 5 males and 7 females. To investigate whether the spectral sensitivities differed between the median and the left lateral ocellus or between individual crickets, we used a mixed model approach to the analyses of repeated measures (MIXED procedure in SAS 9.1.3, SAS Institute Inc., Cary, NC, USA). The repeated variables *ocellus* and *wavelength* were treated as fixed effects. Based on REML (restricted maximum likelihood) information criteria (Wolfinger, 1993), we chose unstructured and first-order auto-regressive covariance structures for *ocellus* and *wavelength*, respectively (Wolfinger, 1996). The denominator degrees of freedom for the tests of the fixed effects were computed by the Kenward-Roger method (Schaalje et al., 2002) and the covariance parameter *cricket*, a random effect, was analyzed by likelihood-ratio statistics (Littell et al., 1996).

The wavelength of peak sensitivity (λ_{max}) was derived from the ERG measurements by fitting templates for the α-band of an 11-cis retinal visual pigment (Seki et al., 1987) to the data (Govardovskii et al., 2000; Stavenga et al., 1993).

Results

We have identified four distinct opsin encoding mRNAs in the cricket *Gryllus bimaculatus* (*Gb*) - more than for any other hemimetabolous insect investigated so far. The deduced proteins vary in length from 377 (*Gb* UV, *Gb* GreenB) to 379 (*Gb* Blue, *Gb* GreenA) amino acids which is very similar to the visual opsins of most insect species. Full-length *Gb* sequences are listed in the appendix to this manuscript.

Molecular classification of cricket opsins

In order to clarify the evolutionary origin of the four opsin paralogs of the cricket, we have reconstructed a molecular phylogenetic tree based on complete amino acid sequences of arthropod opsins (Fig. 1). We included representatives of several insect orders (Coleoptera, Lepidoptera, Diptera and Hymenoptera) as well as all othopteroid insect species (Mantodea and Orthoptera) and chelicerates for which full-length sequence information was available. Ciliary opsins,

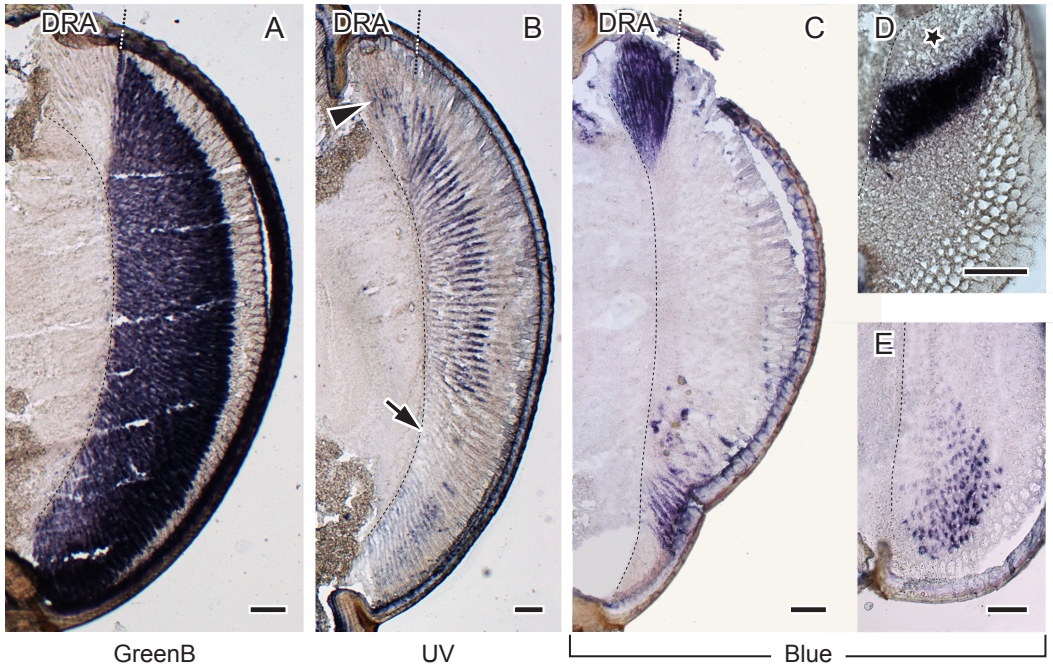

Fig. 2. Opsin mRNA distribution in the compound eye detected by antisense riboprobes for *Gb* GreenB, *Gb* UV and *Gb* Blue. (A-C) Dorso-ventral longitudinal sections including the polarization sensitive dorsal rim area (DRA). (A) *Gb* GreenB is expressed in all eye regions except for the DRA. (B) *Gb* UV positive cells are found in the DRA (arrowhead) and in the main retina excluding an area in the ventral half (arrow). (C) *Gb* Blue is mostly confined to the DRA but also transcribed in a restricted ventral region. (D, E) Cross sections through the upper (D) and the lower part (E) of the eye. All distal receptors in the DRA (D) and some in the ventral retina (E) express *Gb* Blue. Up corresponds to frontal in (D) and to dorsal otherwise. The asterisk in (D) denotes the growth zone of the larval eye. Broken line = basement membrane, scale bars = 100 µm.

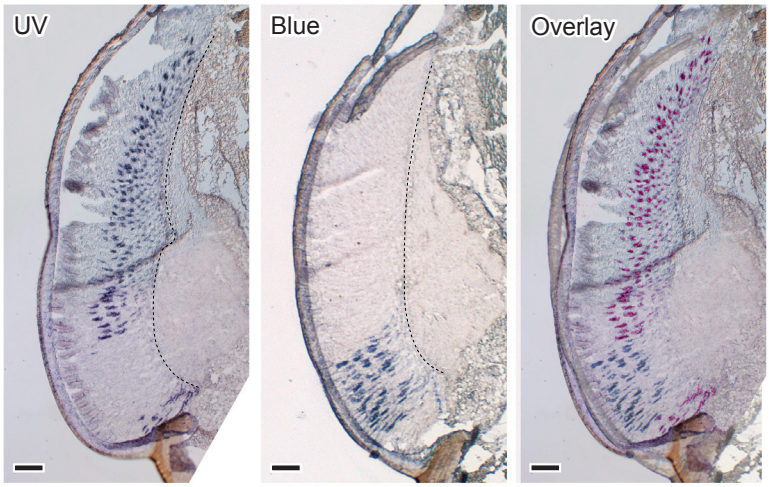

Fig. 3. Localization of *Gb* UV and *Gb* Blue mRNA in the main retina of the compound eye. Consecutive dorso-ventral sections were hybridized with antisense *Gb* UV and *Gb* Blue riboprobes. The right panel shows an overlay of the two pictures to the left with the UV signals recolored in purple in order to discriminate them from the Blue signals. UV and Blue opsin are transcribed in non-overlapping eye regions and at least partly at different levels of the ommatidia. The *Gb* Blue labeling is most intense distally, whereas *Gb* UV is generally detected further proximally. Up corresponds to dorsal in all panels. Broken line = basement membrane, scale bars = 100 µm.

i.e. pteropsin and pteropsin-like proteins, were designated an outgroup. The cricket sequences cluster in the main visual opsin clades of insects: one in the short-wavelength (SW), one in the middle-wavelength (MW) and two in the long-wavelength (LW) branch of the phylogenetic tree. Considering the spectral sensitivities of the compound eyes (Zufall et al., 1989) and ocelli (see below) of *Gryllus bimaculatus* as well as the spatial pattern of opsin expression (see below), the SW, MW and LW sequences can most likely be assigned to ultraviolet-, blue- and green-sensitive visual pigments and were thus termed *Gb* UV, *Gb* Blue, *Gb* GreenA and *Gb* GreenB.

Opsin expression in the retina of the compound eyes

Transcripts of three of the four cricket opsins were detected in the compound eyes: *Gb* GreenB, *Gb* UV and *Gb* Blue. *In situ* probes for *Gb* GreenB labeled the retina outside the DRA (Fig. 2A), probes for *Gb* UV stained photoreceptors in all eye regions except for an area in the ventral half (Fig. 2B) and those for *Gb* Blue marked the DRA and receptors in a restricted ventral region (Fig. 2C). Consecutive cryostat sections hybridized with antisense *Gb* UV and *Gb* Blue riboprobes revealed that the area devoid of *Gb* UV expression coincides with the ventral *Gb* Blue area (Fig. 3). Thus, the retina of the cricket compound eye is spectrally divided into three parts: the polarization-sensitive DRA with blue- and UV-opsin, a newly-discovered ventral area with blue- and green-opsin, and the remainder of the compound eye with UV- and green-opsin.

To some extent, our results allow to relate opsin expression to specific photoreceptors. We denominate the retinula cells of the cricket ommatidium according to the numbering applied by Burghause (Burghause, 1979). In the DRA, the five receptors 1, 2, 5, 6 and 7 contribute to the rhabdom at distal and intermediate levels. Proximally, the short receptor 8 joins in. Cells 3 and 4 do not form microvilli but extend along the whole length of the retinula. Distal cross-sections of DRA ommatidia were labeled completely if hybridized with probes for *Gb* Blue (Fig. 2D), and none of the other cricket opsins was detected distally in the DRA (*Gb* GreenB: Figs. 2A and 4A, E; *Gb* UV: Figs. 2B and 4F; *Gb* GreenA: not shown). Thus, all receptors in the DRA except for the basal cell 8 possibly transcribe *Gb* Blue (Fig. 5). However, we cannot exclude that cells 3 and 4 lack opsin expression completely. Their cross sectional areas are reduced and the absence of a signal in them might thus be hard to notice. A *Gb* UV staining proximally in the DRA (Figs. 2B, 4F and 5) can probably be attributed to cell 8, which is a small, though apparently fully functional photoreceptor (Blum and Labhart, 2000).

In the central part of the retina, the rhabdomeres of all 8 photoreceptors contribute to the rhabdom. The four retinula cells 1, 3, 5 and 7 begin most distally. Below the crystalline cone receptors 2, 4 and 6 join in. Retinula cell 8 and its rhabdomer are developed in the proximal half of each ommatidium only (Burghause, 1979; Sakura et al., 2003). Based on the following observations we assume that the most distal receptors in the central retina transcribe *Gb* GreenB (Fig. 5): All four retinula cells surrounding the tip of the crystalline cone are labeled by probes for *Gb* GreenB in distal cross-sections through the central eye region (Fig. 4B). In longitudinal sections the *Gb* GreenB staining is in general stronger distally than proximally. This is particularly obvious when the signal is less intense due to a shortened development step and therefore more graded (Fig. 4A). At about the level where the *Gb* GreenB labeling becomes weaker, cells stained for *Gb* UV begin (Fig. 4C,D), which suggests that at least one of the more proximal receptors 2, 4 and 6 expresses *Gb* UV (Fig. 5). We assume that the other two cells either transcribe *Gb* UV as well or *Gb* GreenB, since the remaining cricket opsins were not detected in the central retina (*Gb* Blue: Figs. 2C and 3; *Gb* GreenA: not shown). The same applies to cell 8. However, we were unable to identify this small receptor in our sections and thus we also have to consider the possibility that it expresses none of the opsins investigated in this study.

There is evidence that opsin expression in some areas of the main, pigmented part of the retina differs from the one described above. *Gb* Blue is transcribed at a further distal level in the ventral blue-region than *Gb* UV in the central retina (compare Figs. 2B,C and 3). This indicates that *Gb* Blue does not simply replace *Gb* UV expression in the ommatidia of the ventral blue area. If the structure of the ommatidia is the same everywhere in the retina except for the DRA, one must expect that at least one of the four receptors that begin most distally, i.e. retinula cells 1, 3, 5 or 7, transcribes *Gb* Blue. However, the photoreceptor arrangement in the ventral part of the eye of *Gryllus bimaculatus* has not been studied yet. It is therefore possible that *Gb* Blue replaces *Gb* UV in one of the three receptors 2, 4 and 6 which, however, begin at a more distal level in the ommatidia of the ventral blue region than in the central retina. Furthermore, our data suggest that the *Gb* UV expressing cells in the main retina sometimes reach further distally than in the central part of the retina: This concerns for example the ventralmost ommatidia (Fig. 2B) and those directly adjacent to the DRA (Fig. 4F). Apparently, retinal heterogeneity is more complex in the cricket compound eye than previously assumed.

Spectral sensitivities of the ocelli

Apart from the compound eyes, crickets possess a second type of visual organ, the ocelli. The right and the left lateral ocellus are positioned just dorsal of the left and the right antennal base, respectively, whereas the median ocellus is located on the vertex of the forehead. We measured the spectral sensitivities of the median and the left lateral ocellus in adult *G. bimaculatus* by ERG recordings. The results yielded neither a significant difference between individual crickets (χ^2 = 2.7, *df* = 1, *P* = 0.1003 for dark-adaptation, χ^2 = 0.6, *df* = 1, *P* = 0.4385 for light-adaptation) nor between the median and the left lateral ocellus ($F_{1,63.3}$ = 2.01; *P* = 0.1613 for dark-adaptation, $F_{1,44.6}$ = 0.50; *P* = 0.4823 for light-adaptation). Plotting the values for both ocelli on the same graph shows the similarity in shape and peak of the curves (Fig. 6A). Results were therefore pooled before templates for the α-band of an 11-cis retinal visual pigment (Seki et al., 1987) were fitted to the data in a least square sense (Fig. 6B). The models developed by Stavenga (Stavenga et al., 1993) and Govardovskii (Govardovskii et al., 2000) produce equal correlations (0.99 for dark-adaptation and 0.97 for light-adaptation; correlation was calculated as 1 - mean square error).

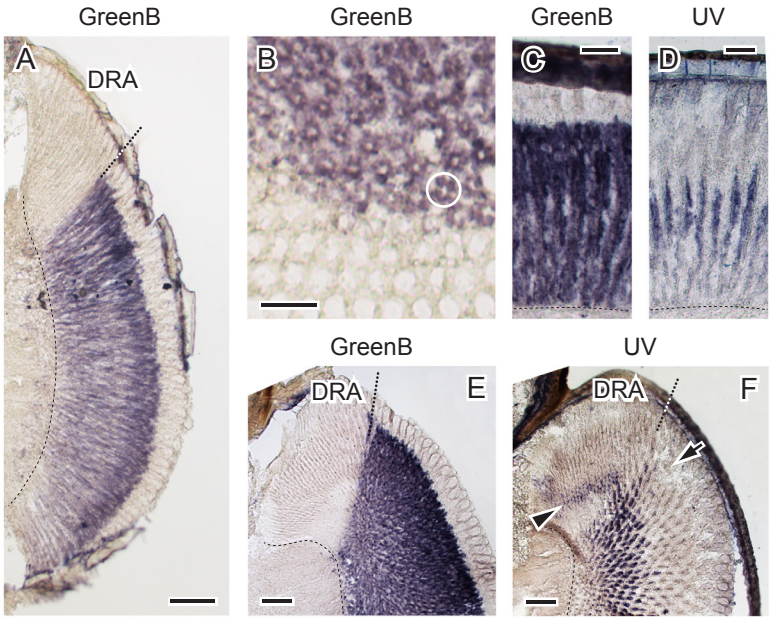

Fig. 4. *Gb* GreenB and *Gb* UV mRNA localization in the compound eye. (A) Longitudinal section showing a less intense and therefore more graded *Gb* GreenB labeling than in Fig. 2A. The staining in the main retina is generally much stronger distally than proximally. (B-D) Distal cross section (B) and longitudinal sections (C, D) through the central part of the eye. (B) All four receptor cells around the tip of the crystalline cone (encircled in one ommatidium) transcribe *Gb* GreenB. (C) At about the level where the *Gb* GreenB labeling becomes weaker, (D) the *Gb* UV staining begins. (E, F) Oblique cross sections through the dorsal part of the compound eye. (F) Whereas *Gb* GreenB cannot be detected in the DRA, (G) *Gb* UV is transcribed in a population of small, proximal receptors (arrowhead). Directly adjacent to the DRA, *Gb* UV is found at a further distal level (arrow) than in the rest of the main retina. Up corresponds to dorsal in (A, E, F), to medial in (B) and to distal in (C, D). Broken line = basement membrane, scale bars = 50 µm in (C, D) and 100 µm otherwise.

For the dark-adapted state the Stavenga and the Govardovskii template give peak absorbances at λ_{max} = 511 nm and 510 nm and for the light-adapted state at λ_{max} = 348 nm and 351 nm respectively. Thus, cricket ocelli are both green- and ultraviolet-sensitive.

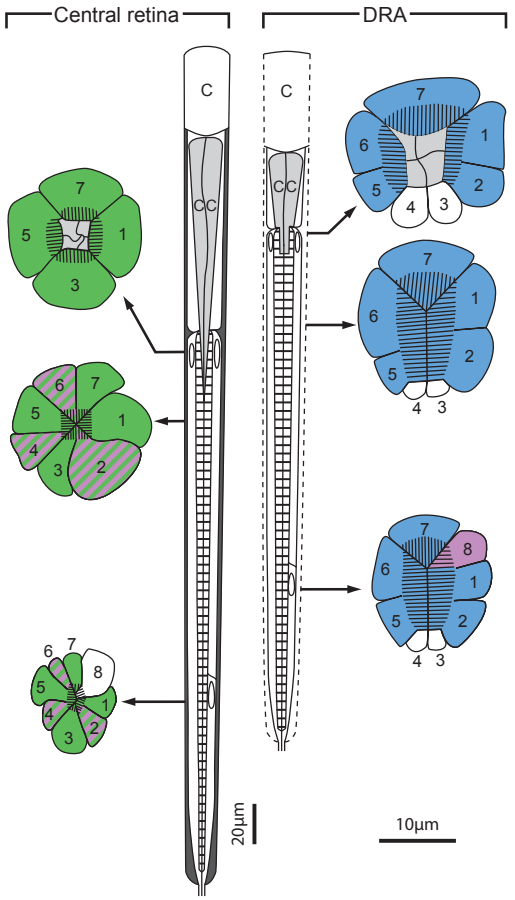

Fig. 5. Opsin expression pattern in ommatidia of the cricket compound eye. Schematic drawing showing a longitudinal section through an ommatidium in the central eye region and in the DRA with cross-sections at different levels as indicated. C = cornea, CC = crystalline cone. Colors denote opsins: Green = *Gb* GreenB, purple = *Gb* UV, blue = *Gb* Blue. Central retina: The four retinula cells 1, 3, 5 and 7 begin most distally and are green-sensitive. Below the crystalline cone receptors 2, 4 and 6 join in. At least one of them is ultraviolet-sensitive and the others are either also ultraviolet- or green-sensitive. Opsin expression in the proximal cell 8 could not be clarified. DRA: All five receptors 1, 2, 5, 6 and 7, which form the rhabdom at a distal level, are blue-sensitive. Cells 3 and 4 do not contribute microvilli but extend along the whole length of the retinula. The small proximal receptor 8 is ultraviolet-sensitive. Vertical and horizontal scale bars refer to longitudinal sections and cross-sections, respectively. Illustration modified after (Burghause, 1979; Nilsson et al., 1987; Sakura et al., 2003).

Opsin expression in the ocelli

None of the three opsins expressed in the compound eyes, i.e. *Gb* GreenB, *Gb* Blue and *Gb* UV, was found in the ocelli. Transcripts of *Gb* GreenA, on the other hand, were detected in the median as well as in both lateral ocelli but not in the compound eyes (Fig. 7). *Gb* GreenA groups in the insect long-wavelength clade of the molecular phylogenetic tree (Fig. 1) and it is therefore most likely that it belongs to the green-sensitive visual pigment ($\lambda_{max} \approx$ 511 nm) that was demonstrated in the ocelli by ERG recordings (see above). Selective depression of the long-wavelength sensitivity by chromatic adaptation revealed the existence of a second ocellar pigment maximally absorbing in the ultraviolet spectral range ($\lambda_{max} \approx$ 350 nm). However, *Gb* UV, the opsin that forms the ultraviolet-sensitive visual pigment found in the compound eyes, is not expressed in the ocelli (Fig. 7). Thus, there must be an additional, yet unknown ocellus-specific opsin in the cricket.

Discussion

Opsin expression in the eyes of Gryllus bimaculatus

Three spectral classes of photoreceptors in the compound eye: In previous, electrophysiological investigations, photoreceptors with peak absorbances in the green (515 nm), blue (445 nm) and UV (332 nm) spectral range were identified in the compound eyes of *Gryllus bimaculatus* (Zufall et al., 1989). Similar results were obtained for *Gryllus campestris*, a closely related species (Labhart et al., 1984). Our data support these three spectral classes of receptors in the cricket. The spatial expression pattern of the visual opsins described in this study also partly coincides with the conclusions drawn from the electrophysiological experiments on the distribution of spectral sensitivities across the eye. However, there are a few important differences.

The DRA is blue- and UV-sensitive: By intracellular recordings only blue receptors were detected in the DRA of *Gryllus bimaculatus* (Zufall et al., 1989). Our own results suggest that all of the long photoreceptors are blue-sensitive, while the proximal cell 8 is UV-sensitive. The latter is rather short (Burghause, 1979) and has therefore probably been missed by all electrophysiological investigations so far. In the DRA of the locust *Schistocerca gregaria*, a related, orthopteroid insect species, two spectral classes of photoreceptors have been reported (Eggers and Gewecke, 1993): blue- and UV-sensitive ones. The polarization sensitivity of the blue cells was on average high, whereas the only UV cell for which the polarization sensitivity could be determined showed a rather low value. In contrast to the cricket, the rhabdomeres of receptors 3 and 4 are not completely reduced in the DRA of the locust. The few microvilli they contribute to the rhabdom show no particular alignment suggesting low polarization sensitivities. It has therefore been argued that cells 3 and 4 constitute the UV receptors (Homberg and Paech, 2002). However, the polarization sensitivity of the one UV cell investigated so far is within the range of values of the blue cells (Eggers and Gewecke, 1993), which means that

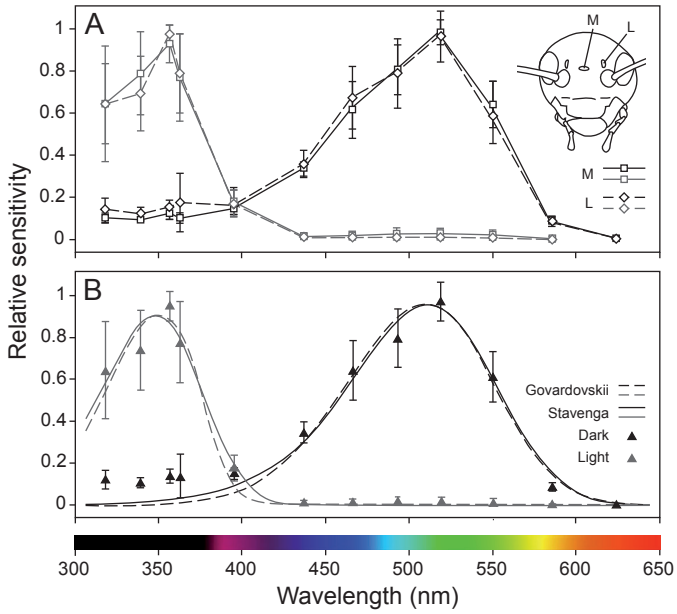

Fig. 6. Spectral sensitivity of the ocelli derived from ERG recordings. (A) Mean spectral sensitivity (± standard deviation) of the median (M, solid lines, open squares, $n = 12$) and the left lateral ocellus (L, broken lines, open diamonds, $n = 12$) under dark-adaptation (black) and light-adaptation with bright long-wavelength illumination (grey). The similarity between the two ocelli in peak sensitivity and shape of the curves is evident. (B) Pooled spectral sensitivity data of both ocelli (mean value ± standard deviation, $n = 24$) under dark-adaptation (black triangles) and light-adaptation (grey triangles) are well fitted by templates for the α-band of an 11-cis retinal visual pigment. The models by Stavenga (solid lines) and Govardovskii (broken lines) yield peak absorbances at 511 and 510 nm for the dark-adapted state and 348 and 351 nm for the light-adapted state, respectively.

the average polarization sensitivity of both receptor types could actually be similar. If the distribution of spectral sensitivities in the locust DRA was the same as in the cricket, one would expect that cell 8 was UV-sensitive. In the locust DRA, receptor 8 is long, beginning at the same distal level as all other retinula cells (Homberg and Paech, 2002). It should therefore be easier to record from it than from the short receptor 8 in the cricket which is only present in the proximal half of the ommatidium (Burghause, 1979). The microvilli of cell 8 are well aligned in both crickets and locusts (Blum and Labhart, 2000; Homberg and Paech, 2002) and thus this cell can be expected to be strongly polarization-sensitive.

A specific ventral area is blue- and green-sensitive: In the pigmented, main part of the cricket compound eye, no blue receptors were identified by intracellular recordings (Zufall et al., 1989). However, our results show that transcripts of the same blue opsin that is expressed in the DRA are also found in a restricted ventral region. Only few cells were recorded electrophysiologically in the ventral part of the eye and it is therefore not surprising that the blue receptors which occur localized and always together with the more abundant green receptors were not detected.

The function of the restricted ventral blue-green region, which is present in adults and larvae of both sexes, remains enigmatic. Regionalization, be it by gradual changes in the number and frequency of receptor types or by confined, principally different parts of the eye, is a common property of the insect visual system (Kelber, 2006). To our knowledge, however, no ventral area comparable to the one of the cricket compound eye has been described to date. It possibly constitutes an adaptation to mediate a specific visual function – similar to the polarization-sensitive DRA of many insect species (Labhart and Meyer, 1999), the part of the dragonfly eye specialized for prey detection (Labhart and Nilsson, 1995) or the mating zone of the honey bee drone (Menzel et al., 1991). In order to understand the function of the newly described blue-green region, morphological and electrophysiological investigations of the photoreceptor properties in the ventral half of the cricket compound eye might be helpful.

The remainder of the compound eye is green- and UV-sensitive: UV receptors were recorded intracellularly only in the dorsal region of the pigmented, main part of the compound eye (Zufall et al., 1989). Our results, in contrast, show that UV opsin is expressed everywhere in the retina except for the ventral blue-green region (Figs. 2B, 3, 4F, 7H). Surprisingly, it is not the UV but the green or blue cells that contribute to the rhabdom at the distalmost level in the cricket compound eye. Since the green and the blue visual pigment have their β-absorption peak in the ultraviolet, this arrangement reduces the absolute sensitivity of the more proximal UV receptors (Warrant et al., 2007).

The ocelli are UV- and green-sensitive: ERG recordings under both dark and long-wavelength adaptation conditions revealed only one spectral type of receptor in the ocelli of the sand field cricket *Gryllus firmus*, the closest relative of *Gryllus bimaculatus* investigated so far. It was most sensitive to green light with an absorption maximum at 520 nm (Lall and Trouth, 1989). The two-spotted cricket *Gryllus bimaculatus*, however, clearly possesses the two peak sensitivities in the UV and blue-green spectral range which are typically found in insect ocelli.

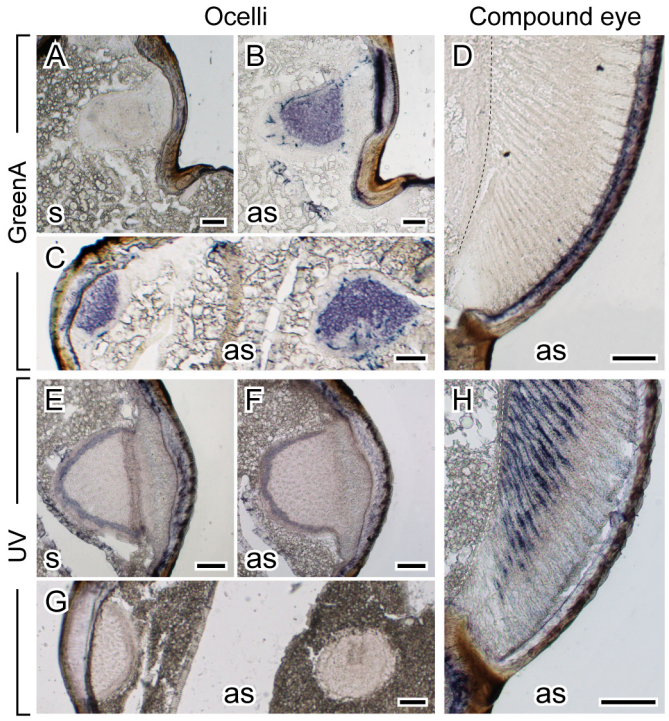

Fig. 7. Localization of *Gb* GreenA and *Gb* UV mRNA in the ocelli and in the compound eyes. Transverse sections of the head were hybridized with sense (s) and antisense (as) riboprobes. (A, B, E, F) Lateral ocellus. (C, G) Lateral ocellus (to the left) sectioned longitudinally and median ocellus (to the right) sectioned tangentially. (D, H) Ventral part of the compound eye. Whereas *Gb* GreenA is expressed in all three ocelli (B, C), it is absent from the retina of the compound eye (D). *Gb* UV, on the other hand, is clearly detectable in the compound eye (H) but cannot be found in the ocelli (F, G). Up corresponds to dorsal in all panels. Broken line = basement membrane, scale bars = 100 μm.

Phylogeny of insect opsins

Origin of the three major clades of insect visual opsins: To root the phylogentic tree of arthropod visual opsins, pteropsin and pteropsin-like sequences were designated as outgroups. While the pteropsin gene has apparently been lost from the *Drosophila* lineage (Velarde et al., 2005), two coding sequences of the red flour beetle (*Tribolium castaneum*) deposited in GenBank cluster with honey bee pteropsin. We assume that these are transcripts of the same gene. They mainly differ in the presence of 45 successive nucleotides, which potentially constitute an additional exon and thus suggest the existence of two splice variants. The remaining 1053 nucleotides deviate in just three positions resulting in two amino acid changes. These minor variations might be due to a polymorphism as only one gene locus could be identified in the genome assembly of the red flour beetle (http://www.Beetlebase.org).

Insect visual opsins fall into three major clades: UV-sensitive SW opsins, blue-sensitive MW opsins and LW opsins whose sensitivities vary from blue-violet (Rh2 in *Drosophila*, Fig. 1) through green to red (e.g. in some Lepidoptera (Briscoe, 2000)). Most holometabolous insect species investigated so far possess at least one opsin of each type. Exceptions such as the red flour beetle *Tribolium castaneum*, which only encodes an SW and an LW opsin, are thought to have lost their MW paralog secondarily (Jackowska et al., 2007). In this study, we have, for the first time, cloned opsins of all three clades in a hemimetabolous insect, the cricket *Gryllus bimaculatus*. The cricket sequences cluster in the phylogenetic tree within the branches formed by opsins of holometabolous species. This confirms the view that the SW, MW and LW visual pigments arose before the holometabolous-hemimetabolous split took place in insects – a hypothesis that has already been proposed on the basis of spectral sensitivity data (Briscoe and Chittka, 2001). A recent study on branchiopod crustaceans, a putative sister group of hexapods including insects, suggests that the divergence of MW and SW insect opsins dates back at least to the last common ancestor of hexapods and branchiopods (Glenner et al., 2006; Kashiyama et al., 2009). The split into an SW-MW and an LW opsin clade occured even earlier in arthropod evolution. Adding the available chelicerate (spider and horseshoe crab) sequences to the phylogenetic opsin tree (Fig. 1) indicates that the origin of these two branches predates the divergence of the Pancrustacea (crustaceans and hexapods) and Chelicerata.

The concomitance of ocelli and compound eyes was followed by opsin divergence: Unlike crickets, honey bees express the same ultraviolet opsin (AmUVop) in both the ocelli and the compound eyes (Velarde et al., 2005). This has also been shown for bumblebees (Spaethe and Briscoe, 2005). The long-wavelength opsins, in contrast, differ between ocelli and compound eyes in all insect species investigated so far. GreenA of the cricket, AmLop2 of the honey bee (Velarde et al., 2005) and Rh2 of

the fruit fly (Pollock and Benzer, 1988) are ocellus-specific (Fig. 1). They are nested within the insect long-wavelength clade and branch off from the opsins expressed in the compound eyes independently at rather basal positions. Chelicerate opsins that were isolated from visual organs presumably homologous to the insect ocelli (Bitsch and Bitsch, 2005; Paulus, 1979), namely from the principal (anterior median) eyes of jumping spiders (Koyanagi et al., 2008) and the median ocelli of the horseshoe crab (Smith et al., 1993), do not cluster with the insect ocellar opsins. Instead, they separate before the insect lineages diversify, after the split into a long-wavelength and a short- to middle-wavelength arthropod opsin clade. Since the origin of the compound eyes and ocelli likely predates the euarthropod subphyla (Bitsch and Bitsch, 2005; Paulus, 1979; Paulus, 2000), this branching pattern suggests that both visual organs primarily expressed the same set of opsins. The concomitance of ocelli and compound eyes was then followed by opsin divergence, which occurred independently in different groups.

Since LW and SW opsins, but no MW opsins have been detected in insect ocelli so far, it would be particularly interesting to investigate whether the intermediate blue shoulder between the UV and green sensitivity peaks in the dragonfly *Anax junius* is due to an MW visual pigment (Chappell and DeVoe, 1975). A general absence of MW opsins from the ocelli could be explained by an early loss of ocellar blue sensitivity in the evolution of insects. Alternatively, the duplicated gene that led to the MW opsin clade might have been expressed in the compound eyes only right from the very beginning.

For a better understanding of visual opsin evolution in the ocelli and the compound eyes, comparative studies on insect species from a greater variety of taxa than investigated so far would be helpful.

List of Symbols and Abbreviations

DRA	dorsal rim area
ERG	electroretinogram
Gb	*Gryllus bimaculatus*
LW	long-wavelength
MW	middle-wavelength
SW	short-wavelength
λ	wavelength
λ_{max}	wavelength of maximal sensitivity

Acknowledgments

We are most grateful to Stephan Neuhauss for providing us with the means and facilities to perform this study and we thank Colette Maurer, Sabine Renninger, Valerie Fleisch, Corinne Hodel, Marion Haug and Oliver Biehlmeier for technical assistance, Stefan Sommer for advice on statistics, Megan O'Connor and Ola Gustafsson for support in data processing, Martin Kohler for help with the figures, Almut Kelber for stimulating discussions and Malin Skog for comments on the figures. This research was partially supported by the "Studienstiftung des deutschen Volkes".

Appendix

Full-length coding sequences of all four cricket opsins described in this paper are listed below.

Nucleotids

Gryllus bimaculatus GreenA: AATGGACAACATTCTGGCACT
TACACCTAGCCTTCTGCAGCCTAAGGCCCCTGAG
GCATGGCAGCAGGTTTCAAATGTGACTGTGGTGGA
TAATGTGCCTCCTGATATGTTACATCTTATTGATGCT
CACTGGTACCAGTTTCCTCCTTTAAATCCACTTT
GGCATGCAATTCTTGGATTTATGATTGGATGTTT
GGGCTTTGTGTCGTGGATGGGTAATGGAGTTGTGATC
TATATCTTTTCTACGACCAAAGGACTTCGCACCCCTTC
CAACCTGCTTGTCGTGAATTTGGCTTTTTCTGATTTC
CTCATGATGGTGGTAATGTCACCACCTATGGTAGT
TAACTGCTTCTATGAAACATGGGTATTAGGAGAACT
GATGTGCCAAATATATGGCATGTGTGGATCCTTGTTT
GGCTGTGCTTCCATTTGGACTATGACAATGATTGCAAT
GGACCGATACAATGTTATTGTAAAGGGCTTAGCAG
GCAAGCCTCTGACTATCAAGACTGCTTTGCTACGCAT
TATTGTAGTGTGGCTCTTTGCTCTAGCATGGACAATT
GCACCACTTTTTGGATGGAACAGATATGTTCCAGAAG
GAAATATGACAGCATGTGGCACTGATTATCT
TAACAAAGATTGGTTCAGTCGCAGTTACATTTTGGTG
TACTCGGTGTTCGTATACTACTTGCCCCTTTTTACGA
TAATCTATTCATACTACTTTATCGTGAAG
GCAGTCGCWGCGCACGAAAAAGCTATGCGCGAACAG
GCAAAGAAAATGAACGTCGCTTCGTTGCGATCG
GCTGAGAACGCCAACACCAGCGCCGAGTGCAAGCT
GGCCAAGGTTGCCCTGATGACAATCTCATTGTGGT
TCATGGCTTGGACTCCATATCTCGTTATCAATTACAT
GGGTGTCTTCCAAGGAGCCAACATTAGCCCGCT
GGCCACTATTTGGGGCTCGCTGTTTGCCAAAGCGAAT
GCAGTTTACAACCCTATCGTATATGGCATCAGCCATC
CAAAGTACAGAGCTGCTCTGAAAGAGAAGCTTCCTT
GCCTTGTGTGTGGACAGACGGAGAGTCCAGAAACAA
CATCGCAAGCTTCAGCTGGCACTACCAACACAAAT
GCTGCTGAGAAGGCATAA

Gryllus bimaculatus GreenB: ATGACCGTCTTACCGAAC
GAGCCGCACTTCAGCGCCTACCAATGGGGCAGCG
GAGGCGGCATGGGCGGCAACATCACCGTCGTC
GACAAGGTGCTGCCGGAAATGATGCACATGGT
GGACGCCTACTGGTACCAGTTCCCTCCCATGAAC
CCGCTCTGGCACGGCCTCCTGGGCTTCGTCATCG
GCGTGCTGGGAGTGATCTCGGTGCTGGGCAACG
GCATGGTCGTCTACATCTTCTGCTCCACCAAGGGCCT
GCGCACGCCCTCCAACCTGCTCGTAGTCAACTT
GGCCTTCTCAGACTTCCTCATGATGTTGGCCATGT
CACCTGCTATGGTCATCAACTGCTACTACGAGAC
CTGGGTGCTGGGGCCACTGATGTGTGAGCTCTACG
GCATGGCAGGGTCCCTCTTCGGTTGCGGCTC
CATCTGGACCATGACCATGATCGCCCTCGATAGGTA
CAACGTCATCGTCAAGGGGCTGTCGGCGAAGCCGAT
GACCAACAAGACGGCTGCCCTGCGCATCTTGT
TCGTGTGGGTCACCTCCATCGCATGGACCATCAT

GCCCTTCTTCGGCTGGAACCGCTACGTGCCCGAG
GGCAACATGACGGCCTGCGGCACGGACTAC
CTGACCAAGACGTGGCAGAGCCGCTCCTACATC
CTCGTCTACTCCTTCTTCGTCTACTTCGCGCCTCTCT
TCACCATCATCTACTCGTACTTCTTCATCGTGCAG
GCCGTCGCCGCCCACGAAAAGGCCATGCGCGAG
CAAGCCAAGAAGATGAACGTGGCGTCCTTGCGATCG
GCCGACAACGCCAACACCAGCGCCGAGTGCAAGCT
GGCCAAGGTGGCTCTCATGACCATCTCTCTGTGGT
TCTTCGCGTGGACCCCCTACCTGGTGATCAACTA
CACTGGCATCTTCGACGGCGCTAAGATCAGCCCTCT
GGCCACCATCTGGAGCTCGCTGTTTGCCAAG
GCCAACGCCGTCTACAACCCCATTGTCTACGGCAT
CAGCCACCCCAAGTACCGCGCGGCGCTGCAAAA
GAAGTTCCCGAGCCTGGCGTGCGCCAACGCCGAG
GACGACACCAGCTCCGTGGCGTCGGGGGCCACCAC
CTGCACCGAAGAGAAGCCTTCGGCGTAA

Gryllus bimaculatus Blue: ATGAACTCCACTACCAGTCTCG
GTGGCGCCCCGATCGCTCTCCCCTACGAGAGCTACGT
GGTGCAACTGCTGGGATGGAATATTCCAGCGGAACA
CATCGAACTTGTTCATCCTCACTGGCGGGGATAT
GAAACACCAAGCAAATTTTGGCATTTTGGATTCGCTT
TCATGTACTTCTGTATTATGGTCATGTCATGTCTAG
GCAATGGAATCGTCCTTTGGATCTTTGGAAC
CACTAAATCATTGAGAACACCATCCAACATGTTTGT
GGTAAACCAGGCCTTGCTTGATATGCTTATGATGATT
GAAATGCCATTGTTTGTTTTAAACTCACTCTTCTAC
CAACGACCAATTGGTTGGGAAGTAGGCTGTGATATC
TACGCCCTGCTAGGATCTGTCTCTGGTATTGGTTCT
GCCATCAACAATGCTGCAATTGCTTATGACAGATATCG
CACCATCGCATTCCCCCTGGATGGGAGGCTGCAGT
TCGGTCATGCAATGGCATTCATTCTTGGCACCT
GGGTTTGGGCGATGCCCTTCTCCCTCCTGCCACTACT
TCGTGTTTGGGGCAGATATGTTCCTGAGGGTTTCCT
TACCACGTGTTCCTTTGATTATTTGACCGACGATGAA
GACACTCGTGTATTCACTGCATCCATCTTTGTTT
GGTCTTATGCCTTTCCTCTGTGTCTCATTATCTTCTTC
TACTGCAAACTTTTTAACCAAGTTCGCTTCCACGA
GAAGATGCTCAAAGATCAGGCAAGGAAAATGAACG
TAAAATCTCTGCAGACCAATCAAGATGCT
GAACAAAAATCTGTTGAAATCCGAATTGCGAAGGTAG
CATTCACAATTTTCTTCCTGTTCTTGTGTTCGT
GGACTCCTTATGCTACTGTGGCAATGATTGGAGCTTTT
GGTAACAGGGCTTTGCTGACGCCTATGTCAACAAT
GATTCCTGCTTTAACTGCAAAGATCGTTTCATGTATT
GACCCATGGATATATGCCATCAACCATCCCAGATTCAG
GGGAGAGCTGCTGCGACGTGCGCCTTGGTTTGGAGT
CAAGGAAATCAACCCATCTGATGTCGGCTCTGTGAC
CACTGATCGCACCACTACTACAGGAACAACCGAGTC
CGTTTCAGCTTAA

Gryllus bimaculatus UV: ATGGAGCTCCAAGGCAGCAAT
GTTTCTCACCTCGGTGTGTGGCGCCCTGAAGCCAG
GTTGGCCACTCGCTTACTGGGGTGGAATGTTCCT
GCCGAGGAGTTAATCCACATCCCGGAGCACTGGCTGA
CATTCCCCGAGCCAGAGGCATTCAGCCACTACCTC
CTTGGCATGCTGTATGTAGCATTCTGTGCTAT
AGCTCTCGTGGGAAATGGACTGGTCATCTGGGTCT
TCAGTTCAGCCAAGTCTCTTCGCACTCCTTCTAATG
TATTTGTTATAAATCTTGCAATTTGTGATTTTATCATGAT
GTTAAAAACACCCATTTTTATATACAATTCATTTAATTT
GGGTTTTGCAATGGGGCAGCTGGGATGTCAAATTTTT
GGTTTCATGGGGTCAATTTCAGGCATAGGAGCT
GCAACAACAAATGCATGCATTGCCTATGACAGATACA
GAGTTATTGCTCGACCATTTGACAGTAAAATGT
CAATAAAAGGTGCCACAATGCTAGTCCTACTTCTCT
GGACATATACTCTACCATGGGCAATAATGCCTCTTTT
GGAAGTTTGGGGAAGATTTGCTCCTGAGGGCTATT
TATCCAGTTGCTCATTTGATTATCTCACAGACACCCCT
GAAAATAATATGTTTGTTCTCTGTATATTCATTTGTTC
CTATGTTATTCCAATGAGCCTGATAATTTATTTTTATTCT
CAAATTGTAAGTCATGTGGTAAATCATGAAAAAT
CACTTAAAGAACAGGCTAAGAAAATGAATGT
GGACTCTCTACGAAGCAATCAACAGCAAAATCAAA
CATCTGCTGAGATACGCATTGCCAAAGTTGCCATT
GGCATATGCTTTCTGTTTGTTGCTTCATGGACTCCG
TATGCAGTATTGGCTCTAATTGGTGCATTT
GGCAACAAAACACTTCTAACACCTGGAGTAACAAT
GATTCCGGCCTGCACTTGCAAAGCTGTAGCTTGCCTC
GACCCTTATGTGTACGCAATCAGCCATCCACGCTATA
GAGTGGAGCTCCAAAAGCGATTGCCATGGCTTTGCAT
AAAGGAACAGACGGCAAGTGATGCAAGTTCAGTT
GCAACAACAACATCAACAAATGCTACTACGACAACT
TCTACATAA

Amino acids

Gryllus bimaculatus GreenA: MDNILALTPSLLQPKAPEAWQ
Q V S N V T V V D N V P P D M L H L I D A H W Y Q F P
P L N P L W H A I L G F M I G C L G F V S W M G N G V V I Y I F
S T T K G L R T P S N L L V V N L A F S D F L M M V V M S P P M V V N C
F Y E T W V L G E L M C Q I Y G M C G S L F G C A S I W T M T M I A M
D R Y N V I V K G L A G K P L T I K T A L L R I I V V W L F A L A W T I A P L F
G W N R Y V P E G N M T A C G T D Y L N K D W F S R S Y I L V Y S
V F V Y Y L P L F T I I Y S Y Y F I V K A V A A H E K A M R E Q A K K M N
V A S L R S A E N A N T S A E C K L A K V A L M T I S L W F M A W T P Y L
V I N Y M G V F Q G A N I S P L A T I W G S L F A K A N A V Y N P I V Y
G I S H P K Y R A A L K E K L P C L V C G Q T E S P E T T S Q A S A G T T N T
N A A E K A

Gryllus bimaculatus GreenB: MTVLPNEPHFSAYQWGSG
G G M G G N I T V V D K V L P E M M H M V D A Y W Y Q F P P M N
P L W H G L L G F V I G V L G V I S V L G N G M V V Y I F C S T K G L R T P
S N L L V V N L A F S D F L M M L A M S P A M V I N C Y Y E T W V L G
P L M C E L Y G M A G S L F G C G S I W T M T M I A L D R Y N V I V K G L
S A K P M T N K T A A L R I L F V W V T S I A W T I M P F F G W N R Y
V P E G N M T A C G T D Y L T K T W Q S R S Y I L V Y S F F V Y F A P L F T I I
Y S Y F F I V Q A V A A H E K A M R E Q A K K M N V A S L R S A D N A N T
S A E C K L A K V A L M T I S L W F F A W T P Y L V I N Y T G I F D G A K I S
P L A T I W S S L F A K A N A V Y N P I V Y G I S H P K Y R A A L Q K K
F P S L A C A N A E D D T S S V A S G A T T C T E E K P S A

Gryllus bimaculatus Blue: MNSTTSLGGAPIALPYESYV
VQLLGWNIPAEHIELVHPHWRGYETPSKFWHFGFAFMY
FCIMVMSCLGNGIVLWIFGTTKSLRTPSNMFVVN
QALLDMLMMIEMPLFVLNSLFYQRPIGWEVGCDIYA
LLGSVSGIGSAINNAAIAYDRYRTIAFPLDGRLQF
GHAMAFILGTWVVAMPFSLLPLLRVWGRYVPEGFLT
TCSFDYLTDDEDTRVFTASIFVWSYAFPLCLIIFFYCKLF
NQVRFHEKMLKDQARKMNVKSLQTNQDAEQKSVEIRI
AKVAFTIFFLFLCSWTPYATVAMIGAFGNRALLTPMST
MIPALTAKIVSCIDPWIYAINHPRFRGELLRRAPWF
GVKEINPSDVGSVTTDRTTTTGTTESVSA

Gryllus bimaculatus UV: MELQGSNVSHLGVWRPEARLA
TRLLGWNVPAEELIHIPEHWLTFPEPEAFSHYLLGMLY
VAFCAIALVGNGLVIWVFSSAKSLRTPSNVFVINLAICD
FIMMLKTPIFIYNSFNLGFAMGQLGCQIFGFMGSISGI
GAATTNACIAYDRYRVIARPFDSKMSIKGATMLVLLLW
TYTLPWAIMPLLEVWGRFAPEGYLSSCSFDYLTDTPEN
NMFVLCIFICSYVIPMSLIIYFYSQIVSHVVNHEK
SLKEQAKKMNVDSLRSNQQQNQTSAEIRIAKVAIGIC
FLFVASWTPYAVLALIGAFGNKTLLTPGVTMIPACTCKA
VACLDPYVYAISHPRYRVELQKRLPWLCIKEQTASDASS
VATTTSTNATTTTST

References

Bernard, G. D. and Stavenga, D. G. (1979). Spectral sensitivities of retinular cells measured in intact, living flies by an optical method. *J. Comp. Physiol. A* **143**, 95-107.

Bitsch, C. and Bitsch, J. (2005). Evolution of eye structure and arthropod phylogeny. In *Crustacea and Arthropod Relationships* (ed. S. Koenemann, R. A. Jenner and F. R. Schram), pp. 185-214. New York: CRC Press, Taylor and Francis Book Inc.

Blum, M. and Labhart, T. (2000). Photoreceptor visual fields, ommatidial array, and receptor axon projections in the polarisation-sensitive dorsal rim area of the cricket compound eye. *J. Comp. Physiol. A* **186**, 119-128.

Briscoe, A. D. and Chittka, L. (2001). The evolution of color vision in insects. *Annu. Rev. Entomol.* **46**, 471-510.

Briscoe, A. D. (2000). Six opsins from the butterfly *Papilio glaucus*: Molecular phylogenetic evidence for paralogous origins of red-sensitive visual pigments in insects. *J. Mol. Evol.* **51**, 110-121.

Briscoe, A. D., Bernard, G. D., Szeto, A. S., Nagy, L. M. and White, R. H. (2003). Not all butterfly eyes are created equal: Rhodopsin absorption spectra, molecular identification, and localization of ultraviolet-, blue-, and green-sensitive rhodopsin-encoding mRNAs in the retina of *Vanessa cardui*. *J. Comp. Neurol.* **458**, 334-349.

Brunner, D. and Labhart, T. (1987). Behavioral evidence for polarization vision in crickets. *Physiol. Entomol.* **12**, 1-10.

Burghause, F. M. H. R. (1979). Die strukturelle Spezialisierung des dorsalen Augenteils der Grillen (Orthoptera, Grylloidea). *Zool. Jb. Physiol.* **83**, 502-525.

Chapman, R. F. (1998). *The Insects*: *Structure and Function*. Cambridge: Cambridge University Press.

Chapman, R. M. and Lall, A. B. (1967). Electroretinogram characteristics and the spectral mechanisms of the median ocellus and the lateral eye in *Limulus polyphemus*. *J. Gen. Physiol.* **50**, 2267-2287.

Chappell, R. L. and DeVoe, R. D. (1975). Action spectra and chromatic mechanisms of cells in the median ocelli of dragonflies. *J. Gen. Physiol.* **65**, 399-419.

Chou, W. H., Hall, K. J., Wilson, D. B., Wideman, C. L., Townson, S. M., Chadwell, L. V. and Britt, S. G. (1996). Identification of a novel *Drosophila* opsin reveals specific patterning of the R7 and R8 photoreceptor cells. *Neuron* **17**, 1101-1115.

Dalal, J. S., Jinks, R. N., Cacciatore, C., Greenberg, R. M. and Battelle, B. A. (2003). *Limulus* opsins: Diurnal regulation of expression. *Visual Neurosci.* **20**, 523-534.

Eaton, J. L. (1976). Spectral sensitivity of ocelli of adult cabbage-looper moth, *Trichoplusia ni*. *J. Comp. Physiol.* **109**, 17-24.

Eggers, A. and Gewecke, M. (1993). The dorsal rim area of the compound eye and polarization vision in the desert locust (*Schistocerca gregaria*). In *Sensory Systems of Arthropods* (ed. K. Wiese, F. G. Gribakin, A. V. Popov and G. Renninger), pp. 101-109. Basel: Birkhäuser Verlag.

Feiler, R., Bjornson, R., Kirschfeld, K., Mismer, D., Rubin, G. M., Smith, D. P., Socolich, M. and Zuker, C. S. (1992). Ectopic expression of ultraviolet-rhodopsins in the blue photoreceptor cells of *Drosophila*: visual physiology and photochemistry of transgenic animals. *J. Neurosci.* **12**, 3862-3868.

Feiler, R., Harris, W. A., Kirschfeld, K., Wehrhahn, C. and Zuker, C. S. (1988). Targeted misexpression of a *Drosophila* opsin gene leads to altered visual function. *Nature* **333**, 737-741.

Fortini, M. E. and Rubin, G. M. (1990). Analysis of cis-acting requirements of the Rh3 and Rh4 genes reveals a bipartite organization to rhodopsin promoters in *Drosophila melanogaster*. *Genes Dev.* **4**, 444-463.

Fryxell, K. J. and Meyerowitz, E. M. (1987). An opsin gene that is expressed only in the R7 photoreceptor cell of *Drosophila*. *Embo. J.* **6**, 443-451.

Glenner, H., Thomsen, P. F., Hebsgaard, M. B., Sorensen, M. V. and Willerslev, E. (2006). Evolution: The origin of insects. *Science* **314**, 1883-1884.

Goldsmith, T. H. and Ruck, P. R. (1958). The spectral sensitivities of the dorsal ocelli of cockroaches and honeybees; an electrophysiological study. *J. Gen. Physiol.* **41**, 1171-1185.

Govardovskii, V. I., Fyhrquist, N., Reuter, T., Kuzmin, D. G. and Donner, K. (2000). In search of the visual pigment template. *Visual Neurosci.* **17**, 509-528.

Grimaldi, D. and Engel, M. S. (2005). *Evolution of the Insects*. Cambridge: Cambridge University Press.

Homberg, U. and Paech, A. (2002). Ultrastructure and orientation of ommatidia in the dorsal rim area of the locust compound eye. *Arthropod Struct. Dev.* **30**, 271-280.

Hu, K. G., Reichert, H. and Stark, W. S. (1978). Electrophysiological characterization of *Drosophila* ocelli. *J. Comp. Physiol.* **126**, 15-24.

Huber, A., Schulz, S., Bentrop, J., Groell, C., Wolfrum, U. and Paulsen, R. (1997). Molecular cloning of *Drosophila* Rh6 rhodopsin: the visual pigment of a subset of R8 photoreceptor cells. *FEBS Lett.* **406**, 6-10.

Jackowska, M., Bao, R., Liu, Z., McDonald, E. C., Cook, T. A. and Friedrich, M. (2007). Genomic and gene regulatory signatures of cryptozoic adaptation: Loss of blue sensitive photoreceptors through expansion of long wavelength-opsin expression in the red flour beetle *Tribolium castaneum*. *Front. Zool.* **4**, 24.

Kashiyama, K., Seki, T., Numata, H. and Goto, S. G. (2009). Molecular characterization of visual pigments in Branchiopoda and the evolution of opsins in Arthropoda. *Mol. Biol. Evol.* **26**, 299-311.

Kelber, A. (2006). Invertebrate colour vision. In *Invertebrate Vision* (ed. E. Warrant and D.-E. Nilsson), pp. 250-290. Cambridge: Cambridge University Press.

Kirschfeld, K., Feiler, R. and Vogt, K. (1988). Evidence for a sensitizing pigment in the ocellar photoreceptors of the fly (*Musca*, *Calliphora*). *J. Comp. Physiol. A* **163**, 421-423.

Kirschfeld, K. and Lutz, B. (1977). Spectral sensitivity of ocelli of *Calliphora* (Diptera). *Z. Naturforsch. C* **32**, 439-441.

Koyanagi, M., Nagata, T., Katoh, K., Yamashita, S. and Tokunaga, F. (2008). Molecular evolution of arthropod color vision deduced from multiple opsin genes of jumping spiders. *J. Mol. Evol.* **66**, 130-137.

Labhart, T. (1986). The electrophysiology of photoreceptors in different eye regions of the desert ant, *Cataglyphis bicolor*. *J. Comp. Physiol. A* **158**, 1-7.

Labhart, T., Hodel, B. and Valenzuela, I. (1984). The physiology of the cricket's compound eye with particular reference to the anatomically specialized dorsal rim area. *J. Comp. Physiol.* **155**, 289-296.

Labhart, T. and Meyer, E. (1999). Detectors for polarized skylight in insects: A survey of ommatidial specializations in the dorsal rim area of the compound eye. *Microsc. Res. Tech.* **47**, 368-379.

Labhart, T. and Nilsson, D.-E. (1995). The dorsal eye of the dragonfly *Sympetrum*: specializations for prey detection against the blue sky. *J. Comp. Physiol. A* **176**, 437-453.

Lall, A. B. (1970). Spectral sensitivity of intracellular responses from visual cells in median ocellus of *Limulus polyphemus*. *Vision Res.* **10**, 905-909.

Lall, A. B. and Trouth, C. O. (1989). The spectral sensitivity of the ocellar system in the cricket *Gryllus firmus* (Orthoptera, Gryllidae). *J. Insect Physiol.* **35**, 805-808.

Littell, R. C., Milliken, G. A., Stroup, W. W. and Wolfinger, R. D. (1996). *SAS System for mixed models*. SAS Institute Inc, Cary, NC: SAS Publishing.

Mayer, G. (2006). Structure and development of onychophoran eyes: What is the ancestral visual organ in arthropods? *Arth. Struct. Dev.*

35, 231-245.
Mazzoni, E. O., Celik, A., Wernet, M. F., Vasiliauskas, D., Johnston, R. J., Cook, T. A., Pichaud, F. and Desplan, C. (2008). Iroquois complex genes induce co-expression of rhodopsins in *Drosophila*. *PLoS Biol.* **6**, e97.
Menzel, J. G., Wunderer, H. and Stavenga, D. G. (1991). Functional morphology of the divided compound eye of the honeybee drone (*Apis mellifera*). *Tissue Cell* **23**, 525-535.
Menzel, R. and Blakers, M. (1976). Colour receptors in the bee eye - morphology and spectral sensitivity. *J. Comp. Physiol. A* **108**, 11-33.
Meyer-Rochow, V. B. (1980). Electrophysiologically determined spectral efficiencies of the compound eye and median ocellus in the bumblebee *Bombus hortorum tarhakimalainen* (Hymenoptera, Insecta). *J. Comp. Physiol.* **139**, 261-266.
Montell, C., Jones, K., Zuker, C. and Rubin, G. (1987). A second opsin gene expressed in the ultraviolet-sensitive R7 photoreceptor cells of *Drosophila melanogaster*. *J. Neurosci.* **7**, 1558-1566.
Mote, M. I. and Goldsmith, T. H. (1970). Spectral sensitivities of color receptors in the compound eye of the cockroach *Periplaneta*. *J. Exp. Zool.* **173**, 137-145.
Mote, M. I. and Wehner, R. (1980). Functional characteristics of photoreceptors in the compound eye and ocellus of the desert ant, *Cataglyphis bicolor*. *J. Comp. Physiol.* **137**, 63-71.
Nilsson, D.-E., Labhart, T. and Meyer, E. (1987). Photoreceptor design and optical properties affecting polarization sensitivity in ants and crickets. *J. Comp. Physiol. A* **161**, 645-658.
Nilsson, D.-E. and Kelber, A. (2007). A functional analysis of compound eye evolution. *Arthropod Struct. Dev.* **36**, 373-385.
Papatsenko, D., Sheng, G. and Desplan, C. (1997). A new rhodopsin in R8 photoreceptors of *Drosophila*: evidence for coordinate expression with Rh3 in R7 cells. *Development* **124**, 1665-1673.
Pappas, L. G. and Eaton, J. L. (1977). Internal ocellus of *Manduca sexta*: electroretinogram and spectral sensitivity. *J. Insect Physiol.* **23**, 1355-1358.
Paulus, H. F. (1979). Eye structure and the monophyly of the Arthropoda. In *Arthropod Phylogeny* (ed. A. P. Gupta), pp. 299-383. New York: Van Nostrand Reinhold.
Paulus, H. F. (2000). Phylogeny of the Myriapoda-Crustacea-Insecta: a new attempt using photoreceptor structure. *J. Zool. Syst. Evol. Res.* **38**, 189-208.
Peitsch, D., Fietz, A., Hertel, H., de Souza, J., Ventura, D. F. and Menzel, R. (1992). The spectral input systems of hymenopteran insects and their receptor-based colour vision. *J. Comp. Physiol. A* **170**, 23-40.
Pollock, J. A. and Benzer, S. (1988). Transcript localization of four opsin genes in the three visual organs of *Drosophila*; RH2 is ocellus specific. *Nature* **333**, 779-782.
Richards, S., Gibbs, R. A., Weinstock, G. M., Brown, S. J., Denell, R., Beeman, R. W., Gibbs, R., Beeman, R. W., Brown, S. J. Bucher, G. et al. (2008). The genome of the model beetle and pest *Tribolium castaneum*. *Nature* **452**, 949-955.
Ruck, P. (1965). Components of visual system of a dragonfly. *J. Gen. Psychol.* **49**, 289-307.
Sakura, M., Takasuga, K., Watanabe, M. and Eguchi, E. (2003). Diurnal and circadian rhythm in compound eye of cricket (*Gryllus bimaculatus*): Changes in structure and photon capture efficiency. *Zool. Sci.* **20**, 833-840.
Salcedo, E., Huber, A., Henrich, S., Chadwell, L. V., Chou, W. H., Paulsen, R. and Britt, S. G. (1999). Blue- and green-absorbing visual pigments of *Drosophila*: ectopic expression and physiological characterization of the R8 photoreceptor cell-specific Rh5 and Rh6 rhodopsins. *J. Neurosci.* **19**, 10716-10726.
Schaalje, G. B., McBride, J. B. and Fellingham, G. W. (2002). Adequacy of approximations to distributions of test statistics in complex mixed linear models. *J. Agric. Biol. Environ. Stat.* **7**, 512-524.
Seki, T., Fujishita, S., Ito, M., Matsuoka, N. and Tsukida, K. (1987). Retinoid composition in the compound eyes of insects. *Exp. Biol.* **47**, 95-103.
Smith, W. C., Price, D. A., Greenberg, R. M. and Battelle, B. A. (1993). Opsins from the lateral eyes and ocelli of the horseshoe crab, *Limulus polyphemus*. *Proc. Natl. Acad. Sci. USA* **90**, 6150-6154.
Sontag, C. (1971). Spectral sensitivity studies on visual system of praying mantis, *Tenodera sinensis*. *J. Gen. Physiol.* **57**, 93-112.
Spaethe, J. and Briscoe, A. D. (2005). Molecular characterization and expression of the UV opsin in bumblebees: three ommatidial subtypes in the retina and a new photoreceptor organ in the lamina. *J. Exp. Biol.* **208**, 2347-2361.
Stavenga, D. G. (1992). Eye regionalization and spectral tuning of retinal pigments in insects. *Trends Neurosci.* **15**, 213-218.
Stavenga, D. G., Kinoshita, M., Yang, E. C. and Arikawa, K. (2001). Retinal regionalization and heterogeneity of butterfly eyes. *Naturwissenschaften* **88**, 477-481.
Stavenga, D. G., Smits, R. P. and Hoenders, B. J. (1993). Simple exponential functions describing the absorbency bands of visual pigment spectra. *Vision Res.* **33**, 1011-1017.
Townson, S. M., Chang, B. S., Salcedo, E., Chadwell, L. V., Pierce, N. E. and Britt, S. G. (1998). Honeybee blue- and ultraviolet-sensitive opsins: cloning, heterologous expression in *Drosophila*, and physiological characterization. *J. Neurosci.* **18**, 2412-2422.
Ukhanov, K., Leertouwer, H., Gribakin, F. and Stavenga, D. (1996). Dioptrics of the facet lenses in the dorsal rim area of the cricket *Gryllus bimaculatus*. *J. Comp. Physiol. A* **179**, 545-552.
Velarde, R. A., Sauer, C. D., Walden, K. K. O., Fahrbach, S. E. and Robertson, H. M. (2005). Pteropsin: A vertebrate-like non-visual opsin expressed in the honey bee brain. *Insect Biochem. Mol. Biol.* **35**, 1367-1377.
Wakakuwa, M., Kurasawa, M., Giurfa, M. and Arikawa, K. (2005). Spectral heterogeneity of honeybee ommatidia. *Naturwissenschaften* **92**, 464-467.
Waloszek, D. (2003). The "Orsten" window - Three-dimensionally preserved Upper Cambrian meiofauna and its contribution to our understanding of the evolution of Arthropoda. *Paleontol. Res.* **7**, 71-88.
Warrant, E., Kelber, A. and Frederiksen, R. (2007). Ommatidial adaptations for spatial, spectral, and polarization vision in arthropods. In *Invertebrate Neurobiology* (ed. G. North and R. J. Greenspan), pp. 123-154. Cold Spring Harbor, New York: Cold Spring Harbor Laboratory Press.
Wilson, M. (1978). Functional organization of locust ocelli. *J. Comp. Physiol.* **124**, 297-316.
Wolfinger, R. (1993). Covariance structure selection in general mixed models. *Commun. Stat. Simulat.* **22**, 1079-1106.
Wolfinger, R. D. (1996). Heterogeneous variance-covariance structures for repeated measures. *J. Agric. Biol. Environ. Stat.* **1**, 205-230.
Yang, E. C. and Osorio, D. (1991). Spectral sensitivities of photoreceptors and lamina monopolar cells in the dragonfly, *Hemicordulia tau*. *J. Comp. Physiol. A* **169**, 663-669.
Zufall, F., Schmitt, M. and Menzel, R. (1989). Spectral and polarized-light sensitivity of photoreceptors in the compound eye of the cricket (*Gryllus bimaculatus*). *J. Comp. Physiol. A* **164**, 597-608.
Zuker, C. S., Montell, C., Jones, K., Laverty, T. and Rubin, G. M. (1987). A rhodopsin gene expressed in photoreceptor cell R7 of the *Drosophila* eye: homologies with other signal-transducing molecules. *J. Neurosci.* **7**, 1550-1557.

Acknowledgements

If you have ever been kept awake by the high-pitched buzzing sound of a mosquito at night, you might have learnt that one can make a difference no matter how small one is. Social insects like ants, termites, bees and wasps teach us yet another important lesson. As some of the most successful organisms on earth, they convincingly convey the message of cooperation: By working together, one can achieve goals that would otherwise be far beyond one's reach.

During my PhD I have often felt like a tiny mosquito buzzing around in the hope that my work would finally have some impact. I was also quite aware of the fact that similar to a termite mount my thesis would never be accomplished without the help of others. I have greatly appreciated the support I got and I deeply thank all the people who have done their best to bring me where I am now.

Thanks so much to my supervisors and colleagues!

Thomas Labhart – for sharing your tremendous knowledge on the secret world of polarized light and polarization vision with me, for your valuable advice and critical comments. You are one of the most accurate and honest persons I have ever met and this is reflected in both your scientific work and your daily attitude. You have accompanied me during my PhD while group members and leaders changed and I always knew that I could count on you.

Rüdiger Wehner – without your consent this thesis would not have been started. I was very fortunate to experience the first time of my PhD in the lively research group that you had established at the University of Zurich. Your passion for science has influenced several generations of students including myself. I remember with pleasure the great lectures you gave and the fascinating stories on the dinner table when we went out with visitors.

Stephan Neuhauss – for "adopting" me and treating me like one of your "own" PhD students when you became head of the department. Without your financial support for my last year this thesis might not have been finished. You have kept the door to your office always open and you have found time to listen to me no matter how busy you were. I admire your open-minded, interdisciplinary research and your uncomplicated and energetic way of getting things done and, of course, I will never forget the delicious turkey you served us for Thanksgiving.

Uwe Homberg – for accepting to be the external member of my PhD committee, for inviting us to visit your group in Marburg and for organizing such a pleasant and interesting stay for us, for bringing up dedicated students that work on polarization vision and tackle the difficult neuronal questions that have to be answered if we truly want to understand skylight navigation.

All former members of the Wehner group – in particular **Schtefan** for sharing your expertise in statistics with me, **Tobias S** for your advice during my initial stages of Matlab programming, **Robyn** for thoroughly proofreading manuscripts, for your amiable character, your open mind and your pioneer spirit, **Midori** (and **Ryuichi**) for helping me catching crickets in Switzerland and on a crazy trip to Tunisia, for your Asian calmness of never panicking in whatever situation you find yourself in, for taking care of me in Japan and for many stimulating discussions, **Marc**, **Markus K**, **Valerie D**, **Karen**, **Susanne**, **Miriam C**, **Eric M**, **Alex U**, **Simone**, **"what's his name"**, **Patrick**, **Denise W**, **Anna**, **Nicole**, **Sabine V** and **Cornelia** for creating a very pleasant working atmosphere.

All current and **past members of the Neuhauss group** – a fresh breeze swept the department when you moved in. Thanks for being such a social, supportive and energetic team. **Sabine R**, **Colette**, **Valerie F**, **Corinne, Annegret**, **Melody**, **Annette** for passing your expertise in the lab on to me, for good advice and enlightening chats in between, **Oli** for never losing your sense of humor and for sharing your knowledge on microscopes with us, **Kaspar** for solving technical problems when everyone else has given up, **Kara** for being so kind to finish what I had to leave incomplete, **Marion**, **Ursina**, **Tiziana**, **Stephanos** and **Martina** for providing a helping hand when it was needed, **Irene** for your amazing organizing skills keeping track of everything, **Matthias G** for never becoming impolite no matter how many people simultaneously want your advice, for introducing me to molecular biology and for a very fruitful collaboration, **Peter F** for administering first aid when I pressed on the wrong side of that stupid razor blade, **Hans** and **Nina** for helping out with feeding the crickets during holidays, **Franzi** for introducing me to electron microscopy, for the patience and stamina with which you collected data on our capricious electron microscope, for your help catching crickets and taking care of them, for always finding a practical solution and for being the strong woman you are.

All current and **past members of the Lund Vision group** and **everyone else at Zootis** – **Almut** for motivating and supporting me in any possible way. Your energy is incredible! **Eva K**, **Malin**, **Torill**, **Henrik**, **Marcus S**, **Ola**, **Yakir**, **Magnus**, **David**, **Olle**, **Lina**, **Marie**, **Linda**, **Emily**, **Megan**, **Thomas N**, **Ronald P**, **Ronald K**, **Eric W**, **Dan**, **Peter E**, **Eric H**, **Josef**, **Rikard**, **Anders**, **Carina**, **Björn**, **Eva L**, **Rita** and **Ylwa** thanks for giving me such a warm welcome, for comforting me in times when I was down and for making sure that I would not forget about the pleasures of life. I am looking forward to the future days that I can spend with you!

Other co-workers and **colleagues** – **Chrissi** for skillfully gluing tiny flies on toothpicks and contributing in many ways to the *Drosophila* project, **Vasco de Medici** and **Steven Fry** for pictures of free-flying *Drosophila*, **Mathias Wernet** for attracting me to the field of molecular research, **Hitoshi Aonuma** and **his group** for giving me the opportunity to work in Japan, which was undoubtedly one of the most memorable times in my life, **Thorsten** for performing the Lorelei in Japanese with me even though we hardly understood a word of what we were saying (in any case, you were the most remarkable Lorelei I have ever seen), **Helmut Heise**, **Marcel Freund**, **Hansjörg Baumann** and **Patrick Scheuble** for excellent technical support.

Vielen Dank, muito obrigada, ありがとう ございました to my friends and my family!

Tommy – dass du mich zum Turnen ab und zu aus dem Labor in den Irchelpark oder ins Sportzentrum gelockt hast. Du bist ein wundervoller Akrobatikpartner und ein ganz besonderer Freund.

Graça – für die gemütlichen Abende bei dir, an denen du mir die Sprache deiner brasilianischen Heimat näher gebracht hast. In meinem ersten Jahr in Zürich, ohne eigene Unterkunft und gesicherte Finanzierung, hast du mir sehr geholfen, denn bei dir habe ich mich stets zu Hause gefühlt.

Katrin und **Denise v O** – ihr wart meine absoluten Traum-Mitbewohner in der Brahmshof-WG: Zwei sympathische, hilfsbereite und verantwortungsbewusste Studentinnen, die auch noch begeistert kochen! Ich hätte es nicht besser treffen können.

Yukari – für deinen ungeheuren Eifer und die Liebenswürdigkeit, mit der du versucht hast, mein Japanisch aufzubessern. Ich bedauere sehr, dass mir gegen Ende meiner Dissertation keine Zeit mehr für Stunden mit Dir blieb.

Elisabeth – für die fesselnden Gespräche über Auslandsprojekte, Benefizveranstaltungen und alternative Architektur beim gemeinsamen Mittagessen.

Mama und **Papa** – dass ihr mich in einem Haushalt großgezogen habt, in dem ein Igel im Garten interessanter war als das Fernsehprogramm. Ihr habt mich früh auf all die kleinen Wunder um mich herum aufmerksam gemacht und dadurch meine Liebe zur Natur geweckt, noch ehe ich richtig laufen konnte. Schließlich ist kein Kinderspielzeug so faszinierend wie Frösche, die vom Rand eines Tümpels ins Wasser hopsen. Ihr habt mir beigebracht, dass man die Antwort auf Fragen finden kann, indem man nachforscht, und ihr habt mich über viele Jahre hinweg großzügig unterstützt, ohne mir je vorzuschreiben, wo mein Weg hingehen sollte. Danke für Eure bedingungslose Liebe, das Vertrauen und die Freiheit, die ihr mir geschenkt habt.

Carmen und **Anne-Theres** – es war großartig, in einem „Dreimädelhaus" aufzuwachsen. Auch jetzt, da wir alle ausgeflogen sind, gehört ihr zu den Menschen, die mir am nächsten stehen. Ihr versteht meine Sorgen und Nöte ohne große Erklärungen.

Alex, Elena und **Samuel** – mit euch hat sich Carmen eine lustige Gefolgschaft zugelegt. Eure wachsende Familie produziert einen Haufen komischer Situationen, über die man herzlich lachen kann. Ein Jahr lang habt ihr mir in der Schweiz Gesellschaft geleistet, bevor es euch zurück nach Deutschland zog.

Florian – auch Dich hat es in die Schweiz verschlagen. So hatte ich das Glück, einen Bauingenieur in meiner Nähe zu wissen, auf dessen Tipps ich zurückgreifen konnte, wenn ich beim Programmieren nicht weiter kam. Ohne dich würde ich wohl noch heute nach einer Möglichkeit suchen, wie man die Richtung eines Winkels auf einer beliebigen Tangentialebene an eine Kugel eindeutig definieren kann.

Oma Magdalene – für Deine lieben Briefe und Anrufe, durch die du mir trotz unserer räumlichen Distanz immer nahe geblieben bist.

Trudi und **Remi** – dass ihr mir in der Schweiz ein zweites Zuhause gegeben habt. Bei euch bin ich stets rührend umsorgt worden.

Christian und **Sylvia** – ihr habt euch regelmäßig nach meinem Befinden erkundigt. Danke für euer Mitgefühl und danke fürs Zuhören!

Martin – für dein Versprechen, immer an meiner Seite zu bleiben. Du hast die Höhen und Tiefen dieser Arbeit mit mir durchlebt. Du hast Nachtschichten eingeschoben, um mir zu helfen, wenn es brenzlig wurde, du hast als Blitzableiter für meine Launen gedient und mir anfangs durch das Klettern und später durch unsere gemeinsamen Tanzstunden einen wunderbaren Ausgleich zur Arbeit geschaffen. Danke für deine Geduld, deine Treue und deine Liebe.

Grants

2004 - 2007	PhD scholarship from the Studienstiftung des deutschen Volkes
2006	Grant from the Hokkaido University for a 3-month research stay in Japan
2002, 2006	Conference travel grants from the Studienstiftung des deutschen Volkes
1998 - 2002	Undergraduate fellowship of the Studienstiftung des deutschen Volkes
1997	Award from the Wolfgang-C.-Wenten-Stiftung for outstanding performance in English

Publications

Henze MJ, Labhart T (2007) Haze, clouds and limited sky visibility: polarotactic orientation of crickets under difficult stimulus conditions. *Journal of Experimental Biology* 210: 3266-3276.

Henze MJ (2005) Der Sehsinn der Chinesischen Zacken-Erdschildkröte. In: Schaefer I (ed) Zacken-Erdschildkröten - Die Gattung *Geoemyda*. *Natur und Tier-Verlag*: 77-83.

Henze MJ, Schaeffel F, Wagner HJ, Ott M (2004) Accommodation behaviour during prey capture in the Vietnamese leaf turtle (*Geoemyda spengleri*). *Journal of Comparative Physiology A* 190: 139-146.

Henze MJ, Schaeffel F, Ott M (2004) Variations in the off-axis refractive state in the eye of the Vietnamese leaf turtle (*Geoemyda spengleri*). *Journal of Comparative Physiology A* 190: 131-137.

PhD related activities

1) International project presentations

07/2008	*Talk at the 2nd International Conference on Invertebrate Vision, Bäckaskog Slot, Sweden:* A small fly under the open sky: How *Drosophila* views the celestial polarization pattern.
03/2008	*Talk at the Department for Cell and Organism Biology, Lund University, Sweden:* Polarization vision and visual pigments in the cricket.
03/2007	*Poster at the 7th Meeting of the German Neuroscience Society, Göttingen, Germany:* Is there a common genetic program to specify polarization-sensitive photoreceptors in insects?
07/2006	*Poster at the 29th European Conference on Visual Perception, St. Petersburg, Russian Federation:* Haze, clouds and a restricted field of view: Can crickets make use of their polarization compass under unfavorable sky conditions?
02/2006	*Talk at the Research Institute for Electronic Science, Hokkaido University, Japan:* Haze, clouds and a restricted field of view: Can crickets make use of their polarization compass under unfavorable sky conditions?
06/2005	*Talk at the Department of Biology, Philipps-University Marburg, Germany:* Cricket polarization vision: Behavioral results.
02/2005	*Poster at the 6th Meeting of the German Neuroscience Society, Göttingen, Germany:* Cricket polarization vision under difficult stimulus conditions.
10/2004	*Talk in an international course on Sensory Ecology at Lund University, Sweden:* Cricket polarization vision under restricted stimulus conditions.

2) Courses

Science:

- International Sensory Ecology course for Post-graduates
Lund University, Sweden

- Signal processing mechanisms in the nervous system of arthropods
- Colloquium for Neurobiology and Behavioral Studies
Zoological Institute, Zürich University

- The Neurobiology of Consciousness
- Computational Neuroscience
Institute for Neuroinformatics, Zürich University

- Design and statistical analysis of biological experiments
Zoological Museum, Zürich University

Key skills:

- Fund raising for research projects
- Management of scientific projects
- Self- and time-management
- Eye-catching posters
PRO-WISS University Zürich

- Presentation skills training
- Visual knowledge communication
Center for Didactics of the ETH Zürich and Zürich University

- Interactive teaching methods
Program to promote young scientists by the Studienstiftung des deutschen Volkes

Computer applications:

- MySql and PHP
- Macromedia Flash
- Adobe GoLive
- Adobe InDesign
- Adobe Illustrator
- Image processing in Adobe Photoshop
- Adobe Acrobat Professional
- Advanced calculations in Excel
IT Center of Zürich University

Languages:

- Japanese for beginners
Language Center of Zürich University and the ETH Zürich

- Swedish for beginners
Adult Education Center Lund, Sweden

I. Haze, Clouds and Limited Sky Visibility: Polarotactic Orientation of Crickets under Difficult Stimulus Conditions.

M. J. Henze, T. Labhart

II. A Small Fly under the Open Sky: How Drosophila Views the Celestial Polarization Pattern.

M. J. Henze, C. Bleul, F. Baumann, T. Labhart

III. Is there a Common Genetic Program to Specify Polarization-Sensitive Photoreceptors in Insects?

M. J. Henze, M. Wernet, T. Labhart

IV. Opsin Divergence and Retinal Regionalization in the Visual System of the Cricket (Gryllus bimaculatus).

M. J. Henze, M. Gesemann, K. Dannenhauer, T. Labhart